Aus der

Klinik und Poliklinik für Psychiatrie und Psychotherapie des Universitätsklinikums Carl

Gustav Carus an der TU Dresden

(Direktor: Prof. Dr. med. Dr. rer. nat. Michael Bauer)

_Die Konnektivität großer Hirnnetzwerke: Was der Ruhezustand des Gehirns uns über phänotypische Variation und pharmakologische Interventionen sagen kann_

_Large-scale brain networks: what the resting brain can tell us about phenotypic differences and pharmacological interventions_

D i s s e r t a t i o n s s c h r i f t

zur Erlangung des akademischen Grades

Doctor rerum medicinalium (Dr. rer. medic.)

vorgelegt

der Medizinischen Fakultät Carl Gustav Carus

der Technischen Universität Dresden

von

M.Sc. Yacila Isabela Deza Araujo

aus La Libertad, Peru

Dresden 2018

1. Gutachter:

2. Gutachter:

Tag der mündlichen Prüfung: (Verteidigungstermin)

gez.:_____

Vorsitzender der Promotionskommission

**CONTENTS**

## LIST OF FIGURES

**LIST OF TABLES**

# ABBREVIATIONS

| | |
|---|---|
| 5-HT | Hydroxytryptamine (Serotonin) |
| ACC | Anterior Cingular Cortex |
| ATD | Acute Tryptophan Depletion |
| ATL | Acute Tryptophan Loading |
| AUC | Area Under The Curve |
| BAL | Balanced |
| BOLD | Blood-oxygen-level dependent |
| COG | Center of Gravity |
| CON | Cingulo-opercular Network |
| CRC | Collaborative Research Centre |
| DAAD | Deutscher Akademischer Austauschdienst (German Academic Exchange Service |
| DMN | Default Mode Network |
| DVARS | temporal Derivative of timecourses (root mean square) variance over Voxels |
| EEG | Electroencephalogram |
| fALFF | Fractional Amplitude of Low Frequency Fluctuations |
| FD | Framewise Displacement |
| FLIRT | FMRIB's Linear Image Registration Tool |
| FNIRT | FMRIB's Non-Linear Image Registration Tool |
| fMRI | Functional Magnetic Resonance Imaging |
| fNIRS | Functional Near-Infrared Spectroscopy |
| FP | Frontoparietal |
| FSL | Functional MRI of the Brain Software Library |
| ICN | Intrinsic Connectivity Networks |
| ICA | Independent Component Analysis |
| ITG | Inferior Temporal Gyrus |
| MEG | Magnetoelectroencephalogram |
| MELODIC | Multivariate Exploratory Linear Optimized Decomposition into Independent Components |
| MNI | Montreal Neurological Institute |
| MTG | Middle Temporal Gyrus |
| OFC | Orbito-frontal Cortex |

| PALM | Permutation Analysis of Linear Models |
|------|----------------------------------------|
| PCG | Pre-central Gyrus |
| PFC | Prefrontal Cortex |
| PHG | Parahippocampal Gyrus |
| ROI | Region of Interest |
| RSFC | Resting-State Functional Connectivity |
| SSRI | Selective Serotonin Reuptake Inhibitor |
| STG | Superior Temporal Gyrus |
| TFCE | Threshold-Free Cluster Enhancement |
| TRP | Tryptophan |
| VBDM | Value-Based Decision-Making |

# ABSTRACT

This doctoral thesis aims to demonstrate the relevance of resting-state functional connectivity (RSFC) for the study of brain function. RSFC refers to the spontaneous brain activity structured in intrinsic connectivity networks. These networks mirror task-based activations and show significant variations across several behavioral domains and phenotypical traits. Furthermore, changes in these networks after, for instance, pharmacological manipulations, may disentangle the specific role of several neurotransmitters systems in normal and pathological functional connectivity. While various neuroimaging techniques enable the detection of intrinsic connectivity networks, data-driven methods, such as independent component analysis, provide a robust spatial representation of brain networks that are distinguishable from physiological signals and scanner noise.

Within the above-mentioned framework, this thesis presents data from two studies designed to better understand 1) individual differences in decision making reflected in intrinsic network connectivity and 2) variations in intrinsic network connectivity following serotonergic manipulations. The first part is the general introduction where I present the theoretical background, the methodology used in both experiments and an overview of the current research related to the studies of this thesis. The second chapter presents the first study, which examined the relationship between a set of value-based decision-making parameters with large-scale intrinsic connectivity networks. Findings of this study revealed that individuals who prefer to gamble in order to avoid a sure loss, exhibit stronger connectivity between the default mode and left frontoparietal systems to their adjacent brain regions, especially to those involved in prospective thinking, affective decision making and visual processing. The third chapter presents the second experimental study, which examined changes in default mode network connectivity after two tryptophan interventions to increase and decrease brain serotonin synthesis, and a control condition. Results of this study showed decreased functional connectivity between the default mode network and emotion-related regions associated with higher serotonin brain levels. Finally, the fourth chapter includes a general discussion that integrates the significance of the findings from both studies. In this section, limitations and recommendations for future research are also considered before presenting the conclusion that highlights the contribution of this work for unraveling the continuous activity of the resting brain.

# CHAPTER 1

## 1. GENERAL INTRODUCTION

*"The fact that the body is lying down is no reason for supposing that the mind is at peace. Rest is sometimes far from restful"*

*Seneca the younger, "On Noise", ~65 AD*

### 1.1.    Resting-state functional connectivity: the silent work of the resting brain

Since ancient times, humans have wondered what the mind (therefore the brain as well) does when it is not involved in an active and conscious task. Is the brain still working, or does it simply "shut down"? In 1979, the accidental discovery of higher frontal blood flow during resting wakefulness was interpreted as an anticipatory response to "simulate behavior" (Ingvar, 1979), but it was not until 1995 when modern neuroscience revealed what really happens when we "are not using" our brain. In 1995, Dr. Bharat Biswal and colleagues mapped, for the first time using functional magnetic resonance imaging (fMRI), spontaneous brain signals in the human sensorimotor cortex in absence of a task or stimulus (Biswal et al., 1995). This investigation undoubtedly demonstrated that the awake brain remains active under resting conditions and introduced the concept of Resting-State Functional-Connectivity (RSFC), a technique that uncovers spontaneous brain fluctuations in the fMRI signal. These fluctuations are temporally correlated across functionally related areas, building detailed maps of complex neural systems which constitute what researchers nowadays call an individual's "functional connectome" (Biswal et al., 2010).

Since the publication of this seminal work, RSFC studies have significantly increased, mainly due to their relatively easy acquisition procedure and the possibility of their use with sensitive population (i.e. psychiatric patients (Woodward & Cascio, 2015), children and elderly (Wang et al., 2012), sedated (Kirsch et al., 2017) and sleeping individuals (Altmann et al., 2016)). Moreover, the use of RSFC is not limited to the neuroimaging domain but it also extends to other forms of brain exploration (e.g. EEG, MEG (Muthuraman et al., 2015), fNIRS (Niu & He, 2014)), allowing the detection of functional connectivity measures and other forms of spontaneous brain activity[1]. To show the increasing popularity of RSFC, a manual search of English-language peer-reviewed RSFC studies was conducted on PubMed[2] and showed a total of 22,855 studies published between 2008 and May 2018 which contained the keywords "Resting-state", "Brain networks" and "Default mode network".

A crucial aspect of RSFC is to understand the kind of brain activity that can be detected under resting conditions. In other words, how are resting-state signals produced? The use of fMRI to monitor regional brain activity was proposed by Ogawa et al. (1990) after his observation of the so-called Blood Oxygen Level Dependent (BOLD) response, which was sensitive to the local concentrations of paramagnetic deoxyhemoglobin (i.e., form of hemoglobin without the bound oxygen) in the brain. Cognitive and behavioral tasks increase metabolic demands in the brain and produce changes in blood flow, resulting in decreases of deoxyhemoglobin and thus increases in the BOLD signal (Hillman, 2014). The current consensus is that BOLD signals are more related to postsynaptic neural activity, reflecting the input to a neuronal population as well as its intrinsic processing (Lauritzen, 2005). In the absence of an overt task, the synchronous resting-state fluctuations are thought to represent changes in blood flow and oxygenation due to spontaneous neuronal activity (Craddock et al., 2009) and still, very little active metabolism (Ekstrom, 2010). A recent computational model suggests that resting-state signals arise from dynamic infra-slow fluctuations of the sodium (Na+) and potassium (K+) ion concentrations in the brain (Krishnan et al., 2018). Consequently, these signals are present in low frequencies (0.01 – 0.2 Hz) and are, therefore, highly susceptible to the influence of other fluctuations in the MRI signal.

Perhaps this last situation and the possibility that RSFC might not represent the underlying neural activity in the same way as task-based fMRI, have triggered an intense

---

[1] Regional Homogeneity (ReHo) and (fractional) Amplitude of Low Frequency Fluctuations (fALFF, ALFF) are also neuroimaging methods to detect and quantify spontaneous activity in the resting brain. However, this work is completely focused on functional connectivity measured in the BOLD signal.
[2] https://www.ncbi.nlm.nih.gov/pubmed/  retrieved in 30.05.2018.

debate that goes back to the beginnings of the technique. A primary criticism is the contamination of resting-state frequencies by physiological noise, such as respiratory and cardiac fluctuations (Birn, 2012) and signals coming from head motion (aperiodic or usually respiratory-rate related; (Power et al., 2012)). Additionally, there might be other sources of noise that need to be carefully controlled, such as equipment generated artifacts and signals from white matter (WM) and cerebrospinal fluid (CSF). In an attempt to overcome these limitations and provide a clear and clean characterization of the organized brain activity under rest, the so-called denoising procedures have emerged in the last years (Pruim et al., 2015a; Salimi-Khorshidi et al., 2014). After denoising, measures of functional connectivity can be detected in the resting-state data. To achieve this, several methodologies are available, each one with advantages and pitfalls that we will discuss next. Model-driven approaches, for instance, allow the detection of correlations between the timecourse[3] in a certain seed region (i.e., brain regions, structures) with the timecourses of all other brain voxels. Seed definition is typically based on strong hypotheses regarding the functional connectivity of a small number of brain regions of interest (ROI) or individual voxel locations of interest (Cole et al., 2010). The obvious disadvantage of this method is the need for strong *a priori* assumptions on the expected connectivity patterns. Moreover, anatomical variations and heterogeneity of brain regions can lead to selection bias (Sohn et al., 2015). Similarly, proximity to pulsating vessels, motion, susceptibility and registration artifacts can reduce signal to noise ratio and thus affect the detection of significant differences within individuals and between groups. In contrast, data-driven analyses permit the exploration of organized brain activity without specific prior model definition, but some of them demand a meticulous visual inspection in order to distinguish noise from resting-state signals. Various other methods are currently available for the detection of RSFC (see Lee et al. (2013) for a review). Most of them intend to present resting-state signals in a coherent way, unravelling spatially consistent patterns across multiple brain regions, which are known as "large-scale brain networks", "resting-state networks" or "intrinsic connectivity networks" and are the primary focus of this doctoral thesis. To provide a complete picture of the methodology and theoretical models used in this work, I present core concepts in the following sections.

---

[3] The evolution of a measurement – in this case, the BOLD signal – over the course of the scanning time.

## 1.2.    Intrinsic connectivity networks

Leading researchers in the resting-state field identified coherent slow fluctuations in the BOLD signal grouped in separate anatomically and functionally plausible networks, which are highly consistent across individuals (Damoiseaux et al., 2006; Fox et al., 2005; Smith et al., 2009a; Yeo et al., 2011) and can be also found in other species (Ortiz et al., 2018). These intrinsic connectivity networks (ICN) comprise specific neuro-anatomical systems involved in motor function, visual and auditory processing, executive functioning and self-oriented cognition. Furthermore, these ICN as well as their subnetworks, exhibit close correspondence with task performance activity (Laird et al., 2011), thus confirming that regions similarly modulated by tasks tend to present correlated spontaneous fluctuations even in the absence of stimuli (Fox et al., 2005). In addition, some studies have demonstrated that the anti-correlation between task-negative and task-positive networks exists in both task-based and RSFC, although this dichotomy remains a matter of debate (see Spreng (2012) for a discussion). After the initial identification of a large set of ICN, additional improvements in modelling and/or data acquisition yielded a more fine-grained network characterization across ages and genders, revealing up to 28 ICN in the human brain (Allen et al., 2011). Fig. 1 displays the most used templates of the existing ICN.

Among all the ICN, the default mode network (DMN) is of particular interest. Raichle and colleagues accidentally discovered this network using positron emission tomography (PET), describing it as a group of regions with decreased metabolic activity during attention-demanding cognitive tasks but increased blood flow while participants rest awake with eyes closed (Raichle et al., 2001). It was therefore, considered a "baseline state of the brain". The DMN is present across different species (Ortiz et al., 2018). In humans, it encompasses the ventromedial prefrontal cortex, the posterior cingulate/retrosplenial cortex, the inferior parietal lobule, the lateral temporal cortex, the dorsal medial prefrontal cortex and the hippocampal formation (which includes entorhinal cortex and parahippocampal cortex) (Buckner et al., 2008b)). The DMN is easily detected in the human brain across different developmental stages, although its regions are only sparsely connected between the ages of seven and nine years (Fair et al., 2008) and the undergoing developmental changes are not uniform across all DMN regions (Supekar et al., 2010). The DMN activity is linked to autobiographical memory, mind-wandering, prospective memory, theory of mind, moral decision making and other forms of self-relevant mental exploration (Andrews-Hanna et al., 2010; Buckner et al., 2008b). Recent research described the pivotal role of the DMN in cognitive processes, suggesting that its level

of activation can be associated with successful performance across goal-directed behaviors (Anticevic et al., 2012; Crittenden et al., 2015).

Overall, the study of RSFC organized into dynamic and anticorrelated ICN, has demonstrated high sensitivity and specificity for detecting individual differences associated with a wide range of domains (e.g., cognitive, perceptual, motoric and linguistic) as well as behavioral traits (e.g., empathy, impulsiveness, risky decision making), and states (e.g., anxiety and psychiatric symptoms). Furthermore, ICN show relevant changes in response to new experiences and pharmacological treatments (for a review see Vaidya and Gordon (2013)) and recently, more sophisticated techniques have demonstrated that brain functional connections can be used as a biomarker of diseases and predictors of treatment outcome (Craddock et al., 2009; Drysdale et al., 2017; Emerson et al., 2017). To expand on the above-mentioned body of information, the current thesis investigated changes of ICN associated with 1) phenotypic traits and 2) pharmacological manipulations.
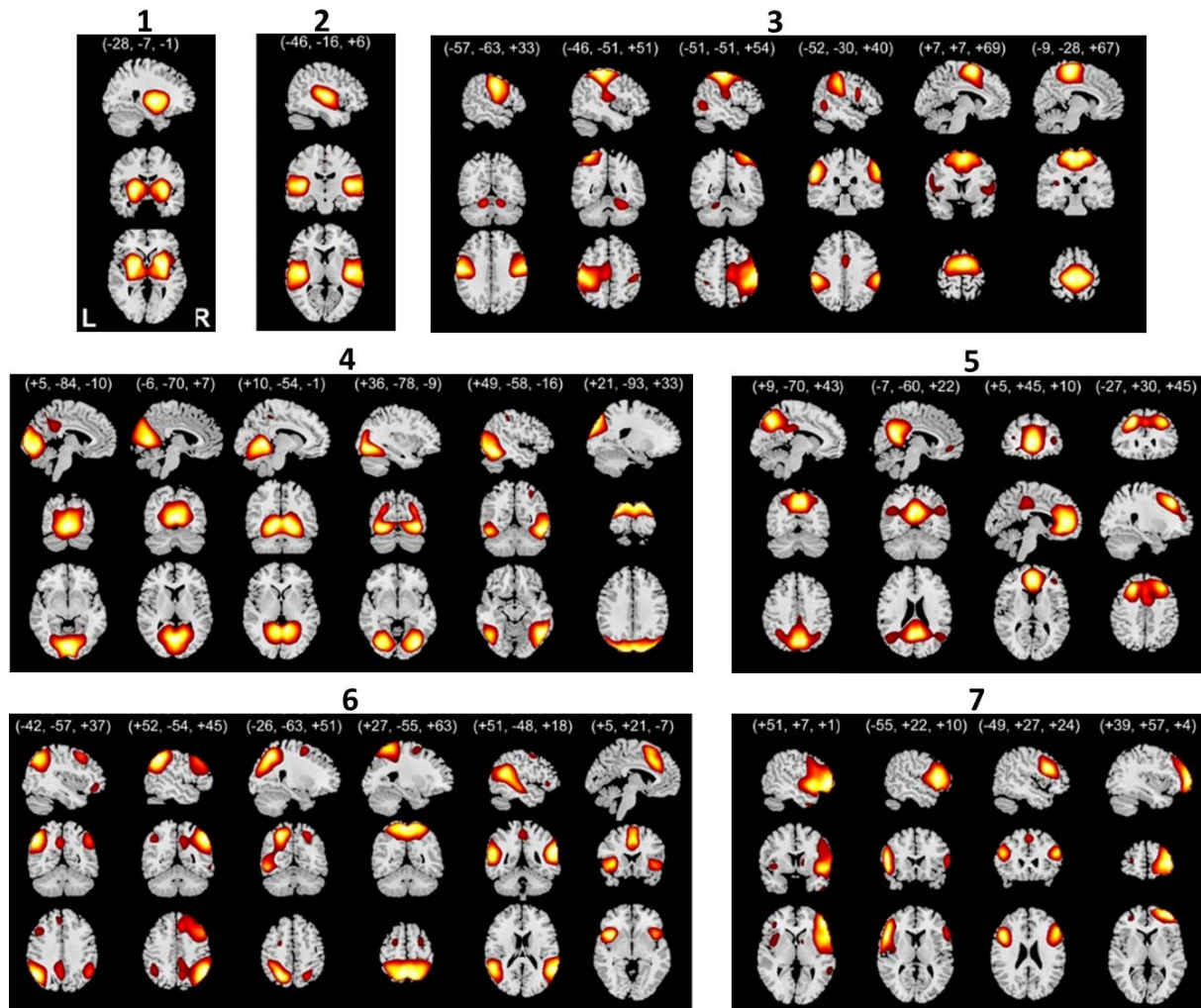
**Figure 1.** Spatial maps of 28 intrinsic connectivity networks detected in a sample of 603 subjects using Independent Component Analysis (ICA). Basal ganglia network = 1, auditory network = 2, sensorimotor networks = 3, visual networks = 4, default-mode networks = 5, attentional networks = 6 and frontal networks = 7. Adapted from Allen et al. (2011).

### 1.2.1. ICN and phenotypic variability

The application of noninvasive techniques for examining brain function helps to investigate the *in vivo* neural correlates of both normal and pathological behaviors. In this specific case, RSFC consistently described distributed networks across different behavioral domains, which might be partially or completely disturbed under pathological conditions (Siegel et al., 2016).

One of the most stable findings is the association between higher executive functions and stronger within-network connectivity in frontoparietal, cognitive control and default mode systems (Hearne et al., 2016). This link supports the idea of interplay between cortical systems involved in top-down control underlying the deployment of cognitive resources in a goal-directed manner. Conversely, the disruption of this apparent harmonic configuration is associated with aberrant decision making such as pathological impulsivity (Shannon et al., 2011), addictions (Ding et al., 2013; Zhu et al., 2015) and risk-seeking behaviors (DeWitt et al., 2014). The disruption of default mode systems is a common finding in these disorders, perhaps characterizing a cognitive style with predominant self-referential thoughts and therefore less participation of networks associated with cognitive control processes (Greicius et al., 2003). Furthermore, a failure in the suppression of default modes of cognition might result in less goal-directed behavior and illustrate the momentary lapses in attention observed, for example, in ADHD and related disorders (Castellanos et al., 2008; Han et al., 2016).

Other phenotypic traits have been associated with the interplay between various ICN. For instance, stronger interactions between DMN, cognitive control and attentional brain systems were described in more creative individuals (Beaty et al., 2015; Beaty et al., 2018; Shi et al., 2018). In a similar manner, personality domains associated with emotional reactivity can be predicted by the interconnectivity between frontal hubs and limbic regions (Adelstein et al., 2011; Hsu et al., 2018), suggesting that vulnerability traits respond to a distinct involvement of emotion-related structures.

Although we remain cautious in deducing causality between brain connectivity and the observed behavior, disentangling how the variability of ICN relates to phenotypic traits may in the first place, help elucidate the functional significance of these networks and in the second place, help us to understand how brain networks integrate information through the complex pattern of neural connections (Smith et al., 2015), and how these connections are associated with normal and disruptive behaviors. In this sense, the relationship between intrinsic brain connectivity and decision-making profiles is of particular relevance, since it may contribute to the prompt implementation of prevention strategies, especially in young and vulnerable populations.

### 1.2.2. ICN and pharmacological manipulations

Traditionally, the effects of pharmacological interventions in the brain were assessed with positron emission tomography (PET). However, the dose-radiation restriction makes this technique unsuitable for repeated crossover studies in humans. Similarly, task-based pharma-fMRI is valuable for hypothesis testing, but it is virtually impossible to standardize in translational or large-scale clinical studies. These facts among others (see Khalili-Mahani et al. (2017) for a review) encouraged the use of pharma-RSFC[4] as a noninvasive technique to examine the neural fluctuations caused by pharmacological interventions. In addition, recent studies highlight the importance of pharma-RSFC as a translational tool, suggesting that it can be used as a potential biomarker for drug development (Smucny et al., 2014).

Pharma-RSFC was used for the first time by Kiviniemi et al. (2000) who showed the effects of thiopental in the spontaneous fluctuations of sensory cortices in anesthetized children. Subsequent studies demonstrated that other anesthetic agents such as propofol (Monti et al., 2013) and chloral hydrate (Wei et al., 2013) affect the overall ICN's activity, indicating that the global state of consciousness and brain metabolism can be detected through pharma-RSFC. This technique was also extended to the investigation of aberrant connectivity among drug addictions (Moeller et al., 2016), suggesting that chronic drug use alters excitatory and inhibitory processes and consequently, modifies the connectivity of networks subserving attentional, emotional, and inhibitory functions (Goldstein & Volkow, 2011). This is particularly important in understanding the behavioral manifestations that might maintain and promote addictive behaviors.

Likewise, modulation of ICN in patients and healthy individuals has been described after dopaminergic (Carbonell et al., 2014; Cole et al., 2013; Esposito et al., 2013; Flodin et al., 2012; Kelly et al., 2009; Vytlacil et al., 2014) and serotonergic agents (Klaassens et al., 2016; Klaassens et al., 2015; McCabe et al., 2011; van de Ven et al., 2013; Zanchi et al., 2016), among others. Changes in brain networks associated with the symptomatic manifestations of several neuropsychiatric disorders are of particular relevance to pharma-RSFC, since they might help to explain the mechanism of action of certain pharmacological interventions. For example, connectivity changes in brain regions with dense serotonergic innervation (i.e. hippocampus, cingulate cortex, precuneus) that belong to the DMN, have

---

[4] Since it is acquired under resting conditions, cerebral blood flow (CBF) is also considered a measure in pharma-RSFC. However, this work is only focused on BOLD activity, measured with RSFC.

been described in mood disorders (Posner et al., 2013; Wang et al., 2015). This may reflect depressive biases toward internal thoughts at the cost of engaging with the external world (Kaiser et al., 2015). Given the implication of the serotonergic system in the regulation of emotion and cognition (Cowen & Browning, 2015; Jenkins et al., 2016), connectivity changes that arise after challenging this system may represent a potential biomarker for the understanding of depressive symptomatology.

In conclusion, pharma-RSFC is still a growing field that should advance with caution. In this vein, the use of robust and unbiased ICN maps is particularly relevant. Different methods for the identification of ICN from resting-state data were already mentioned in the first part of this introduction. However, due to their robustness and interpretability, the neuroimaging community has repeatedly endorsed the application of a computational and statistical technique known as Independent Component Analysis.

## 1.3.    Independent Component Analysis

Independent Component Analysis (ICA) is a highly multivariate method that considers the relationships between all voxels simultaneously and offers continuous improvements regarding its application in brain exploration (i.e., EEG (Raduntz et al., 2015), fMRI artifact removal (Pruim et al., 2015a; Salimi-Khorshidi et al., 2014), brain parcellation (Wu et al., 2015) and task-based activity (Gess et al., 2014)). The theoretical framework of ICA is presented next.

ICA is a method originated from signal processing research which relies on the blind source separation algorithm (BSS; Jutten and Herault (1991)). This algorithm is used to separate simultaneously all the unknown, independent, linear and non-Gaussian sources from a mixing matrix. ICA is typically applied to solve the "cocktail party problem", where this method can effectively separate sources from an auditory scene if this scene is recorded with multiple microphones positioned at different locations in a room. Each microphone yields a different weighted combination of the sources according to their proximity to them and if the number of microphones and sources is the same, simple assumptions about the statistical properties of sources (e.g. non-Gaussianity) are enough to derive the source signals from the mixtures (McDermott, 2009).

ICA was introduced in neuroimaging research by McKeown et al. (1998) who concluded that this method could successfully distinguish between task-related activity and other artifactual components in the fMRI signal based on weak assumptions about their spatial distributions and without a priori assumptions about their time courses (McKeown et al., 1998). Typically, spatial ICA is performed in neuroimaging and considers the data with $n$ voxels measured at $p$ different time points as a $p\ x\ n$ matrix $X$ that can be represented as

$$X = AS$$

where $X$ is the mixture (observed data), $A$ is the mixing matrix (estimated) and $S$ are the sources (estimated). This implies that the sources are maps that are maximally independent, i.e. non-overlapping and the mixing matrix represents activate timecourses of the sources. Then, using the *infomax* algorithm (Bell & Sejnowski, 1995) the sources are estimated by optimizing an *unmixing matrix* $W = A^{-1}$ so that $S = W\ X$ contains mutually independent rows. In this doctoral thesis we used a slightly different ICA approach called Probabilistic ICA (PICA; Beckmann and Smith (2004)). PICA assumes that the time courses of the fMRI data (i.e., p-dimensional vectors of observations) are generated from a set of q (< p) spatial maps (i.e., statistically independent non-Gaussian sources) via a linear and instantaneous mixing process corrupted by additive Gaussian noise η(t):

$$x_i = As_i + \eta_i$$

*where $x_i$ are the individual measurements at voxel location $i$, $s_i$ are the non-Gaussian source signals contained in the data *and $\eta_i$ is the Ga*ussian noise. The noise covariance is isotropic at every voxel location $\eta_i \sim G(0, \sigma^2 \Sigma i)$. Although the similitude with a standard general linear model (GLM) where the matrix is pre-specified prior to model fitting, PICA estimates the mixing matrix $A$ from the data (Beckmann et al., 2005).

ICA offers several advantages for neuroimaging research. For example, it requires no *a priori* hypothesis or model of brain activity because it is a multivariate, data-driven approach. Similarly, when conducted on a group level, ICA facilitates the estimation of robust independent components that capture the temporal and spatial patterns at the individual level. Moreover, in the specific case of PICA, the general characteristics of the noise present in the fMRI signal are considered, yielding more interpretable and robust spatial maps that represent ICN among other signals of noninterest (Beckmann et al., 2005).

Yet some methodological challenges exist. Since this method is also sensitive to detecting structured noise, physiological artifacts and motion can affect the reliability of the component detection (Zuo et al., 2010). In addition, the initial ICA estimation may turn into a highly exploratory process in which the number of components (i.e. ICN + noise) is not given beforehand and should be tested repeatedly, consuming time and computational resources. The final model selection should neither under-fit (i.e., too few components that contain merged networks and noise) nor over-fit (i.e., too many components that contain fragmented networks and noise) the signal. Once the ideal model has been estimated, the data require a fine visual inspection to ensure that well-known ICNs are represented in grey matter with minimum overlap in white matter (white matter signals should ideally be removed before ICA). To achieve this last step, spatial correlations between the resulting components and ICN templates can be performed (Reineberg et al., 2015).

For statistical analyses on a group level, one common approach is to obtain single representations of each ICN. The ICN resulting from ICA are then used as templates in regressions analysis (e.g. back-projection (Calhoun et al., 2001), dual regression (Beckmann et al., 2009)). The work reported in this doctoral thesis used a dual regression approach, which is a multivariate regression analysis to identify subject-specific networks and their related time courses that capture within or between-group differences. Another proposed approach is to use predefined networks as templates (e.g. maps obtained from larger groups and publicly available) and directly proceed with the dual regression analysis. This way, higher variability which may bias the group ICN, can be avoided at the individual level.

All in all, ICA has emerged as a powerful tool for investigating organized spontaneous brain activity contained in ICN. Based on the notion that RSFC is susceptible to inter-individual differences and pharmacological challenges, this work joins a large field of ongoing research aiming to demonstrate the validity and robustness of this technique for uncovering the restless activity of the brain.

## 1.4. Summary: research objectives and study hypotheses

### 1.4.1. Study 1

Based on the postulated phenotypic variability of RSFC across behavioral domains, this study investigated the relationship between large-scale ICN and value-based decision-making domains (i.e. delay-aversion, risk seeking for losses, risk seeking for gains, risk-aversion) in a large cohort of young individuals.

**Research questions:**

1. Do these ICN have a different connectivity strength in more impulsive and risk-seeking young individuals?

2. Is the connectivity between the ICN and other brain regions different in more impulsive and risk-seeking young individuals, as proposed by Cox et al. (2010) and DeWitt et al. (2014)?

3. Are *risk seeking for losses* and *risk averse* behaviors associated with different intrinsic connectivity patterns in young individuals?

### 1.4.2. Study 2:

Based on the serotonergic modulation of the default mode network (DMN) and the implication of this network in depressive symptomatology, this study examined changes in the DMN following two tryptophan interventions and a control condition to manipulate brain serotonin synthesis.

**Research questions:**

1. How do different brain serotonin levels influence the DMN functional connectivity?

2. Are the DMN changes following serotonergic manipulation, similar to the connectivity patterns displayed by depressed patients?

3. Are the effects of our pharmacological challenge similar to the effects reported on the DMN after other serotonergic agents (i.e. SSRI (Klaassens et al., 2015; van de Ven et al., 2013), SNRI (Posner et al., 2013)?

4. Are the DMN connectivity changes following serotonergic manipulations related to changes in mood, anxiety, impulsive choice or sleepiness ratings?

# CHAPTER 2

**2. STUDY I:  Risk seeking for losses modulates the functional connectivity of the default mode and left frontoparietal networks in young males**

## 2.1. Abstract

Value-based decision making (VBDM) is a principle that states that humans and other species adapt their behavior according to the dynamic subjective values of the chosen or unchosen options. The neural bases of this process have been extensively investigated using task-based fMRI and lesion studies. However, the growing field of resting-state functional connectivity (RSFC) may shed light on the organization and function of brain connections across different decision-making domains. With this aim, we used independent component analysis to study the brain network dynamics in a large cohort of young males (N = 145) and the relationship of these dynamics with VBDM. Participants completed a battery of behavioral tests that evaluated delay aversion, risk seeking for losses, risk aversion for gains, and loss aversion, followed by an RSFC scan session. We identified a set of large-scale brain networks and conducted our analysis only on the default mode network (DMN) and networks comprising cognitive control, appetitive-driven, and reward-processing regions. Higher risk seeking for losses was associated with increased connectivity between medial temporal regions, frontal regions, and the DMN. Higher risk seeking for losses was also associated with increased coupling between the left frontoparietal network and occipital cortices. These associations illustrate the participation of brain regions involved in prospective thinking, affective decision making, and visual processing in participants who are greater risk-seekers, and they demonstrate the sensitivity of RSFC to detect brain connectivity differences associated with distinct VBDM parameters.

**Keywords:**

*Value-based decision making*
*Intrinsic connectivity networks*
*Probabilistic discounting for losses*
*Default mode network*
*Frontoparietal network*

## 2.2.    Introduction

An extensive body of literature has already investigated the influence of several personality traits and psychological constructs on value-based decision-making (VBDM) during adolescence and early adulthood (Franken et al., 2008; Romer, 2010; Zermatten et al., 2005). However, a limited scope still exists, because the prior research usually focused on single constructs at a time. Beyond these earlier behavioral studies, this investigation offers a complementary neuroimaging approach for understanding the neural underpinnings of an array of VBDM components (i.e., delay aversion, risk seeking/risk aversion, and loss aversion) in healthy young males.

Delay aversion is often taken as an indicator of impulsivity and is usually assessed with delay-discounting tasks in experimental environments (Ainslie, 1975). Individuals may benefit from impulsive behavior because it allows them to take advantage of unexpected opportunities when quickly exploiting their options (Dickman, 1990). However, high degrees of impulsivity are related to a broad range of maladaptive behaviors, principally in young individuals (Story et al., 2014). In a similar manner, risk seeking has been pointed out as a predisposing factor for the development of addictive disorders and delinquent behavior during adolescence (Blum & Nelson-Mmari, 2004; Burnett et al., 2010; Steinberg, 2008), especially in male participants (Ball et al., 1984). Conversely, high risk aversion (taken as the other extreme of the risk spectrum), as well as high loss aversion (Kahneman & Tversky, 1979), might indicate a negative learning bias that increases the risk of depression and anxiety disorders (Smoski et al., 2008).

On the neural level, task-based fMRI experiments and lesion studies have shown the brain circuitry underlying some of the behaviors mentioned above: Frontostriatal regions (i.e. medial prefrontal cortex, ventral striatum) are implicated in valuation processes and reinforcement learning (Bartra et al., 2013; Peters & Buchel, 2011; Ripke et al., 2012; Rushworth et al., 2011), whereas the so-called cognitive control network (i.e. posterior parietal cortex, lateral prefrontal cortex, anterior insula, and anterior cingulate cortex) was associated with the decision phase during intertemporal and probabilistic choices (Marco-Pallares et al., 2010; McClure et al., 2004; Ripke et al., 2015; Ripke et al., 2012; Weber & Huettel, 2008). Additionally, developmental neuroimaging studies have postulated that stronger activation of regions involved in reward processing (e.g. nucleus accumbens) during adolescence encourages sensation seeking and risk taking at these ages (Barkley-Levenson & Galvan, 2014; Braams et al., 2015; Galvan et al., 2007).

24

A complementary investigation of brain networks can be achieved through resting-state functional connectivity (RSFC), a robust technique for exploring low-frequency fluctuations (~ 0.01 – 0.1 Hz) in the BOLD signal (Biswal et al., 1995). Resting state fluctuations are coherently organized into intrinsic connectivity networks (ICN) that are believed to recapitulate task-based/stimulus activity (Mennes et al., 2010; Smith et al., 2009b) and exhibit variations according to the different phenotypic characteristics of an individual (Vaidya & Gordon, 2013). These networks can be investigated using independent component analysis  (ICA; Beckmann & Smith, 2004), a reliable method that allows the separation of ICNs from artifactual signals (Cole et al., 2010) and thus supports the exploration of organized neural activity. The possibility that these ICNs differ across distinct VBDM styles has already promoted study of the relationship between various VBDM constructs and RSFC in young and vulnerable populations (Cservenka et al., 2014; Weissman et al., 2015; Whelan et al., 2012). However, further investigations analyzing several VBDM components in a single study will increase our understanding of the neural bases of these behaviors.

Recent insights into the resting-state circuitries that may characterize impulsive decision-making have described weaker connectivity between regulatory (frontal) and appetitive- drive (limbic) regions (Davis et al., 2013). Additionally, hyperconnectivity between the DMN and motor planning regions was also reported in the same group of participants (Shannon et al., 2011), suggesting that higher activity at rest of limbic and motor regions may predispose young individuals to impulsive decision-making. Similarly, hyperconnectivity between subcortical limbic structures (i.e. nucleus accumbens, amygdala) and middle frontal cortices may underlie the expression of risky behaviors in adolescents (DeWitt et al., 2014). On the other hand, risk-averse decision-making seems to follow the same activation pattern in both task-based and resting-state fMRI, with participation of a brain circuit comprising the right inferior frontal gyrus and insular cortex (Christopoulos et al., 2009; Cox et al., 2010; Preuschoff et al., 2008). Although these findings indicate that the functional brain architecture may accurately reflect individual differences in VBDM, studies with larger samples of healthy participants are still necessary in order to observe the neural dynamics that may underlie risky and impulsive choices at young ages. Furthermore, the relation between risky behaviors and RSFC has only been investigated in the gain domain (i.e., risk seeking/risk aversion for gains), but the distinction between gains and losses has not been reported thus far.

In the present study, we examined RSFC and its relation to VBDM, expressed through four constructs (delay aversion, risk aversion for gains, risk seeking for losses and loss

aversion) in a large cohort of young males. We hypothesized that the basal ganglia and default mode networks would exhibit higher functional connectivity in more delay-averse and risk-seeking participants, illustrating more reward-driven traits and therefore weaker functional connectivity in the cognitive-control and executive networks. Finally, we explored the relationship between brain functional networks, risk seeking for losses, and loss aversion, since existing studies have described the engagement of single brain structures, but the functional dynamics under rest have not yet been studied.

## 2.3.    Materials and Methods

The study protocol was approved by the local ethics committee of Charité Universitätsmedizin Berlin and Technische Universität Dresden and was in accordance with national legislation and the Declaration of Helsinki. All participants provided written informed consent and received monetary compensation.

### 2.3.1.    Participants

This study included data from 145, 18-year-old, right-handed, healthy males, selected from a total sample of 201 individuals who took part in the ongoing longitudinal fMRI study "Learning dysfunctions in young adults as predictors for the development of alcohol use disorders" (LeAD, www.lead-studie.de; clinical trial number: NCT01744834) within the research group "Learning and habituation as predictors of the development and maintenance of alcoholism" funded by the Deutsche Forschungsgemeinschaft (DFG).  In this study, we used the sample already reported by Bernhardt et al. (2017) with the addition of two participants who were abstinent from alcohol and therefore not included in other studies from this research group (for details, see the description in Supplementary Material Fig. S1). All participants were recruited in Berlin and Dresden through their respective residents' registration offices and were screened in order to exclude current or previous history of neurological or psychiatric diseases, drug abuse or dependence (except for nicotine dependence and alcohol abuse) and MRI incompatible conditions.

### 2.3.2. Value-based decision-making assessment

In the first session, participants completed an extensive behavioral and clinical assessment that included the Value-based decision-making battery (VBDM; see Fig. 2). This set of tasks employs a Bayesian learning scheme to estimate the delay-discounting rate as well as the probability discounting rates for gains and losses, and loss aversion.
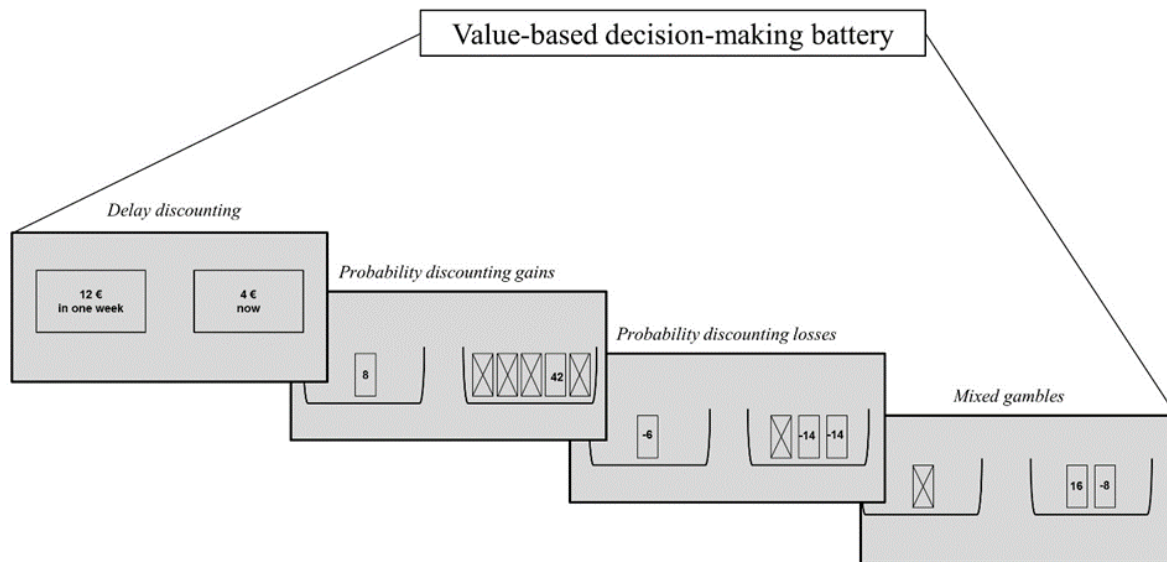


**Figure 2**. Value-based decision-making battery with trial examples for each task. During all tasks, offers are randomly assigned to presentation on the left or the right side of the screen. There was no time limit for the selection in a given trial and no feedback after the choice. The selected choices were indicated within a red frame before presenting the next offer. Participants were informed that they would be paid based on a randomly selected trial that they chose in each task. Crossed out boxes represent the odds against winning or losing in the probabilistic tasks. In mixed gambles task the crossed out box represents the option to reject the gamble (Pooseh et al., 2017).

Delay aversion was assessed with a delay discounting (DD) task with 30 trials, in which participants needed to choose between receiving a smaller immediate amount of money or a greater delayed one (e.g., €2  now or €8  in one week). Monetary rewards ranged from €0.30 to €10. The evaluation of the offers is best described by a hyperbolic function (Mazur, 1988; Odum, 2011)

$$V = A/(1 + kd),$$

where V represents the subjective value of the amount A after a delay D in days (available delays: 3, 7, 14, 31, 61, 180 and 365 days) and k is a free parameter representing the discount rate. Larger k values represent preference for immediate amounts and therefore higher delay aversion.

The second and third tasks assessed risk aversion for gains and risk seeking for losses, using probability discounting for gains and losses, respectively (PDG and PDL; both with 30 trials), where participants needed to choose between a sure amount that they could win or lose and the probability of winning/losing a larger amount of money (e.g. 75% probability of winning €5  or winning €2  for sure, or a 50% probability of losing €8  or losing €3  for sure). The probability values were set to 2/3, 1/2, 1/3, 1/4, and 1/5. The amounts ranged from €0.30 to €10 for PDG and -0.30 to -10€ in PDL.  Probability discounting can also be well described by a hyperbolic function (Green et al., 1999; Rachlin et al., 1991)

$$V = \frac{A}{1 + k\theta},$$

where V is the subjective value of a probabilistic amount A, k is a parameter that reflects the individual discounting rate due to the probability of the reward, and θ represents the odds against receiving the probabilistic amount $(\theta = [1 - p]/p)$  where p is the probability of receipt. In the probability discounting for gains, risk-averse behavior is defined as the preference for the certain amount over the probabilistic one, reflected by larger k values. On the other hand, probability discounting for losses produces larger k values when participants prefer the probabilistic offer over the certain one, therefore, exhibiting a more risk-seeking behavior (Shead & Hodgins, 2009).

The final task measuring loss aversion presented mixed gambles (MG; 40 trials), in which participants received a credit of €10 at the beginning of the game and then needed to

decide whether to accept or reject an offer with a 50/50 chance of either gaining one amount of money or losing another amount (e.g., refusing to gamble or accepting a gamble that offered either winning €15 or losing €8). The amounts ranged from €1 to €40 for gains and -€5 to -€20 for losses. The value function here was given by

$$V = \frac{1}{2(G - \lambda L)},$$

where V is the expected value of the gamble. The coefficient 1/2 expresses a 50/50 chance of gaining or losing, G and L are the amounts of gains and losses, respectively, and $\lambda$ is a measure of behavioral loss aversion that can be computed as the ratio of the contributions of loss to gain magnitude in the participant's decisions. Larger $\lambda$ values indicate higher loss aversion and are produced when participants reject the gamble because they perceived high differences between gains and losses (Tom et al., 2007).

In all tasks, the likelihood of choosing between the two offers followed a softmax probability function $P(a1 \mid k, \beta) = 1/(1 + exp\,(\beta(V2 - V1)))$, where V1 and V2 are the subjective values of the offers and $\beta$ > 0 serves as a consistency parameter such that its large values correspond to a high probability of taking the most valuable action. The algorithm started from liberal prior distributions on the parameters and, after observing a choice at each trial, updates the belief about the parameters using the Bayes's rule $P(k, \beta | choice) \propto P(choice | k, \beta) P(k, \beta)$. The procedure continued for 30 (40 in Mixed Gambles) trials to reach a stable estimation. The estimates at the final trial were considered the best-fitting parameters for a participant. Further information is provided in Supplementary Material 2; details regarding the mathematical framework can be found in Pooseh et al. (2017); and application of the battery in a clinical cohort is reported in Bernhardt et al. (2017).

Summary statistics and pairwise correlations were calculated using SPSS 22.0 (IBM-SPSS, Chicago, IL, USA) on the nonlogarithmic VBDM scores. To be used as regressors in the resting-state analysis (see the Single Network Analysis section), the resulting main discounting parameters (k) were log-transformed in order to approximate them to a normal distribution. The mixed gambles parameter ($\lambda$) was normally distributed, therefore no transformation was necessary. To maximize the availability of the data, multiple imputation (MI; (Little & Smith, 1987) was used to complete missing completely at random (MCAR) VBDM scores of nine participants who had only one incomplete subtest

29

and Winsorization (Dixon, 1960) was used to change one extreme score (See the Results section). These processes did not change the descriptive statistics of the main scores.

### 2.3.3. MR data acquisition

The scanning protocols were identical in both study centers. The scanning session took place during a second appointment. Six-minute resting state fMRI scans were acquired on a 3 T whole-body Magnetom Trio Tim MRI Scanner (Siemens Medical, Erlangen, Germany) equipped with a 12-channel head coil using a single-shot gradientecho planar imaging (EPI) sequence with a repetition time (TR) of 2.41s, an echo time (TE) of 25 ms, a flip angle of 80°, field of view of 192 × 192 mm, matrix size of 64 x 64 and voxel size of 3 mm x 3 mm x 2 mm. A total of 148 resting-state volumes were acquired, each consisting of 42 transversal slices (2 mm thick, 1 mm gap), tilted axially parallel to the anterior-posterior commissural line. For registration purposes, a T1-weighted high-resolution anatomic scan of the magnetization-prepared rapid gradient echo (MPRAGE) was acquired (TR = 1.90 s, TE = of 2.52 ms, TI = 1100 ms, flip angle of 9°, FOV = 256 × 224 mm2, 192 slices, 1 mm x 1 mm x 1 mm voxel size, slice thickness of 1 mm and no gap). Participants were given earplugs to protect hearing and foam pads to minimize head movement. They were instructed not to think about anything in particular and to lie as still as possible with their eyes closed.

### 2.3.4. Image preprocessing

The resting-state fMRI data were preprocessed using the Functional Magnetic Resonance Imaging of the Brain (FMRIB) Software Library (FSL Version 5.0.8, www.fmrib.ox.ac.uk/fsl; (Jenkinson et al., 2012)). Because movement has a great impact on functional connectivity, DVARS (with D referring to temporal derivative of the time courses and VARS referring to the RMS variance over voxels) and framewise displacement (FD; Power et al. (2012)) were calculated on the resting state data prior to any other preprocessing step with the tool fsl_motion_outliers. Participants whose sequences showed more than 10% of volumes over the 0.5 % Δ BOLD for DVARS and/or over 0.5 mm for FD were excluded from the subsequent analysis (see Supplementary Material 1).

Preprocessing steps included motion correction with MCFLIRT, brain extraction of the EPI data with BET, spatial smoothing with a Gaussian kernel of full width at half maximum of 5mm and high-pass temporal filter at 100s. Registration parameters were derived from nonsmoothed and nonfiltered data. For registration, the T1-weighted images were registered to a common stereotaxic space (MNI152; 2 mm x 2 mm x 2 mm spatial resolution) using a 12 degree-of-freedom nonlinear registration implemented in FNIRT (warp resolution: 10 mm) and then, each participant's functional dataset was registered to their corresponding T1-weighted image using a 6 degree-of-freedom linear affine transformation with FLIRT. After this process, all images were visually inspected to ensure the accuracy of the registration. Finally, FD measures were calculated again after preprocessing to ensure that the existing volumes with high motion were adequately handled by the motion correction algorithm. A more stringent cut-off was used with these data (FD ≥ .2 mm). One participant who exhibited more than 10% of volumes over this threshold was discarded from the high-level analysis.

### 2.3.5. Generation of intrinsic connectivity networks

We used group probabilistic independent component analysis as implemented in MELODIC Version 3.14 (Beckmann & Smith, 2004) to generate a set of spatially independent components (IC). The first stage of this group process uses principal component analysis (PCA) to temporally demean and concatenate all datasets, treating them as if they were a huge single dataset. However, this stage becomes excessively computationally demanding as the number of time points and participants increases. For this reason, we used the recently implemented MIGP algorithm (MELODIC´s Incremental Group-PCA; (Smith et al., 2014)) which has been shown to be more accurate than the current approaches used for multisubject resting-state studies with the advantage of having very low computing memory requirements. Following the process, the data were whitened and projected into a 50 dimensional subspace, variance was normalized and finally the estimated intensity maps were divided by the standard deviation of the residual noise and thresholded by fitting a Gaussian/gamma mixture model to the distribution of voxel intensities within spatial maps and controlling the local false-discovery rate (FDR) at $p < .5$.

### 2.3.6. Single-network analyses

It should be noted that there is no current consensus about the ideal number of ICs, although the existing literature reports that higher dimensionalities produce a better brain parcellation and subdivision of networks, whereas low-order models are useful for identifying large-scale brain networks (Ray et al., 2013). Following the suggestion of Szewczyk-Krolikowski et al. (2014), a model order of 50 ICs (explaining 65% of the total variance) was found optimal to detect the basal ganglia among other 13 large-scale brain networks. Higher dimensionalities were also explored, (70 ICs, 89 ICs) without any significant improvement.

To identify participant-specific spatial maps and associated time courses of the 14 ICNs, we performed a dual regression approach (Beckmann et al., 2009; Filippini et al., 2009). During the first stage of this regression, the group-level spatial maps representing the identified 14 ICNs were linearly regressed against the functional data of each participant, resulting in individual time series for every ICN (spatial regression). In the second stage, these time series were normalized and regressed against the resting-state datasets of the corresponding participant (temporal regression) to estimate subject-specific voxel-to-network spatial maps of every network. To remove sources of spurious variance that might affect estimation of the participants' ICNs, the six individual motion parameters obtained during motion correction and time courses of white matter and CSF were added as nuisance regressors during this stage (Cole et al., 2013; Klumpers et al., 2012). To extract these last time courses, individual white matter and CSF masks were generated from the structural images and transformed into a participant-specific functional space before extracting their corresponding time series (see Supplementary Material 3).

This dual regression approach differs from other group-ICA methodologies (e.g. "back-projection"; Calhoun et al. (2001)) in the way temporal and spatial dynamics at the subject level are estimated. In this method, the estimated spatial maps do not depend on the initial participant-specific major eigenspaces (PCA) and therefore, may lie outside the network's boundaries (Beckmann et al., 2009). The regression coefficients contained in the resulting spatial maps from dual regression represent the weighted voxels associated with specific signal variations for a specific network. The strength of the voxel-to-network connectivity is given by the value of these coefficients (Cole et al., 2013; Klaassens et al., 2016).

Six ICNs were chosen as networks of interest due to their previously reported implication in decision making and related processes (frontal, default mode, left and right frontoparietal, cingulo-opercular and basal ganglia networks (Davis et al., 2013; Shannon et al., 2011; Tom et al., 2007; Zhou et al., 2014)). The resulting participant-specific maps of every network were concatenated across participants and saved in 4D files. The six networks of interest were tested voxel-wise for associations with the behavioral scores, using a nonparametric test based on criteria of exchangeability (10,000 permutations as implemented in FSL–Randomise; (Nichols & Holmes, 2002)) that included one GLM for each network with all four VBDM scores (demeaned log k and λ), a dichotomous variable to control for scan site and mean DVARS measures to account for BOLD changes associated with motion that could not be removed by regression of the motion parameters. To assess the potential collinearity between the regressors of the model, we calculated the variance inflation factor (VIF). The highest VIF score (1.09) indicated that our model does not have a collinearity problem (VIF threshold = 5; (Mumford et al., 2015). A gray-matter mask was used during permutation testing. The results were identified using threshold-free cluster enhancement (TFCE; (Smith & Nichols, 2009)). A multiple-comparison correction was carried out voxel-wise using FDR at a nominal significance level of q < .05 using the fdr command in FSL. This procedure yielded an adjusted threshold of p < .0077. Further correction was carried out to account for the 24 test performed (four VBDM scores and six ICN), setting the significant p < .0003. As we previously mentioned, our results were not restricted to the networks' boundaries, thus brain regions could exhibit significant changes in connectivity either inside or outside a given network (Reineberg et al., 2015). After permutation testing, the resulting significant regions indicated that the strength of the coupling between these regions and the tested network was associated with a given VBDM score.

## 2.4.    Results

### 2.4.1.  Behavioral results

Summary statistics of the obtained VBDM scores, pairwise correlations, and the numbers of imputed and Winsorized scores are presented in Table 1. The resulting discounting parameters (k) for Delay Discounting are comparable to those observed previously in healthy individuals which are typically lower than in those with substance use disorders (Amlung et al., 2017). Further analyses showed that the participants of the

present study were more risk-averse for gains (Probability Discounting for Gains), more risk-seeking for losses (Probability Discounting for Losses), and more loss-averse (Mixed Gambles) than a sample of alcohol-dependent patients (Bernhardt et al., 2017). Negative correlations between Probability Discounting for Losses and Delay Discounting denoted that more risk- seeking (for losses) participants were more patient. Similarly, a negative correlation between Probability Discounting for Losses and Mixed Gambles indicated that more risk-seeking (for losses) participants were not influenced by the difference between gain and loss in making the gamble.

We found no significant differences between the VBDM scores from the two research sites (see Supplementary material, Table S1). Additionally, we controlled for possible associations between VBDM scores and motion parameters, since a positive correlation between impulsivity and in-scanner motion has been reported in resting-state studies (Kong et al., 2014). The Spearman's rank correlations resulting from these analyses were no higher than .06 (see the supplementary material, Table S2).

**Table 1.** Descriptive statistics and correlations between the VBDM scores

| | Median | IQR | $PDG_k$ | | $PDL_k$ | | $MG_\lambda$ | |
|---|---|---|---|---|---|---|---|---|
| | | | $\rho$ | $p$ | $\rho$ | $p$ | $\rho$ | $p$ |
| $DD_k$ | 0.01 | 0.05 | $-0.01$ | 0.88 | $-0.19$ | 0.01 | 0.01 | 0.85 |
| $PDG_k$ | 0.72 | 0.59 | - | - | 0.03 | 0.68 | 0.13 | 0.11 |
| $PDL_k$ | 0.55 | 0.70 | - | - | - | - | $-0.23$ | $<0.01$ |
| $MG_\lambda$ | 1.40 | 1.22 | - | - | - | - | - | - |

N = 145;

IQR: Interquartile range; $\rho$: Spearman's rank correlation coefficient

DD: Delay Discounting; PDG: Probability Discounting Gains; PDL: Probability Discounting Losses; MG: Mixed Gambles

Imputed and winsorized scores: DD (2), PDG (3), PDL (1/1), MG (3)

### 2.4.2. Intrinsic connectivity network selection

From the 50 initially estimated ICs, nine were identified as large-scale brain networks according to the templates from Smith et al. (2009b), using a cross-correlation analysis implemented with the fslcc tool (see the supplementary material, Table S3). Five other ICs were also considered as plausible ICNs after visual inspection of the peak activations, inspection of plots of the time series obtained from the first stage of the dual regression and comparison with other existing templates (Laird et al., 2011; Ray et al., 2013). The remaining 36 components were deemed movement artifacts, scanner drifts, and other activations of noninterest (i.e., white matter, CSF). Spatial maps of the 14 ICNs are described in Table 2 and presented in Fig. 3.

**Table 2:** Intrinsic connectivity networks (ICN) identified in a sample of N = 145 participants.

| % Explained variance | ICN name | Regions |
|---|---|---|
| **Networks of interest** | | |
| 1.89 | Basal ganglia | Thalamus, putamen and pallidum. |
| 2.01 | Left fronto-parietal | Left middle frontal gyrus, right and left inferior frontal gyrus, left inferior parietal lobule, left middle temporal gyrus and left angular gyrus. |
| 2.10 | Right fronto-parietal | Right IFG, right MFG, right inferior parietal lobule, right middle temporal gyrus, right and left angular gyrus. |
| 2.13 | Frontal | Frontal pole, paracingulate gyrus. |
| 2.20 | Cingulo-opercular | Anterior insula, dorsal anterior cingular cortex, supramarginal gyrus, dorsolateral prefrontal cortex and thalamus. |
| 2.22 | Default mode | Ventromedial PFC, precuneus, posterior cingulate cortex (PCC) and angular gyrus. |
| **Other networks** | | |
| 2.10 | Fronto-temporal | Inferior frontal gyrus, superior temporal gyrus. |
| 2.13 | Cerebellar | Cerebellum. |
| 2.22 | Medial visual | Occipital pole, lingual gyrus. |
| 2.33 | Lateral visual | Lateral occipital cortex and temporo-occipital cortex. |
| 2.35 | High visual | Cuneal cortex. |
| 2.36 | Dorsal attention | Lateral occipital cortex, superior parietal lobule and frontal eye fields (FEF). |
| 2.48 | Lateral sensorimotor | Post-central gyrus, supplementary motor area. |
| 2.54 | Sensorimotor | Supplementary motor area, sensorimotor cortex and secondary sensorimotor cortex. |

Networks are listed according to the percentage of explained variance. Regions forming a given ICN were identified using the Probabilistic Harvard-Oxford Cortical and Subcortical Structural Atlases.
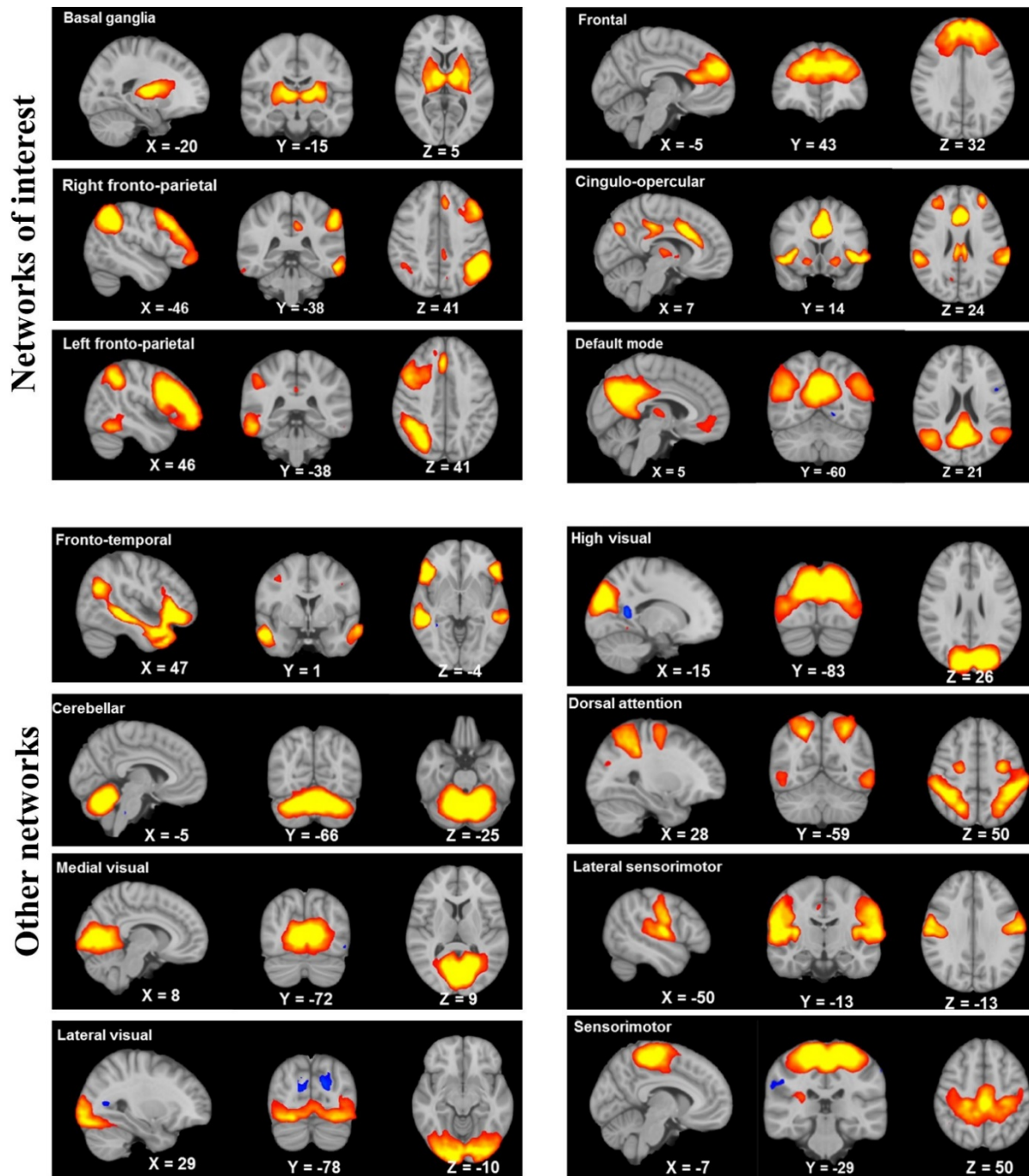
**Figure 3**. Spatial maps of the 14 ICNs listed in Table 2, displayed in neurological orientation (right = right) and thresholded at *z* ≥ 4. The z-scoring was carried out on the group ICs by dividing the voxel-wise estimated spatial maps by the standard deviation of the residual noise (Beckmann & Smith, 2004). The networks of interest are depicted at the top of the image. Brain areas were identified using the Harvard-Oxford Cortical and Subcortical Structural Atlases.

### 2.4.3.  VBDM scores and single network variations

We found that increased connectivity between the DMN and the bilateral parahippocampal gyri was associated with higher risk seeking for losses, as measured with the Probability Discounting for Losses task. The same scores were associated with higher connectivity between the DMN and both the right frontal pole and small clusters in the right inferior temporal gyrus and left orbitofrontal cortex (Fig. 4A, all *ps* < .0003, FDR-corrected). Moreover, increased connectivity between the left frontoparietal network and clusters located in the left occipital pole/cuneus and left lateral occipital cortex was also associated with higher Probability Discounting for Losses scores (Fig. 4B, all *ps* < .0003, FDR-corrected). The complete results are presented in Table 3.

## A. Connectivity with the default mode network
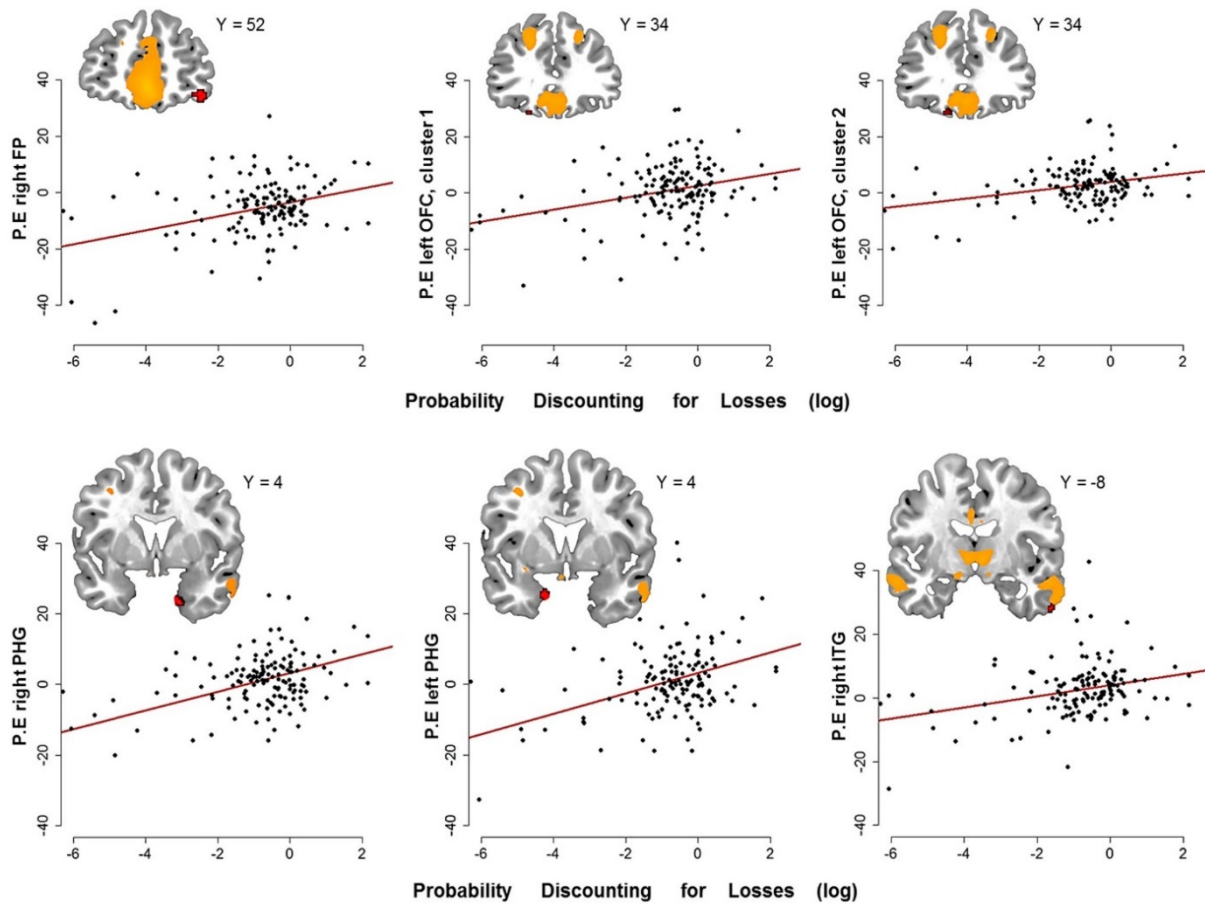


## B. Connectivity with the left fronto-parietal network
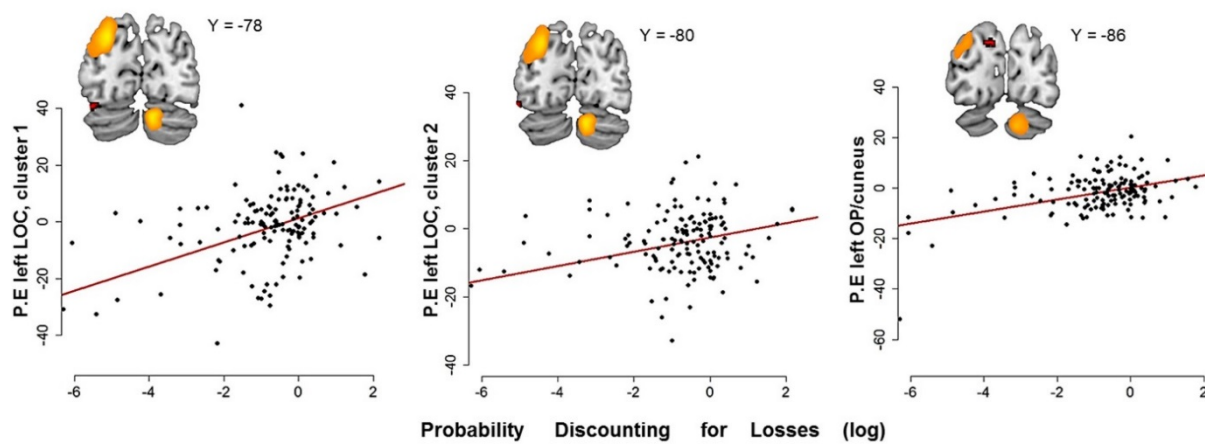
**Figure 4.** Higher risk seeking for losses (measured with the *probability discounting for losses* task) was associated with increased functional connectivity between (A) the default mode network (DMN) and bilateral parahippocampal gyri (PHG), right frontal pole (FP), right inferior temporal gyrus (ITG), and left orbitofrontal cortex (OFC); and (B) the left frontoparietal network (FPN) and left occipital pole/cuneus, and lateral occipital cortex (LOC). In all brain figures, the DMN and the left FPN regions are displayed in orange in the online version of the figure, and the significant clusters are shown in red. The scatter plots below the brain figures show the PDL scores (in a logarithmic scale on the *x*-axis) and the parameter estimates ("P.E") of the significant clusters extracted from the participant-specific DMN and left FPN (in arbitrary units on the *y*-axis). The brain figures are displayed from anterior to posterior coronal plane in neurological orientation, with MNI coordinates (Y) next to each brain figure. Significant clusters are displayed at *p < .0003*, false discovery rate (FDR) corrected at *q < .05* and adjusted for 24 tests. Brain areas were identified using the Harvard-Oxford Cortical and Subcortical Structural Atlases.

**Table 3:** Higher risk seeking for losses (*Probability Discounting for Losses* task) was associated with increased functional connectivity between two ICN and the following brain regions:

| ICN | Region | N° voxels | MNI coordinates (COG) | | | *t |
|---|---|---|---|---|---|---|
| | | | X | Y | Z | |
| Default mode | Right PHG | 148 | 20 | 4 | -32 | 3.99 |
| | Left PHG | 98 | -18 | 2 | -32 | 4.20 |
| | Right FP | 36 | 40 | 52 | -14 | 5.14 |
| | Right ITG | 9 | 60 | -8 | -38 | 3.54 |
| | Left OFC | 7 | -20 | 34 | -22 | 3.80 |
| | Left OFC | 6 | -14 | 34 | -22 | 4.03 |
| Left fronto-parietal | Left OP/cuneus | 46 | -8 | -90 | 28 | 5.27 |
| | Left LOC | 16 | -38 | -78 | -20 | 4.95 |
| | Left LOC | 9 | -48 | -80 | -14 | 3.63 |

PHG, parahippocampal gyrus; FP, frontal pole; ITG, inferior temporal gyrus; OFC, orbitofrontal cortex; OP, occipital pole; LOC, lateral occipital cortex; COG, center of gravity. MNI coordinates and regions were identified using the Probabilistic Harvard Oxford Cortical and Subcortical Structural Atlases. *Uncorrected *t* statistics within regions. All significant clusters correspond to an adjusted p-value of p < .0003, computed using thr false discovery rate (FDR) at *q < .05* and corrected for 24 tests (six networks and four VBDM scores; original threshold: *p < .0077*).

No significant associations were found neither for the remaining VBDM scores (delay discounting, probability discounting for gains, and mixed gambles) nor for the other selected ICN (frontal, basal ganglia, cingulo-opercular, or right frontoparietal).

## 2.5. Discussion

To our knowledge, this is the first study to investigate resting-state functional connectivity and its relation to a set of different value-based decision-making parameters. Our findings show that individuals who were more risk seeking for losses—that is, who prefer a larger but only probable loss to a smaller but certain loss (as measured with the *probability discounting for losses* task)— exhibited increased connectivity between the DMN and bilateral hippocampal gyri and frontal regions. Higher risk seeking for losses was also associated with greater connectivity between the left frontoparietal network, the occipital pole, and lateral occipital regions.

The "medial temporal lobe subsystem" of the DMN has been implicated in mnemonic scene construction (Andrews-Hanna et al., 2010), as well as in the integration of autobiographical memories into current processing (Buckner et al., 2008b). Along this line, research in economic decision-making has already delineated a model involving the frontotemporal axis of the DMN as a binding neural pathway that connects internal memories with prospective actions (Buckner et al., 2008b) and that might subserve self-related simulations of future scenarios in which, for example, potential losses did not occur. Although the notion is speculative, the participation of mnemonic processes in risk-seeking (for losses) individuals may also be supported by increased connectivity between the DMN and the bilateral parahippocampal gyri (PHG), brain structures that are highly involved in contextual associations and episodic memory. In addition, the PHG shows several anatomical and functional connections with anterior and posterior hubs of the DMN (Aminoff et al., 2013). Even when memory and decision making are studied independently, there is unquestionable integration of both functions for decomposing the representations of past experiences and integrating them to future events, aiming to produce adaptive behaviors (Murty et al., 2016). Given the complexity of these functions, our findings do not allow us to draw strong conclusions about their association, but they encourage future research to study the interplay between memory and risk-seeking choices.

Higher risk seeking for losses is also associated with increased coupling between the DMN, the frontopolar cortex and small clusters located in left orbitofrontal regions. In this regard, neuroeconomic research has described specialized neurons within the OFC that appear to code the value of an expected reward and in this way, guide behavior toward more advantageous options (Schoenbaum et al., 2011). Similarly, task-based fMRI has shown that the coupling between frontal DMN areas and the frontal pole provides information about the value of unchosen options and represents the value that these options might have in the near future (Rushworth et al., 2011).

Finally, our findings showed that higher risk seeking for losses modulated the coupling between the left frontoparietal network and occipital regions. This network has typically been associated with risk taking and impulsiveness in both task-based and resting-state studies (Vaidya & Gordon, 2013; Weber & Huettel, 2008), as well as with adaptive control and flexibility (Dosenbach et al., 2007). In the present study, the biggest cortical area connected with the frontoparietal network was the left occipital pole/cuneus, which is mainly involved in basic visual processing (Grill-Spector & Malach, 2004). Further studies have related the activity of this area with behavioral engagement (Zhang & Li, 2012) and risk-taking reactivity, especially in adolescents (Tamura et al., 2012) and in pathologies with aberrant decision making (Crockford et al., 2005). Similar to our findings, Tamura et al. (2012) reported greater activation of the cuneus in response to the observation of high risk-taking actions in late adolescents. Despite their existing methodological differences (i.e., resting-state, task-based fMRI), these studies suggest potential implications of the visual system in the expression of more risk-seeking behaviors in young individuals.

Prior research has investigated the relation between RSFC and risky behaviors only in the gain domain (i.e., risky choices to obtain higher gains). However, our study presents a different approach in which risk seeking for gains and losses was assessed separately according to the well-grounded prospect theory (Kahneman & Tversky, 1979). This theory describes how risk is evaluated when potential gains or losses are involved. In the gain domain, the observation that the value of a gain is discounted (i.e., less attractive) due to the risk of not receiving it has been termed *risk seeking for gains*. In the loss domain, the value of a loss is similarly discounted when a probability is added. However, due to the prospect of losing nothing at all, the discounted offer is perceived as the most attractive one and has a higher likelihood to be chosen. Therefore, this behavior has been termed *risk seeking for losses*. Usually, risk seeking for gains is interpreted as a facet of impulsivity and has been associated with mental

disorders. Risk seeking for losses, on the other hand, indicates instead how susceptible individuals are to certain negative outcomes and how eager they are to avoid them. Increased risk seeking for losses therefore presents a more anxious decision-making style that may be understood as being opposite to an impulsive style. Data from our lab support this reasoning by showing that patients who suffer from alcohol use disorder exhibit increased risk seeking for gains and reduced risk seeking for losses (Bernhardt et al., 2017). In summary, we believe that impulsive choices in the gain *and* loss domain are characterized by increased risk seeking for gains but reduced risk seeking for losses.

Perhaps the above-mentioned differences between gains and losses played a role in the lack of connectivity changes in the networks comprising the cortico-striatal and dopaminergic circuits, which are generally involved in impulsivity and reward-related behaviors (Baik, 2013; Weiland et al., 2014). For instance, connectivity changes in key regions of the basal ganglia and the cingulo-opercular network have previously been reported in both risk-taking and risk-averse behaviors (Cox et al., 2010; DeWitt et al., 2014), but changes in these networks were not evident in our study. Likewise, the relation between delay discounting, probability discounting for gains, and RSFC seems to be stronger in conduct and addiction disorders (Wei et al., 2016; Zhu et al., 2015), but more sensitive techniques seem to be necessary for the detection of such differences in healthy samples. Nevertheless, our results provide, for the first time, insight into the brain's functional architecture that may underlie risk seeking with respect to losses in healthy young males.

### 2.5.1. Limitations

Our results must be viewed in light of several limitations. Our group-level analysis was carried out using nonparametric permutation testing, a method that provides an effective control for Type I error rates (Eklund et al., 2016), while requiring minimal assumptions about the data for valid statistical inference (Nichols & Holmes, 2002). Even when these facts favored the use of permutation tests with our data (Beckmann et al., 2009), we are aware that the biggest disadvantage of this method is weak control of outlying data points, as was recently shown by Mumford (2017). Another factor to consider is that the cluster sizes reported for three brain regions were smaller than the recommended k = 10 (Lieberman & Cunningham, 2009), as a result of the conservative statistical threshold applied. Therefore, for completeness, we reported all clusters that passed correction for multiple testing, but refrained from deep discussion of the results were the clusters contain fewer than ten voxels. Finally, our sample was restricted to a population of healthy, 18-

year-old participants. Thus, it remains unclear whether our results can be generalized to older or younger individuals. Moreover, our sample was restricted to male participants. Existing studies have described remarkable gender differences in risk-seeking behaviors (Ball et al., 1984) and associated negative consequences (Turner & McClure, 2003), but, to date, only the study of Zhou et al. (2014) has addressed gender functional connectivity differences linked to risk-seeking behavior. Therefore, we believe that future decision-making research will benefit from the inclusion of both genders and different age ranges.

### 2.5.2. Conclusion

In summary, delay-averse, risk-averse for gains and loss-averse behaviors did not influence the functional connectivity of large-scale brain networks in our sample, whereas risk seeking (as measured by probability discounting for losses), modulated the expansion of the default mode and left frontoparietal network to their adjacent areas, particularly those areas relevant for self-oriented prospective thinking, affective decision-making and visual processing. These findings suggest that distinct connectivity patterns of large-scale brain networks may underlie individual differences in decision making in healthy populations, and they strengthen the role of RSFC as a potential biomarker of different VBDM facets.

## 2.6. Notes

### 2.6.1. Author contribution

## 2.7. Supplemental Material Study I

### 2.7.1. Fig. S1. Process of including and excluding participants for analyses



| | |
|---|---|
| 201, 18 year-old, right-handed healthy participants were recruited from Berlin and Dresden. | • 7 participants had missing behavioral data.<br>• 1 participant was diagnosed with alcohol dependence. |
| 193 participants completed the fMRI session. | • 1 participant did not complete the resting state sequence.<br>• 4 participants presented structural brain anomalies detected in the anatomical MRI images by a neuro-radiologist. |
| Resting state data of 188 participants were preprocessed. | • 12 participants presented excessive motion during the fMRI sequence (> 10% volumes over 0.5 % Δ BOLD for DVARS and/or > 0.5 mm for FD). 1 participant remained with more than 10% of frames over 0.2 mm for FD after preprocessing.<br>• Data from 30 participants had to be rejected due to partial head coverage, poor data quality, registration problems and other scanner artifacts. |
| **145 participants were considered for the complete analysis (including 2 subjects abstinent from alcohol who were not considered in other studies).** | |

### 2.7.2. Value-based decision-making battery

The VBDM battery (Pooseh et al., 2017) is a set of four computerized tasks which use a Bayesian adaptive approach for the presentation of binary choices.

Besides collecting samples of data from real participants, simulations were performed in order to justify the algorithm in terms of reproducibility of the parameters for individual assessments and to test the reliability of the estimation procedure in a group-level analysis. Predefined values of the discounting and loss aversion parameters were reliably recovered.

Finally, comparison with standard methods showed that our algorithm outperforms an amount adjusting procedure in finding the indifference point for combinations of given immediate amounts, discounting rates and delays. It also performs better in terms of estimating preset discounting rates. Furthermore, we were able to adjust both the amount and delay/risk at the same time. This gives more flexibility in providing new offers.

The VBDM battery, including instructions, binary choices, and outcomes, is implemented using MATLAB, Release 2010a (The MathWorks, Inc., Natick, MA, USA) and Psychtoolbox 3.0.10, based on the Psychophysics Toolbox extensions (Brainard, 1997; Pelli, 1997), and is also available under GNU Octave. The settings of the tasks, including reward types and ranges, temporal delays, probabilities for gains and losses, and gambling, together with the instructions and payment schemes, are easily accessible through the source code provided upon request.

### 2.7.3. Generation of masks and regressors of noninterest

Segmentation of white matter and CSF from the brain-extracted structural images was carried out with FAST (Zhang et al., 2001) and thresholded with fslmaths (80% of tissue-type likelihood; (Biswal et al., 2010)). FLIRT (Jenkinson et al., 2002) was used for transforming the white matter and CSF masks from the subjects' structural space to their corresponding functional space. Fslmaths was used again for re-binarise the masks after transformation. Preprocessing of the resting state data was carried out a second time, only with motion correction and without temporal and spatial filtering. The white matter and CSF time courses were then extracted with fslmeants from this set of non-filtered data and merged with the individual motion parameters obtained with MCFLIRT during motion correction. Finally, this set of regressors was used during the second stage of dual regression.

**Table S1.** Differences in VBDM scores between the groups from Berlin and Dresden (N =145) were analyzed using a Mann-Whitney U test for asymmetrically distributed variables. Values are displayed as median and Interquartile range (IQR).

| VBDM scores | Dresden (75) | | Berlin (70) | | |
|---|---|---|---|---|---|
| | **Median** | **IQR** | **Median** | **IQR** | ***p*-value** |
| $DD_k$ | 0.01 | 0.05 | 0.01 | 0.06 | 0.44 |
| $PDG_k$ | 0.68 | 0.69 | 0.76 | 0.53 | 0.35 |
| $PDL_k$ | 0.48 | 0.76 | 0.58 | 0.67 | 0.04 |
| $MG_\lambda$ | 1.53 | 1.35 | 1.15 | 1.24 | 0.07 |

*Significance was considered at p < 0.0125, corrected for multiple comparisons.
DD: Delay discounting
PDG: Probability discounting gains
PDL: Probability discounting losses
MG: Mixed gambles

**Table S2.** Spearman's rank correlation between the VBDM scores and motion parameters. This analysis was performed in order to control for individual differences in decision-making traits that may influence movement inside the scanner, as postulated by Kong et al. (2014).

| | **Spearman's rho** | | | | | | | |
|---|---|---|---|---|---|---|---|---|
| | **$DD_k$** | | **$PDG_k$** | | **$PDL_k$** | | **$MG_\lambda$** | |
| | ρ | p | ρ | p | ρ | p | ρ | p |
| **DVARS** | − 0.07 | 0.41 | − 0.12 | 0.14 | 0.06 | 0.42 | − 0.02 | 0.76 |
| **FD** | − 0.08 | 0.30 | − 0.17 | 0.03 | − 0.03 | 0.76 | 0.00 | 0.91 |

DVARS: Temporal derivative of time courses (D) root-mean-squared of the variance over voxels (VARS)
FD: Framewise displacement
DD: Delay discounting
PDG: Probability discounting gains
PDL: Probability discounting losses
MG: Mixed gambles

**Table S3.** Cross-correlation results between the 10 ICN from Smith et al., (2009) and IC of our study in order of appearance during their initial projection.

| ICN from Smith et al. (2009b) | IC number | Cross-correlation coefficient: $r$ |
|---|---|---|
| Medial visual | IC 12 | 0.71 |
| Lateral visual | IC 7 | 0.66 |
| Dorsal attention | IC 4 | 0.33 |
| Default mode | IC 13 | 0.80 |
| Cerebellum | IC 18 | 0.45 |
| Sensorimotor | IC 0 | 0.41 |
| Cingulo-opercular | IC 14 | 0.41 |
| Right frontoparietal | IC 22 | 0.60 |
| Left frontoparietal | IC 25 | 0.69 |

# CHAPTER 3

## 3. STUDY II: Acute Tryptophan Loading Decreases Functional Connectivity between the Default Mode Network and Emotion-Related Brain Regions

## 3.1.    Abstract

It has been shown that the functional architecture of the default mode network (DMN) can be affected by serotonergic challenges and these effects may provide insights on the neurobiological bases of depressive symptomatology. To deepen our understanding of this possible interplay, we used a double-blind, randomized, cross-over design, with a control condition and two interventions to decrease (tryptophan depletion) and increase (tryptophan loading) brain serotonin synthesis. Resting-state fMRI from 85 healthy subjects was acquired for all conditions three hours after the ingestion of an amino acid mixture containing different amounts of tryptophan, the dietary precursor of serotonin. The DMN was derived for each participant and session. Permutation testing was performed to detect connectivity changes within the DMN as well as between the DMN and other brain regions elicited by the interventions. We found that tryptophan loading increased tryptophan plasma levels and decreased DMN connectivity with visual cortices and several brain regions involved in emotion and affect regulation (i.e. putamen, subcallosal cortex, thalamus, frontal cortex). Tryptophan depletion significantly reduced tryptophan levels but did not affect brain connectivity. Subjective ratings of mood, anxiety, sleepiness and impulsive choice were not strongly affected by any intervention. Our data indicate that connectivity between the DMN and emotion-related brain regions might be modulated by changes in the serotonergic system. These results suggest that functional changes in the brain associated with different brain serotonin levels may be relevant to understand the neural bases of depressive symptoms.

**Keywords:**

*Serotonin*
*Tryptophan*
*Resting-state fMRI*
*DMN connectivity*

### 3.2. Introduction

The brain's default mode network (DMN) has emerged as a landmark in cognitive and affective neuroscience since its first description in 2001 (Raichle et al., 2001). It is now generally accepted that the synchronized activity between its regions might play a critical role for integrating representational information across the cortex (Margulies et al., 2016). Recently, it has been shown that pharmacological challenges may impact the functional architecture of the DMN, especially in regions with elevated receptor density for particular neurotransmitters (e.g. cingulate cortex; Klaassens et al. (2015)).

Specifically, DMN regions receive dense serotonin (5-hydroxytryptamine, 5-HT) innervations (Saulin et al., 2012). Serotonergic ascending fibers from the dorsal raphe nucleus project onto the lateral cerebral cortex and the hypothalamus, the basal forebrain, and the amygdala. Further projections from the latter regions continue to the cingulate cortex, the medial cerebral cortex and the hippocampus (Hornung, 2003), which are parts of the DMN (Buckner et al., 2008a). Presumably as a result of this innervation, changes in the functional coherence of the DMN following serotonergic medication were observed, especially in brain regions involved in mood and attention regulation (Klaassens et al., 2016; Klaassens et al., 2015; Posner et al., 2013; van de Ven et al., 2013).

Among serotonergic interventions, acute tryptophan challenges are well-established techniques to manipulate the synthesis of 5-HT in the central nervous system in a transitory and marginally invasive manner. Although direct measures of tryptophan influx into the human brain are currently not possible, the effectiveness of these challenges has been demonstrated by several animal studies (Biskup et al., 2012; Grimes et al., 2000; Lieben et al., 2004) and indirect measures of 5-HT levels in humans (e.g. CSF, (Williams et al., 1999; Young & Gauthier, 1981)). These interventions reduce or enhance the availability of the essential amino acid tryptophan, the dietary precursor of 5-HT in the brain, and thus help to investigate the role of the serotonergic system in the modulation of cognitive functions and mood among others (Lindseth et al., 2015; Silber & Schmitt, 2010).

Although simplistic and refined through the years, the hypothesis of a dysfunction in the serotonergic system as a primary factor in the aetiology of affective disorders (Cowen & Browning, 2015) has promoted the use of tryptophan challenges in the study of depressive symptomatology (Lindseth et al., 2015). In addition, an aberrant DMN connectivity was found in depressed individuals, establishing a neural model that helps to explain the states of

excessive rumination, i.e. DMN hyperconnectivity, and deficits in goal-directed behavior, i.e. hypoconnectivity between DMN and cognitive control systems, that characterize this disorder (Kaiser et al., 2015). Consequently, DMN changes following tryptophan manipulations might provide relevant clues regarding the origin of depressive symptomatology.

Existing studies investigating the effects of tryptophan depletion on DMN connectivity describe reduced functional connectivity of the precuneus and enhanced functional connectivity of the frontal cortex in healthy (Helmbold et al., 2016; Kunisato et al., 2011) and psychiatric (Biskup et al., 2016) populations. In contrast, tryptophan loading, a less-used intervention, led to greater connectivity between frontal DMN regions and the lateral PFC (Kroes et al., 2014). However, the use of relatively small samples and a single tryptophan condition limits the conclusions that can be drawn from these investigations.

While the effects on 5-HT synthesis obtained after tryptophan challenges seem to be rapid (Biskup et al., 2012; Dingerkus et al., 2012), animal models have shown that low or single doses of SSRIs increase 5-HT concentrations to a level that floods somatodendritic 5-HT1A autoreceptors, which in turn may cause a subsequent 5-HT depletion-like state with its corresponding behavioral manifestations (Cools et al., 2008) instead of an expected increase in 5-HT levels. This mechanism of action might explain why DMN changes in healthy subjects after single doses of SSRIs mirror those obtained after tryptophan depletion in posterior parts of the DMN (Helmbold et al., 2016; Klaassens et al., 2015; Kunisato et al., 2011; van de Ven et al., 2013). On the other hand, the action of serotonergic manipulations on frontal DMN regions seems to be less clear, showing both increases and decreases in connectivity after either SSRIs (Klaassens et al., 2016; Klaassens et al., 2015) or tryptophan manipulations (Helmbold et al., 2016; Kunisato et al., 2011). Hence, further investigations are still necessary in order to understand how different brain 5-HT levels affect the functional coherence of the DMN.

The aim of our study was to investigate the effects of serotonergic manipulations on the functional architecture of the DMN in healthy subjects following two tryptophan interventions, namely: acute tryptophan depletion (ATD) and acute tryptophan loading (ATL). Both interventions were tested against a balanced condition (BAL), which provided the recommended daily intake of tryptophan for adults (see Experimental procedure). To observe how different brain 5-HT levels may affect the DMN connectivity, we also investigated possible linear relationships between both interventions (ATD – ATL). Based on previous findings and

the existing literature, we hypothesized that ATD would decrease the functional connectivity of posterior parts of the DMN (i.e precuneus and PCC) but increase the connectivity of frontal and medial parts of the DMN (i.e. vmPFC, retrosplenial cortex, angular gyrus) whereas ATL would have opposite effects. The methodology used in this study also allowed us to investigate connectivity changes between the DMN and other brain regions following each tryptophan manipulation (i.e. voxel-to-network connectivity). Additionally, we used similar behavioral measures as previous studies that reported more impulsive choices as well as higher anxiety and depression levels after ATD, and increasing sleepiness after ATL (Dougherty et al., 2010; Lindseth et al., 2015; Silber & Schmitt, 2010). Finally, we investigated possible associations between functional connectivity changes and these behavioral measures.

## 3.3. Materials and Methods

### 3.3.1. Participants

One hundred and twelve healthy participants completed the three sessions of the study. Of these, we discarded five participants who received accidentally the same mixture in all sessions, four participants with excessive movement during the resting-state scan (see Image preprocessing), four participants with structural brain anomalies (e.g. cysts, enlarged ventricles) detected by a neuroradiologist, two participants who did not complete one resting state scan and 12 participants with limited brain coverage or scanner artifacts in one or all resting-state sessions. Therefore, data from 85 participants (41 females; $M_{age}$ = 32.68 years, $SD_{age}$ ±5.81, range = 21-42) were analyzed in this study. These participants form part of the sample already reported by Neukam et al. (2018). The detailed recruitment process is described in the Supplementary Material 1.

Participants gave written informed consent and received monetary compensation for their participation. The study protocol was approved by the local ethics committee of the Technische Universität Dresden and was in accordance with national legislation and the Declaration of Helsinki.

### 3.3.2. Experimental procedure

Participants took part in three sessions and received one of the following drinks: acute tryptophan depletion (ATD), balanced (BAL) or acute tryptophan loading (ATL) in a randomized, double-blind, placebo-controlled (BAL), crossover study, with at least one

week between sessions (elapsed days between sessions: M = 23, SD = 25). The dose of amino acids in the mixtures was adjusted to participant's body weight (Dingerkus et al., 2012; Moja et al., 1988) and contained the same amount of large neutral amino acids (LNAA) but differed in the amount of tryptophan. In the ATD condition, tryptophan was completely absent, the BAL condition contained 7 mg/kg body weight (equivalent to the recommended daily allowance for adults (Richard et al., 2009)) and the ATL condition contained 70 mg/kg body weight. The dose of large neutral amino acids (LNAA) was constant for every participant across sessions: L-phenylalanine (132 mg/kg), L-leucine (132 mg/kg), L-isoleucine (84 mg/kg), L-methionine (50 mg/kg), L-valine (96 mg/kg), L-threonine (60 mg/kg) and L-lysine (96 mg/kg). To maximize the effects of the intervention, we provided a list of low-protein food that the participants were allowed to have for dinner and told them to fast overnight before each experimental day. Participants arrived either at 8.30 a. m or 10.30 a.m., received instructions about the study procedure and the possible side-effects of the intervention (e.g. sleepiness, drowsiness, nausea, vomiting) and drank the assigned mixture prepared by an independent experimenter who did not conduct the session. Additional details about the experimental procedure are provided in Supplementary Material 2.

### 3.3.3. Biochemical measures

A venous catheter (Braunüle®) was inserted in the participant's arm at the beginning of each session in order to draw blood samples in tubes (Sarstedt, Germany) with ethylenediaminetetraacetic acid (EDTA) at four time points (T0 = baseline, T1 = one hour, T2 = three hours and T3 = six hours after ingestion of the mixture) to measure the concentrations of tryptophan and LNAA in blood plasma. Blood samples were immediately centrifuged at 4000g and 4°C for 10 minutes and 1 ml plasma was stored in two Eppendorf capsules in a -81°C fridge. Plasma analyses for the concentrations of tryptophan and LNAA were conducted at the Department of Chemistry and Food Chemistry of the Technische Universität Dresden as described in Henle et al. (1991). Complete blood samples from 71 participants were available for analysis.

The ratio of tryptophan to the sum of the other LNAA (TRP/∑LNAA) in the peripheral blood at each time point was calculated as the best estimate of the intervention effects in each session (Dingerkus et al., 2012). For statistical analyses, the area under the curve (AUC) was computed using the 4 time points. Before calculating the AUC, all four time

points were normalized by subtracting the values of T0 from all time points, thereby accounting for inter-individual differences in baseline blood levels. These AUC scores were entered into a repeated-measures ANOVA.

### 3.3.4. Behavioral assessment

Statistical analyses were conducted using SPSS for Windows (release 22.0, IBM Corp., Armonk, IL, USA). Participants completed an extensive behavioral assessment and several self-report questionnaires. The questionnaires reported in this manuscript are the State-Trait Anxiety Inventory (STAI-State, (Spielberger, 1983)), the Karolinska Sleepiness Scale (KSS, (Akerstedt & Gillberg, 1990)) and a 9-item Visual Analogue Scale (VAS: heightened, excited, balanced, depressed, lethargic, activated, sad, relaxed, stressed (In-house assessment, ZI, Mannheim, Germany)). These questionnaires were applied in the order mentioned above at the four time points of the session. Additionally, we assessed impulsive choice using three tasks of the Value-Based Decision-Making battery (see Pooseh et al. (2017) for a complete description). Briefly, risk aversion for gains and risk seeking for losses were assessed using probability discounting for gains and losses respectively. In these tasks, participants needed to choose between a sure amount that they could win or lose and the probability of winning/losing a larger amount of money (e.g., 75% probability of winning €5 or winning €2 for sure, or a 50% probability of losing €8 or losing €3 for sure). The resulting main discounting parameters from these tasks (k) were log-transformed in order to approximate them to a normal distribution. Finally, loss aversion was assessed with a mixed gambles task. In this task, participants received a credit of €10 at the beginning of the game and then needed to decide whether to accept or reject an offer with a 50/50 chance of either gaining one amount of money or losing another amount (e.g., refusing to gamble or accepting a gamble that offered either winning €15 or losing €8). These three tasks were administered at a single time point after the fMRI session. Due to missing data the number of complete behavioral datasets ranged from 82 to 85. Other behavioral and cognitive measures as well as demographic information were acquired (see Neukam et al. (2018) and Supplementary Material 3). The study design including the number of participants in each session and condition and a schematic overview of one study session are depicted in Fig. 5.

In order to test intervention effects (ATD and ATL vs. BAL) and effects between interventions (ATD vs. ATL) on the three behavioral ratings, we subtracted the scores

obtained at baseline (T0) from the scores obtained before the scan session (T2) and performed a repeated-measures ANOVA with the resulting scores. Results were Bonferroni-corrected for 14 comparisons. If the F-test indicated significant differences, post-hoc paired t-tests were performed to determine directionality of the effects.
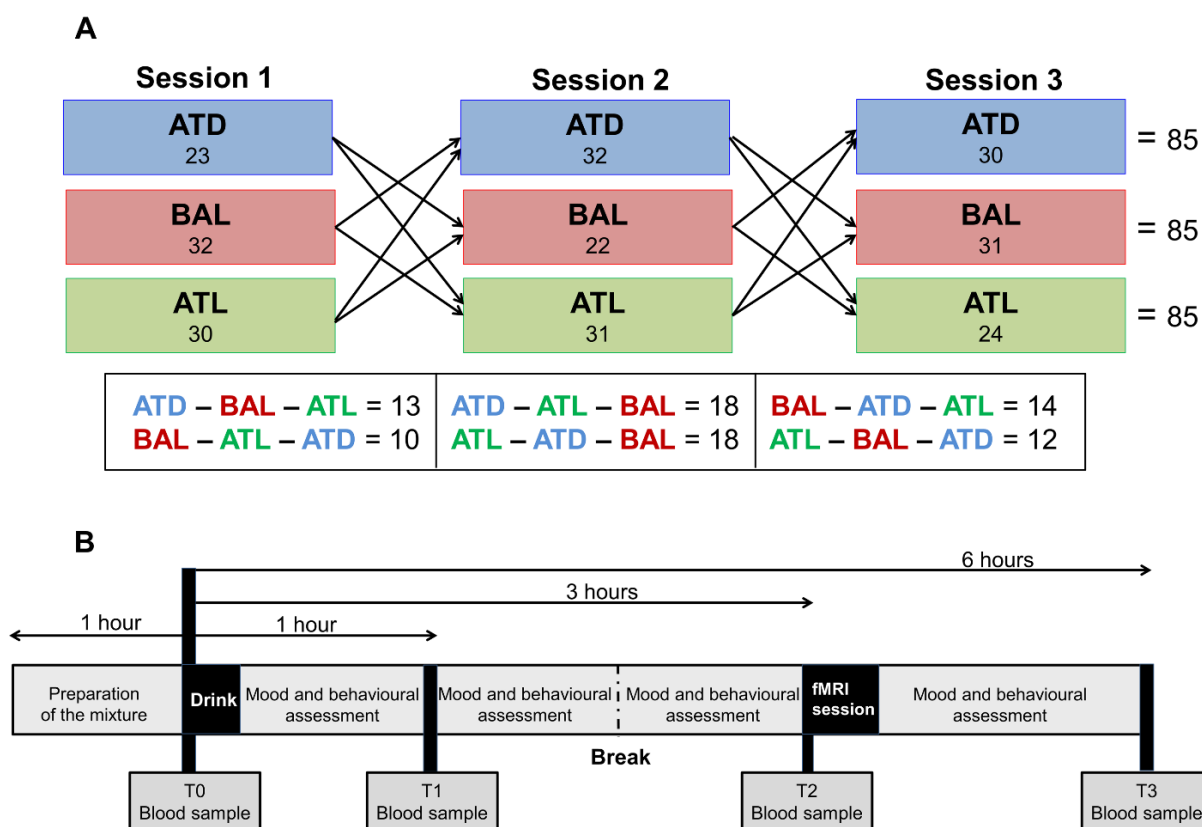


**Figure 5.** Study design. Part A shows the study design with the cross-over randomization of the tryptophan interventions (ATD = acute tryptophan depletion, BAL = balanced, ATL = acute tryptophan loading), the final number of participants for each intervention and session (N = 85) and the number of participants in each possible order of interventions. Part B shows the timeline of a study session. The mixture was prepared one hour before the participant arrived. At T0, the first blood sample was taken as a baseline measure of tryptophan plasma concentrations, followed by the ingestion of the mixture and mood and behavioral assessments. Additional blood samples were taken one, three and six hours after the ingestion of the mixture. The fMRI session was carried out three hours after the drink.

### 3.3.5. MR data acquisition

All fMRI sessions were carried out three hours after the ingestion of the mixtures because previous research (Dingerkus et al., 2012) and our pilot tests showed after this time, the lowest and highest tryptophan peaks in ATD and ATL respectively. The resting-state fMRI sequence was performed after a decision-making task and a short break. fMRI data were collected on a 3 Tesla whole-body MRI Scanner Magnetom Trio Tim (Siemens Healthcare GmbH, Erlangen, Germany) equipped with a 32 channel head coil using a single-shot gradient echo-planar imaging (EPI) sequence with repetition time (TR) of 2.41s, an echo time (TE) of 25 ms, a flip angle of 81°, 42 2 mm-thick slices and 1 mm slice gap, field of view of 192 × 192 mm2 with a matrix size of 64 x 64, 3 mm isotropic resolution and a bandwidth of 2112 Hz/Px. A total of 150 resting-state volumes were acquired, tilted slightly from axially to coronal to be parallel to the anterior/posterior commissural line. For registration purposes, a T1-weighted high-resolution anatomical scan was acquired with a 3D magnetization prepared - rapid gradient echo (MP-RAGE) sequence (TR = 1.90 s, TE = of 2.26 ms, TI = 900 ms, flip angle of 9°, FOV = 256 x 256 mm2, 176 slices, 1 mm x 1 mm x 1 mm voxel size with slice thickness of 1 mm and 200 Hz/Px bandwidth). Participants were given earplugs for noise protection and foam pads to minimize head movement. They were instructed not to think about anything in particular and to lie as still as possible while fixating on a black crosshair presented on the center of a white screen. An eye-tracking camera was used to monitor the participants and to ensure that they remained awake during the whole resting-state session.

### 3.3.6. Image preprocessing

For each participant, framewise displacement (FD: a sum of the absolute values of the temporal derivatives of the volume-by-volume changes in the translational and rotational realignment estimates (Power et al., 2012)), was calculated on the raw data prior to any preprocessing step using the tool fsl_motion_outliers. Four participants with more than 10% of volumes over a FD of 0.5 mm were excluded from the analysis (Deza Araujo et al., 2018). The resting-state fMRI data were preprocessed using the Functional Magnetic Resonance Imaging of the Brain (FMRIB) Software Library (FSL Version 5.0.9, www.fmrib.ox.ac.uk/fsl; (Jenkinson et al., 2012)). The first four volumes of each functional scan were discarded to allow for magnetic equilibration, resulting in 146 volumes per subject and intervention. Preprocessing steps included motion correction with MCFLIRT, brain extraction of the EPI data with BET, spatial smoothing with a 5mm Gaussian kernel

of full-width at half maximum, ICA-based denoising using ICA-AROMA (Pruim et al., 2015) and high-pass temporal filtering of 0.01 Hz. Registration was applied on the denoised functional data using the registration parameters derived from non-smoothed and non-filtered data. For registration, individual resting-state images were aligned to their corresponding T1-weighted image using a boundary-based registration algorithm (BBR (Greve & Fischl, 2009)). The T1-weighted images were registered to MNI space (MNI152; 2 mm x 2 mm x 2 mm spatial resolution) using a nonlinear registration implemented in FNIRT (warp resolution: 10 mm). The same transformation was applied to the filtered EPI images. After this process, all images were visually inspected in order to ensure accuracy of the registration.

### 3.3.7. Generation and analysis of the default-mode network

We used a template-based approach, which has been validated by previous studies (Klaassens et al., 2016; Klaassens et al., 2015) and reliably provides spatial maps of established large-scale brain networks. Briefly, we used the 10 templates from Smith et al. (2009b) to derived the networks identified in more than 1600 studies. These templates included: high, medial and lateral visual networks, default-mode network, cerebellar network, sensorimotor network, auditory network, cingulo-opercular network, right and left frontoparietal networks (See Supplementary Material Fig S3 (Smith et al., 2009b)). To obtain an individual representation of each network, we used a dual regression analysis (Beckmann et al., 2009). Here the templates were linearly regressed against the functional data of each subject, resulting in individual time courses (spatial regression) for each one of the 10 networks. These time courses were normalized and then regressed against the corresponding functional datasets (temporal regression) to estimate 10 subject-specific voxel-to-network spatial maps for each subject and pharmacological condition. Additional individual mean time courses from white matter, cerebrospinal fluid and the six subject-specific motion parameters were added during the last stage of the dual regression to remove sources of spurious variance and residual motion (see Supplementary Material 4). As a multivariate approach, this dual regression procedure allowed the estimation of a "clean" representation of the DMN in which temporal and spatial signals that this network shares with other networks, were removed. In the dual regression approach, the estimated maps do not depend on the initial subject-specific major eigenspaces (PCA) and therefore, may lie outside the network's boundaries (Beckmann et al., 2009). The voxel-wise regression coefficients contained in the resulting spatial maps represent the

synchronization between BOLD temporal dynamics at a given voxel and the mean BOLD time courses of a specific network. The strength of the voxel-to-network connectivity is given by the value of these coefficients (Klaassens et al., 2016; Klaassens et al., 2015). Only the spatial maps representing the DMN were used in the higher-level analysis (85 subjects x 3 interventions = 255 DMN maps).

Due to the unknown distribution of the data, non-parametric testing was used for group-level analyses. To delineate the effects of intervention on the DMN, a repeated-measures ANOVA was performed, with "intervention" (ATD, BAL, ATL) as a within-subject factor. We used Faster Permutation Inference as implemented in Permutation Analysis of Linear Models – PALM version 99a  (Winkler et al., 2015), with 500 permutations and a tail approximation procedure which fits a Pareto distribution to the tail of the distribution used for correction of the p-values (Winkler et al., 2016a). Exchangeability blocks were specified in the model for allowing permutations to happen within subjects (Winkler et al., 2015). We implemented directional contrasts to compare if the within DMN connectivity and the voxel-to-network connectivity were stronger or weaker after a given intervention with respect to baseline levels (ATD > BAL, BAL > ATL, ATD < BAL, BAL < ATL) and between both interventions (ATD < ATL, ATD > ATL). Results were family-wise error (FWE) corrected at .05 using Threshold-Free Cluster Enhancement – TFCE, a method that generates a voxel-wise output image in which the values represent the amount of cluster-like local spatial support (Smith & Nichols, 2009). Further FWE correction over the six tested contrasts was performed, using the option "corrcon" implemented in PALM (Winkler et al., 2016b), which takes into account the dependencies that might exist between contrasts. These comparisons of subject-specific maps indicated which brain areas (within or outside the DMN map) are stronger connected to the DMN under one condition with respect to the other.

Additionally, we tested potential repetition effects. To this aim, a repeated measures ANOVA with "intervention" (ATD, BAL, ATL) as a within-subjects factor and "intervention order" (i.e. the six possible order combinations of the interventions. See Fig. 5) as between-subject factor, was used. A significant interaction between these two factors would indicate that the observed effects on DMN connectivity are driven by the repetition of the resting-state scan and not solely by a given intervention.

Due to postulated gender differences in brain 5-HT metabolism (Nishizawa et al., 1997), we explored whether gender moderates the effects of the tryptophan interventions. To this end, a third repeated-measures ANOVA was included, with "intervention" as a within-subject factor and "gender" (males, females) as a between-subject factor. These additional models were also tested using 500 permutations, with a tail approximation as implemented in PALM, yielding voxel-wise maps identified with TFCE and corrected at .05.

We compared the mean FD measures in a repeated measures model to test whether in-scanner motion differed between interventions or sessions.

### 3.3.8. Analyses of brain-behavior associations

To determine potential brain-behavior associations, we performed Pearson correlations between the behavioral scores and the brain regions with significant intervention effects on DMN connectivity. Specifically, the difference of regional parameter estimates between two interventions (e.g. BAL – ATL) was correlated with their corresponding difference in behavioral scores (e.g. $KSS_{BAL} - KSS_{ATL}$).

### 3.4. Results

#### 3.4.1. Effects of intervention on blood plasma levels of tryptophan and $\sum$LNAA

To test the effects of our interventions in the peripheral blood, TRP/$\sum$LNAA AUC scores and free tryptophan measures were calculated. Significant main intervention effects were found in the measures of free tryptophan in peripheral blood ($F_{2,142}$ =235.52; p = 1.76 x $10^{-28}$) and in the TRP/$\sum$LNAA AUC scores ($F_{2,142}$ = 334.30; p = 1.15 x $10^{-33}$). Contrast analyses revealed significant increases for free tryptophan from ATD to BAL ($F_{1,70}$= 65.44; p = 1.13 x $10^{-11}$) and from BAL to ATL ($F_{1,70}$ = 174.55; p = 8.23 x $10^{-21}$). In the same manner, contrasts analysis for TRP/$\sum$LNAA AUC scores revealed significant increases from ATD to BAL ($F_{1,70}$ = 67.40; p = 7.5 x $10^{-12}$) and from BAL to ATL ($F_{1,70}$= 250.28; p = 8.2 x $10^{-25}$). Graphic representations of these effects are displayed in Fig. 6. Detailed results of this analysis as well as other measures (free tryptophan and TRP/$\sum$LNAA) are provided in Supplementary Table S4.

Finally, neither gender nor intervention order had any effect on tryptophan plasma measures (all *ps* > *.2*).
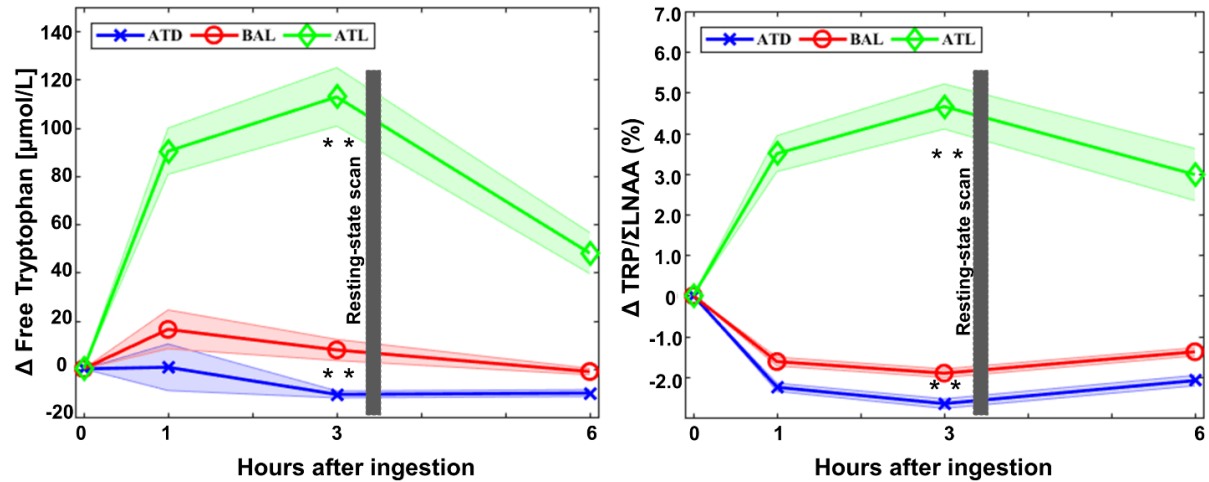
**Figure 6.** Pharmacokinetics of the acute tryptophan intervention: In both graphs, the x axis displays the four time points of blood sampling. On the left graph, the y axis displays the plasma levels of free tryptophan. On the right graph, the ratio of tryptophan to the sum of the other large neutral amino acids (TRP/∑LNAA) is shown. The resting-state scan was carried out after a decision-making task, 3.5 hours after the ingestion of the mixture. The abbreviations are acute tryptophan depletion (ATD), balanced (BAL) and acute tryptophan loading (ATL). The shaded areas indicate bias-corrected and accelerated (BCa) 95% confidence intervals. The graph includes complete data from 71 participants. ** $P < .0001$.

### 3.4.2. Effects of intervention on mood, vigilance and impulsive choice

None of the behavioral scores survived Bonferroni correction for 14 comparisons. For completeness, we reported uncorrected p-values (main effects of intervention and pair-wise comparisons) in Table 4.

**Table 4**. Summary statistics of the difference between T2 (before the scan session) and T0 (baseline) for the behavioral assessment in each tryptophan intervention. None of the comparisons survived Bonferroni correction for 14 tests. Asterisks indicate *ps < .05*, uncorrected for multiple comparisons

| Test | ATD Mean (SD) | ATD - BAL p-value | BAL Mean (SD) | BAL-ATL p-value | ATL Mean (SD) | ATD-ATL p-value | Main effects p-value |
|---|---|---|---|---|---|---|---|
| STAI-G X1-state | 1.12 (5.00) | 0.85 | 1.36 (5.40) | 0.80 | 1.61 (4.11) | 0.62 | 0.88 |
| KSS | 1.41 (2.08) | 0.27 | 1.17 (1.96) | 0.006* | 1.86 (2.13) | 0.19 | 0.04* |
| VAS-heightened (mm) | -6.83 (24.83) | 0.94 | -7.03 (24.56) | 0.31 | -3.64 (17.56) | 0.35 | 0.52 |
| VAS-excited (mm) | -9.32 (28.92) | 0.23 | -5.01 (19.41) | 0.43 | -8.03 (23.52) | 0.68 | 0.49 |
| VAS-balanced (mm) | -0.44 (28.33) | 0.74 | -1.80 (24.25) | 0.40 | -5.69 (30.81) | 0.25 | 0.49 |
| VAS-depressed (mm) | 2.04 (16.63) | 0.06 | 7.05 (21.80) | 0.32 | 4.07 (16.36) | 0.28 | 0.14 |
| VAS-lethargic (mm) | 14.02 (28.41) | 0.52 | 11.15 (27.61) | 0.28 | 16.04 (29.43) | 0.65 | 0.55 |
| VAS-activated (mm) | -10.68 (22.15) | 0.70 | -9.38 (19.06) | 0.63 | -11.08 (24.43) | 0.91 | 0.87 |
| VAS-sad (mm) | 3.55 (13.52) | 0.30 | 1.41 (13.30) | 0.62 | 2.68 (18.31) | 0.55 | 0.55 |
| VAS-relaxed (mm) | -6.20 (21.79) | 0.37 | -3.79 (24.80) | 0.02* | -12.74 (26.46) | 0.12 | 0.06 |
| VAS-stressed (mm) | -1.80 (13.54) | 0.03* | 5.52 (24.12) | 0.48 | 3.73 (15.83) | 0.01* | 0.04* |
| PDG$_{logk}$ | 0.37 (0.85) | 1.00 | 0.31 (1.04) | 1.00 | 0.23 (0.82) | 0.51 | 0.38 |
| PDL$_{logk}$ | -0.15 (0.99) | 0.28 | -0.38 (1.25) | 0.35 | -0.33 (1.52) | 0.63 | 0.34 |
| MG$_\lambda$ | 143 (0.98) | 1.00 | 1.48 (1.13) | 1.00 | 1.44 (1.13) | 1.00 | 0.89 |

N = 82-85

STAI-G X1= State-Trait Anxiety Inventory – state, scale X1

KSS = Karolinska Sleepiness Scale

VAS = Visual Analogue Scale, mm = millimeters

PDG = Probability discounting gains (k on log scale)

PDL = Probability discounting losses (k on log scale)

MG = Mixed gambles (lambda)

### 3.4.3. Effects of intervention on DMN connectivity

Compared to the control condition (BAL), acute tryptophan loading (ATL) reduced significantly the DMN functional connectivity in bilateral medial prefrontal regions ($p_{FWE}$ = .03). The same intervention reduced the functional connectivity between the DMN and clusters located in the putamen ($p_{FWE}$ = .02), subcallosal cortex ($p_{FWE}$ = .03), left thalamus ($p_{FWE}$ = .03) and bilateral occipital regions ($p_{FWE}$ = .02 and .04). All these connectivity changes were unrelated to variations in behavioral scores (all *ps* > .20). Cluster sizes and summary statistics for the significant results are presented in Table 5. A graphical representation of all intervention effects on the significant regions is presented in Fig. 7.

Compared to the control condition (BAL), acute tryptophan depletion (ATD) numerically decreased the DMN connectivity with small clusters in the left middle temporal gyrus (k = 42) and the right orbitofrontal cortex (k = 7). Importantly, these marginal effects did not survive correction for the six contrasts of interest ($p_{FWE}$ = .30. Supplementary Table S5).

No significant differences in DMN connectivity were found between both interventions (ATD vs. ATL).

Regarding possible confounders or moderators, framewise displacement analyses revealed no differences in-scanner motion between interventions or session (all *ps* > .10). Moreover, no interaction between intervention order and interventions were found, indicating that the repetition of the resting-state scan did not affect DMN connectivity. No significant gender-by-intervention interaction on DMN connectivity could be found, indication that interventions had comparable effects for males and females.

**Table 5**. Brain regions that showed significant decreases in functional connectivity to the DMN under ATL compared to BAL.

| Brain regions | Cluster size (voxels) | t-values | *p*-values | MNI coordinates (COG) X | Y | Z |
|---|---|---|---|---|---|---|
| Right Putamen | 1058 | 4.41 | 0.02 | 20 | 10 | -2 |
| Left frontal orbital cortex | 349 | 4.69 | 0.02 | -30 | 18 | -14 |
| Left subcallosal cortex | 153 | 4.09 | 0.03 | -2 | 28 | -26 |
| Left frontal medial cortex | 118 | 4.29 | 0.03 | -12 | 44 | -10 |
| Right frontal orbital cortex | 108 | 4.29 | 0.03 | 38 | 34 | 0 |
| Left thalamus | 96 | 4.53 | 0.03 | -10 | -2 | 4 |
| Left occipital pole | 80 | 5.54 | 0.02 | -2 | -92 | 4 |
| Right frontal medial cortex | 49 | 4.42 | 0.03 | 14 | 44 | -10 |
| Left frontal pole | 41 | 3.83 | 0.04 | -36 | 44 | -8 |
| Left frontal pole | 16 | 4.14 | 0.04 | -14 | 44 | -24 |
| Right middle frontal gyrus | 14 | 4.13 | 0.04 | 36 | 32 | 26 |
| Right middle frontal gyrus | 11 | 4.02 | 0.04 | 34 | 24 | 22 |
| Right occipital pole | 10 | 4.34 | 0.04 | 14 | -90 | 10 |
| Left thalamus | 10 | 3.73 | 0.04 | -10 | -12 | -2 |

Voxel dimensions = 2x2x2 mm. Peak t values within cluster are uncorrected. P-values are FWE-corrected and adjusted for the six comparisons performed. MNI coordinates represent the center of gravity (COG). Brain areas were identified using the Harvard-Oxford Cortical and Subcortical Structural Atlases.
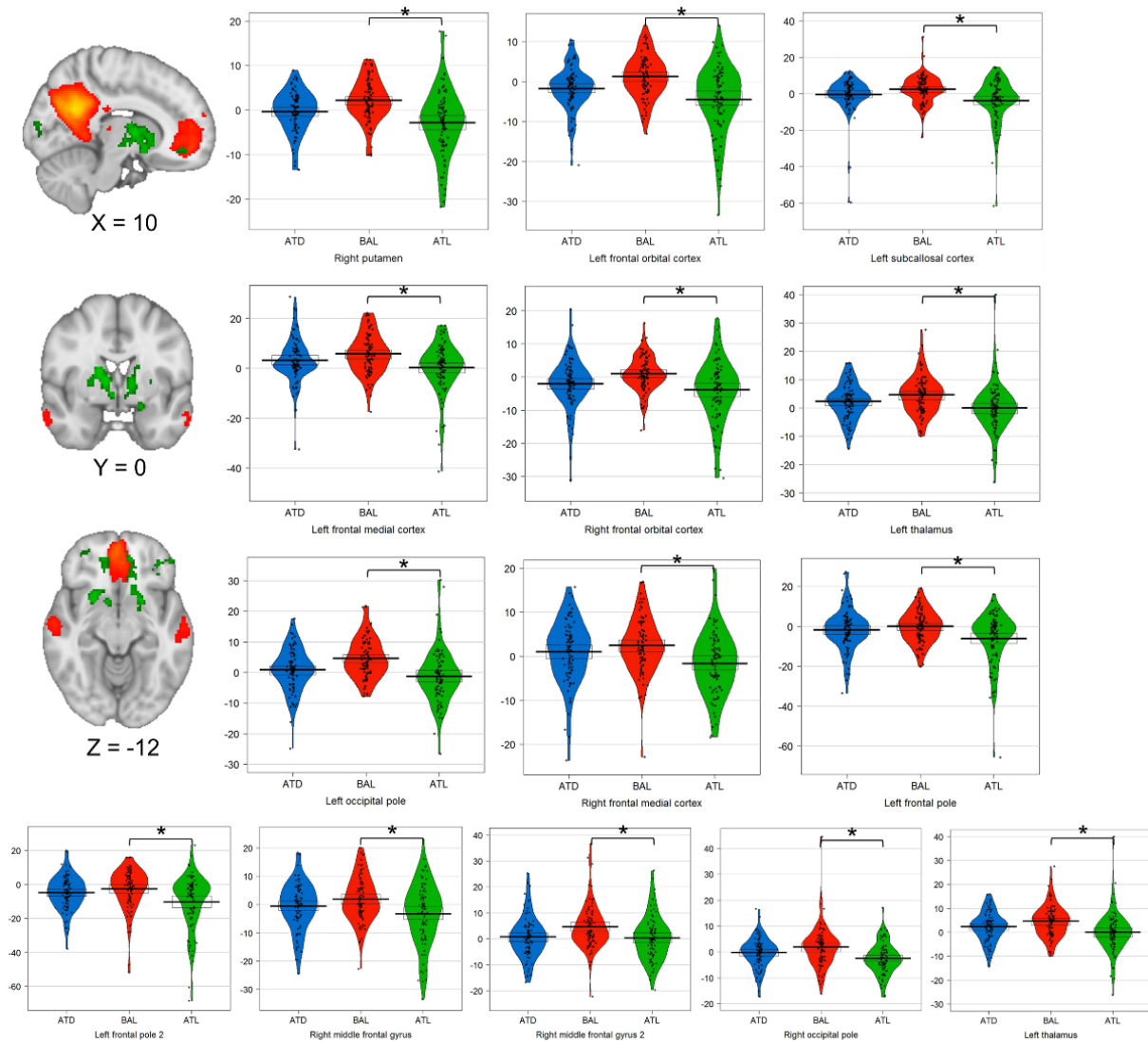
**Figure 7.** Changes in DMN functional connectivity following tryptophan manipulations. The image slices on the left side show the spatial map of the DMN (precuneus, PCC, mPFC, retrosplenial cortex, hippocampus) as identified by Smith et al. (2009) displayed in red-orange. The clusters with decreased functional connectivity to the DMN after acute tryptophan loading (ATL) are displayed in green colors. MNI coordinates are presented below each image. Images are displayed in radiological orientation (left = right). The plots represent the distribution of the parameter estimates (in arbitrary units) of the brain regions that were affected by the tryptophan manipulations (as shown in Table 5. Horizontal lines on the plots represent means and 95 % confidence intervals. *$P < .05$, FWE corrected and adjusted for six comparisons performed.

### 3.5.     Discussion

This study is the first to use both, tryptophan depletion and loading, together with a control condition to manipulate brain 5-HT levels and investigate related changes in DMN functional connectivity in a large cohort of healthy adults. We found that, compared to the control condition (BAL), higher brain 5-HT levels (ATL) decreased the functional connectivity within the DMN and between this network and other brain regions. Contrary to previous findings, lower brain 5-HT levels (ATD) did not yield any significant changes on DMN connectivity. Finally, behavioral measures of mood, sleepiness, vigilance and impulsive choice were neither strongly affected by our interventions nor related to any DMN connectivity change.

In partial agreement with our hypotheses, higher brain 5-HT levels (ATL) resulted in lower functional connectivity within anterior regions of the DMN (i.e. bilateral medial frontal cortex) but did not increase the functional connectivity of posterior DMN regions. Moreover, the same intervention decreased the functional connectivity between the DMN and the middle frontal gyrus, left frontal pole and bilateral orbitofrontal cortex. Frontal DMN regions are involved in emotion regulation, introspection and future thinking (Buckner et al., 2008a), processes that have a close relationship with serotonergic function and are generally affected in mood disorders (Dainer-Best et al., 2018; Meneses & Liy-Salmeron, 2012). Similarly, the dense serotonergic innervation of the orbitofrontal cortex indicates that an adequate 5-HT modulation of this area is crucial for behavioral flexibility and regulation of emotional responses (Roberts, 2011). Given the anatomical proximity and the existing connections between the orbitofrontal cortex and the frontal hub of the DMN (i.e. medial prefrontal cortex); (Kahnt et al., 2012)), serotonergic-induced changes in the functional connectivity of these regions may be relevant to understand, for example, mood improvements observed after the administration of serotonergic medications.

In the same way, higher brain 5-HT levels (ATL) reduced the connectivity between the DMN and the thalamus and putamen. These structures form part of the limbic-cortical-striatal-pallidal-thalamic circuits (LCSPT), which are primarily involved in emotional processing, affect regulation and are also implicated in the pathophysiology of mood disorders (Drevets et al., 2008a; Greicius et al., 2007). Moreover, PET studies have revealed high serotonin synthesis capacity rates in these areas (Okazawa et al., 2000; Saulin et al., 2012), indicating their susceptibility to different 5-HT levels.

The decreased connectivity between the DMN and a cluster located in the subcallosal cortex following ATL deserves special attention. The subcallosal cortex comprises the adjacent ventromedial PFC and Brodmann areas 24 and 25 (Vogt et al., 1995) and plays a fundamental role in affective valuation of stimuli and expression of negative emotions (Drevets et al., 2008b). Functional and structural changes in the subcallosal cortex and its adjacent areas are observed in mood and depressive disorders (Drevets et al., 2008b). Furthermore, this area exhibits high densities of 5-HT transporters and 5-HT1A receptors (Varnas et al., 2004), which may enhance its susceptibility to serotonergic manipulations (Talbot & Cooper, 2006). An increased functional connectivity between the DMN and the subgenual prefrontal cortex (sgPFC), the caudal portion of the subcallosal area, is a common finding in depressive disorders (Berman et al., 2011; Greicius et al., 2007). In addition, a recent model proposed that this hyperconnectivity may explain depressive rumination by means of a two-system interaction: the DMN that brings in self-referential processes and the sgPFC that provides emotional loading to these processes (Hamilton et al., 2015).

An elevated connectivity of the DMN is consistently reported in depression (Berman et al., 2011; Greicius et al., 2007; Hamilton et al., 2011; Lois & Wessa, 2016; Sheline et al., 2009; Ye et al., 2015) and individuals at high risk for depression (Posner et al., 2016), illustrating potential neural signatures of disrupted self-referential processing and poor impulse control (Kaiser et al., 2015), functions that are closely related to serotonergic activity (Cha et al., 2018; Dainer-Best et al., 2018). In this light, serotonergic manipulations such as antidepressant agents, were found to normalize the elevated DMN connectivity in depressed patients (Posner et al., 2013) and, similar to our findings, decrease the connectivity between DMN regions and subcortical regions in healthy individuals (McCabe & Mishor, 2011), pointing to a plausible neural substrate of depressive symptoms that can be targeted by medication.

In contrast to the effects of ATL on DMN connectivity and previous studies (Biskup et al., 2016; Helmbold et al., 2016; Kunisato et al., 2011), depleting tryptophan yielded only small effects that failed to reach statistical significance. Furthermore, these effects were numerically in the same direction as ATL i.e., if anything ATD slightly decreased connectivity to the DMN.

While our blood measures indicated that ATD significantly lowered plasma tryptophan levels, the lack of robust neural effects may arise from differences in 5-HT stores among our participants or the presence of adaptive brain processes (Young, 2007) that might prevent significant decreases of brain 5-HT in our healthy individuals compared to psychiatric

populations (Biskup et al., 2016). Furthermore, methodological differences may also explain why others have reported ATD effects. For example, seed-based approaches provide more power due to strong a priori hypotheses regarding the functional connectivity of the seed region and, therefore, capture more subtle connectivity changes (Eisner et al., 2017). Similarly, other ATD studies use resting-state data but analyze measures, like fractional amplitude of low-frequency fluctuation (ALFF; (Kunisato et al., 2011)), that do not quantify functional connectivity (Di et al., 2013). In addition, we suspect that ATD might have smaller effects than found by previous small studies, which leads to an overestimations of effect sizes (Fanelli et al., 2017). In contrast, our study was performed in a larger sample (n = 85), which provided sufficient power (1 − β = .80) to detect small- to medium- sized effects at the behavioral and network level (α = .05; dz = .34) and medium-sized effects at the voxel level (α = .001; dz = .50) (Faul et al., 2007), but still ATD effects were not evident. Lastly, we acknowledge that all these interpretations are speculative and certainly merit future in-depth investigation.

At the behavioral level, none of our measures showed significant changes after correction for multiple testing. Regarding the effects of ATD on mood and anxiety, decreases in these scores are mostly reported in depressed or recovered depressed patients, perhaps reflecting a selective vulnerability of the serotonergic system (Fusar-Poli et al., 2006). In addition, depressed patients might also exhibit associations between mood scores and functional connectivity strengths (Posner et al., 2013; Wang et al., 2015; Zhu et al., 2012), in which symptomatic improvements are correlated with reductions in functional connectivity (Wang et al., 2015). In a similar manner, the effects of ATL on these measures may depend on the initial state of the serotonergic system of the individuals. For example, large doses of tryptophan during the daytime may have calming effects in healthy adults but reduce sleep latency and increase subjective ratings of sleepiness in individuals with sleep disturbances (Hartmann, 1982; Silber & Schmitt, 2010). Since we investigated healthy volunteers, it is not surprising that these changes and associations were not statistically reliable in our study. Lastly, although the serotonergic system is involved in the expression of impulsive behaviors (Miyazaki et al., 2012), our measures of impulsive choice were neither affected by any intervention nor related to functional connectivity changes. Behavioral analyses of this lab support these observations, showing that impulsive choice is not affected by transient changes of tonic 5-HT, but modulated by individual differences in the serotonergic system (Neukam et al., 2018). Nevertheless, our results highlight the role of higher 5-HT brain synthesis as a modulator of the connectivity between the DMN and brain regions involved in emotion processing. One might speculate that diminished serotonergic function in these areas leads to

a hyperconnectivity with the DMN and therefore, promotes depressogenic cognition, but caution is warranted due to the known neurobiological differences between depressed patients and healthy individuals and the distributed nature of depression (Pandya et al., 2012).

### 3.5.1. Limitations

Our study has some limitations. First, it has been shown that short scan lengths impact the reliability of the resting-state data across sessions (Birn et al., 2013), which at the same time, reduces the statistical power and allows the detection of only large effect sizes. Future studies might use improved scanning protocols including longer scanning times (e.g. 9-12 minutes; (Birn et al., 2013)) and accelerated EPI sequences with much shorter TRs (i.e. multiband) which may yield more stable estimates of connectivity strengths, allowing the detection of smaller effects that were not evident in our study (e.g. ATD). In addition, study designs with pre- and post-intervention scans would provide a more stable baseline against which the conditions of interest can be compared. Second, the resting state scan was performed after a decision-making task and a short break (about 2 minutes). Therefore, possible carry-over effects from the previous task cannot be ruled out. To discard these potential confounds, well-tailored studies entirely dedicate to investigate resting-state activity are encouraged. Finally, despite the extended use of tryptophan challenges for more than forty years up to now, the specificity of their action on the serotonergic system remains a matter of debate (Crockett et al., 2012; van Donkelaar et al., 2011). Therefore, further animal and human research is still needed to draw stronger conclusions about the impact of tryptophan challenges on brain 5-HT levels.

### 3.5.2. Conclusion

To sum up, our study is the first to use both ATD and ATL, together with a baseline condition in the same subjects to shed light on acute connectivity changes of the DMN following serotonergic manipulations. Our results expand a large body of ongoing research regarding the serotonergic modulation of the DMN (Biskup et al., 2016; Helmbold et al., 2016; Klaassens et al., 2015; Kunisato et al., 2011; Posner et al., 2013; van de Ven et al., 2013). More specifically, our data support the notion of decreased connectivity between the DMN and emotion-related regions after increasing brain 5-HT levels and suggest that these functional changes represent a key feature for the understanding of the neural basis of depressive symptomatology.

### 3.6.    Acknowledgments

### 3.7. Supplemental Material Study II

#### 3.7.1. Recruitment process

For the first phase of the recruitment process, 15750 letters were sent to randomly selected addresses provided by the registration office of Dresden, Germany. These addresses included an equal number of males and females stratified by age (between 20 and 40 years old). Of those, 1382 individuals answered to our invitation and were telephonically screened by trained psychologists. Exclusion criteria included pregnancy, corrected binocular visus below 0.8, current somatic disease requiring medical treatment, any psychiatric disorders that required pharmacological treatment within the last year, a lifetime history of organic psychiatric disorders (for ICD-10: organic psychiatric disorders (F0), opiate, cocaine, stimulants, hallucinogens, inhalants, or poly-substance dependence, schizophrenia or related personality disorders (F2), affective disorders (F3)) and MRI incompatible conditions. After the telephone screening, 611 participants were invited to a baseline session which included IQ and behavioral assessment as well as weight, height, visus test and blood taking. Four blood samples (36 ml) were collected by venepuncture in 9 ml ethylenediaminetetraacetic acid (EDTA) tubes (Sarstedt, Germany). Three tubes were sent to a collaborating laboratory for genotyping analysis. Results of these analyses are reported elsewhere (Neukam et al., 2018). The blood of the fourth tube was immediately processed by adding 81 µl Aprotinin and centrifuged at 3500 rpm for 8 minutes at 4°C. After this process, the plasma was stored in a fridge at -81°C for the posterior analysis of hormones. All participants were informed about the second phase of the study, provided written informed consent and received monetary compensation at the end of the baseline session.

One hundred and seventy participants were reinvited for the main study. Of those, we excluded: 21 participants due to nausea or vomiting during the first visit, 12 during the second visit and two during the third visit. Additionally, 23 participants could not or refuse to participate after the first or second session. Therefore, one hundred and twelve participants successfully completed all three sessions. Further analysis-specific criteria were applied, resulting in 85 eligible participants for the analyses. The recruitment workflow is depicted in Fig. S2.
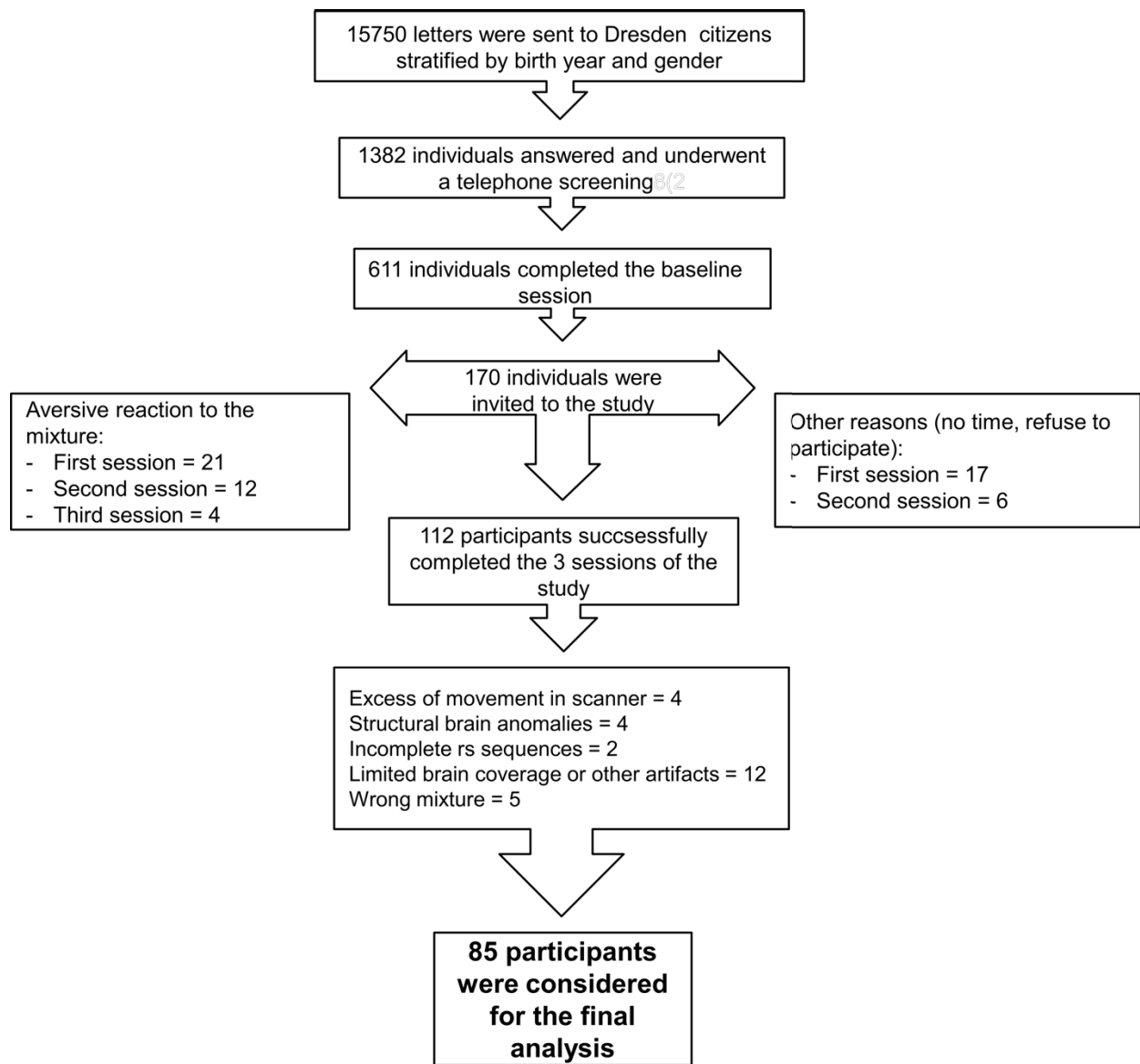
**Fig. S2.** Recruiting and exclusion procedure leading to the final behavioral and imaging datasets.

### 3.7.2. Experimental procedure

In order to minimize negative side effects, the mixtures were prepared in accordance with the participants' body weight (Dingerkus et al., 2012; Moja et al., 1988; Zepf & Poustka, 2008). The mixtures were prepared by a commercial manufacturer (Amino-Factory, Lindenberg, Germany) and mixed about 1 hour before ingestion with 100 ml of warm water and 200 ml of a citric soft drink, resulting in identical tasting drinks for all conditions. Sugar-free candies and extra water were offered ad libitum to minimize the unpleasant taste of the drink. All participants had a urine drug screen at the first visit only (Kombi/DOA10-Schnelltest, MAHSAN Diagnostika GmbH, Reinbek, Germany) and tests for breath alcohol (Alcotest 6810, Drägerwerk AG & Co. KGaA, Lübeck, Germany) and breath carbon monoxide concentration (CO Monitor, Bedfont Scientific Ltd, ME1 3QX, England) at the beginning of each session.

### 3.7.3. Behavioral and mood assessment

An extensive behavioral and mood assessment was conducted during the following three hours after the ingestion of the mixture and before and after the fMRI scan. In addition to the questionnaires reported in the main section of the study, in each session and immediately after the ingestion of the mixture, we evaluated physical activity with the German version of the International Physical Activity Questionnaire (Booth, 2000)). State-related questionnaires acquired for a single time, one hour after the ingestion of the mixture in all sessions included the Beck Depression Inventory (Beck et al., 1961), the Perceived Stress Scale (Cohen et al., 1983) and the State Trait Anxiety Inventory (STAI; (Spielberger, 1983). Demographic and trait-related information were acquired only during the first session and included the German versions of the Snaith-Hamilton Pleasure Scale (Snaith et al., 1995), the Buss-Perry Aggression Questionnaire (Buss & Perry, 1992) and the Melbourne Decision Making Questionnaire (Mann et al., 1997). Finally, other behavioral and cognitive functions related to serotonergic functions were also evaluated during all study sessions. They go beyond the scope of this manuscript and are reported elsewhere (Neukam et al., 2018).

### 3.7.4. Generation of nuisance regressor for Dual regression:

Segmentation of white matter and CSF from the brain-extracted structural images was carried out with FAST ((Zhang et al., 2001) and thresholded with fslmaths (80% of tissue-type likelihood; (Biswal et al., 2010)). FLIRT (Jenkinson et al., 2002) was used for transforming the white matter and CSF masks from the subjects' structural space to their corresponding functional space. Fslmaths was used again to re-binarise the masks after transformation. Preprocessing of the resting state data was carried out a second time, only with motion correction and without temporal and spatial filtering. The white matter and CSF mean time courses were then extracted with fslmeants from this set of non-filtered data and merged with the individual motion parameters obtained with MCFLIRT (the estimated translation along and rotation around the x, y and z axes) during motion correction. Finally, this set of regressors was used during the second stage of dual regression.
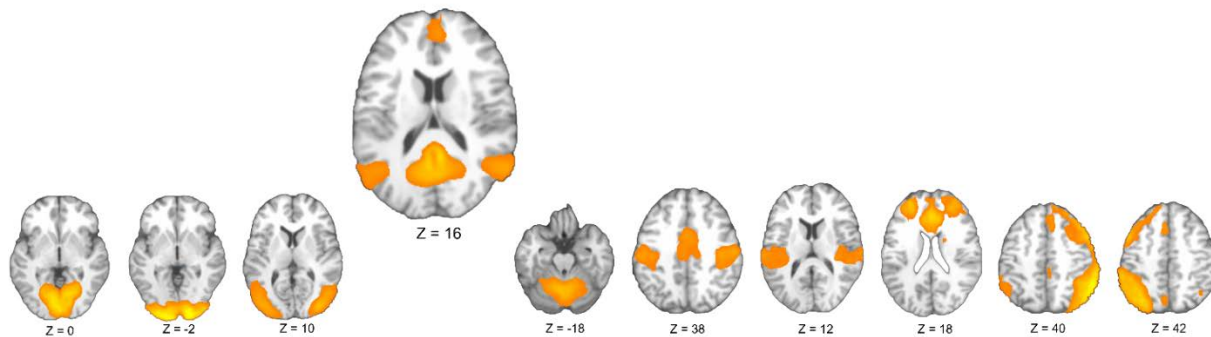


**Fig. S3**. Large-scale brain networks identified in more than 1600 studies by (Smith et al., 2009b). From left to right: high, medial and lateral visual networks, default-mode network, cerebellar network, sensorimotor network, auditory network, cingulo-opercular network, right and left fronto-parietal networks

### 3.7.5. Supplemental results

**Table S4**

TRP/∑LNAA peripheral blood plasma levels

| Time points | ATD | BAL | ATL |
|---|---|---|---|
| | Free tryptophan [µmol/L] | | |
| | Mean (SD) | Mean (SD) | Mean (SD) |
| T0 | 31.90 (7.55) | 33.36 (7.88) | 32.31 (7.12) |
| T1 | 29.13 (10.21) | 48.05 (22.41) | 121.98 (41.59) |
| T2 | 21.52 (9.60) | 42.50 (19.72) | 145.64 (52.72) |
| T3 | 21.87 (9.08) | 33.00 (10.85) | 80.38 (38.01) |
| | TRP/∑LNAA (%) | | |
| | Mean (SD) | Mean (SD) | Mean (SD) |
| T0 | 3.79 (0.64) | 3.89 (0.75) | 3.84 (0.60) |
| T1 | 1.54 (0.52) | 2.32 (0.73) | 7.30 (1.80) |
| T2 | 1.13 (0.60) | 2.02 (0.64) | 8.41 (2.29) |
| T3 | 1.70 (0.76) | 2.53 (0.82) | 6.70 (2.71) |
| | AUC: TRP/∑LNAA (%): Normalized with respect to T0 | | |
| | Mean (SD) | Mean (SD) | Mean (SD) |
| | -13.14 (2.42) | -9.01 (3.24) | 20.80 (11.57) |

N = 71

TRP/∑LNAA (%) = Ratio of tryptophan to the sum of large neutral amino acids, in per cent.

**Table S2**

Additional DMN connectivity results in the contrast ATD < BAL

| Brain region | N° voxels | MNI coordinates (X, Y, Z) | Peak t-value | p-value |
|---|---|---|---|---|
| Middle temporal gyrus | 42 | -50, -58, 8 | 4.27 | 0.068 |
| Frontal orbital cortex | 7 | 24, 14, -16 | 3.94 | 0.077 |

P-values; uncorrected for the six contrasts tested
MNI coordinates correspond to the center of gravity

# CHAPTER 4

---

## 4. GENERAL DISCUSSION

*"They who dream by day are cognizant of many things which escape those who dream only by night".*

*Edgar Allan Poe*

### 4.1.    Research objectives and summary of results

The aim of my doctoral thesis was to examine the importance of RSFC to detect significant functional brain activity associated with both value-based decision-making profiles and after serotonergic challenges. Briefly, in the first study, we presented a well-powered investigation from a large cohort of young adult males (N = 145), comparing a set of value-based decision-making (VBDM) parameters with large-scale ICN, as characterized by an independent component analysis (ICA) and a dual regression approach. Our findings showed that individuals who prefer to gamble in order to avoid a sure loss, exhibited stronger connectivity between the default mode and left frontoparietal systems to their adjacent brain regions, especially to those regions involved in prospective thinking, affective decision-making and visual processing. Although our results are presented as exploratory and follow a somewhat conservative statistical correction procedure, they represent an important contribution for cognitive neuroscience and lay the groundwork for a deeper understanding of the neurobiological bases of impulsive and risk-seeking behaviors. The second study sought to investigate how different brain serotonin (5-HT) levels modulate the connectivity of one of

the most important ICN in the brain, i.e. the default mode network (DMN). Results showed that higher brain 5-HT levels decrease the functional connectivity between the DMN and brain regions involved in emotion regulation. Although in a healthy sample (N = 85), these results mirror the connectivity changes obtained after serotonergic medication in depressed patients and, therefore, suggest a potential link between aberrant DMN connectivity and serotonin levels underlying mood disorders. Both studies are well-powered and present novel methodologies for disentangling the contribution of the ICN to observable human behaviors. Next, I will present a discussion of both studies followed by an integrative approach.

## 4.2. Risk seeking for losses is associated with changes in default mode and frontoparietal systems

As argued in the introduction, one main advantage of the ICA algorithm is that it provides an optimal partition of the fMRI signal into a set of spatio-temporal components, which are thought to represent discrete networks in the brain. In the first study, the ICA algorithm was able to identify 14 ICN in our sample, corresponding to default-mode, frontal, cingulo-opercular, two frontoparietal, basal ganglia, cerebellar, dorsal attention, frontotemporal, three visual and two sensorimotor networks (Fig. 3). Even if this is not the main finding of the study, the identification of ICN in the data have two important methodological implications. First, it confirms the existence of large-scale ICN described in prior work (Damoiseaux et al., 2006; Laird et al., 2011; Smith et al., 2009a). Second, it validates visual inspection as a robust technique for the distinction between noise and ICN, following existing guidelines of neuroimaging research (Griffanti et al., 2017; Kelly et al., 2010).

The main findings confirm the implication of default mode and cognitive control systems in the expression of risky behaviors, although following a different approach in which risk seeking for gains and losses were evaluated separately. This different approach provides novelty to our work, and for the first time, characterized the connectivity profile of risk-seeking (for losses) individuals. Interestingly, the DMN was found to have a regulatory function, especially during young ages when cognitive control and inhibitory networks are still under development (Fair et al., 2008; Uddin et al., 2011). Similarly, frontoparietal networks are dynamic and flexible control systems capable of interacting with other major networks and providing effective top-down control of behavior (Zanto & Gazzaley, 2013). There was no difference in within network connectivity, namely, the strength of both networks did not vary

across decision-making profiles. However, we did observe that individuals who prefer to gamble in order to avoid a sure loss exhibited stronger coupling between the DMN, parahippocampi, OFC and frontopolar regions. The same scores were associated with stronger coupling between the left frontoparietal network and visual areas. Given the implication of both networks in cognitive processes (although the specific role of the DMN in cognition is not fully understood (Margulies et al., 2016)), one might speculate that our findings support the notion of higher activity of these networks associated with a more cautious cognitive style (i.e. prefer the higher but probabilistic loss). Contrary to other studies (Li et al., 2013; S. Wang et al., 2017), we did not observe functional changes associated with delay discounting, loss aversion and risk seeking for gains. While several methodological differences might have caused these results (e.g. bigger sample size, different techniques for resting-state analyses), we needed to consider the complexity of the VBDM constructs assessed in this study (which are tightly mathematically and cognitively defined). Hence, replication of these findings is encouraged. Nonetheless, our results show how the conceptualization of ICN have advanced our understanding beyond a modular view of the brain. We believe that these findings will be of broad interest to researchers keen on integrative approaches to personality research, neuroimaging and decision-making.

## 4.3. Higher serotonin brain synthesis decreases DMN connectivity

The main finding of this study is the decreased DMN connectivity following higher brain 5-HT synthesis. These connectivity changes involved visual cortices, suggesting the contribution of 5-HT circuits to the regulation of posterior attentional and visuospatial systems (Talbot & Cooper, 2006). Most of these connectivity changes were located in brain regions implicated in emotion expression and affect regulation, resembling those changes observed in mood disorders after antidepressant medication (Posner et al., 2013). The serotonergic system plays a significant role in the regulation of mood states (Cowen & Browning, 2015). Consequently, our results can be viewed as evidence of the postulated relationship between DMN hyperconnectivity and depressive symptomatology (Berman et al., 2011; Hamilton et al., 2015).

Changes in the synchronized activity of the DMN indicate differences in phenotypical characteristics (De Pisapia et al., 2016), genetic variations (Glahn et al., 2010) and might be relevant for understanding several neuropsychiatric conditions (for a review see Buckner et al.

(2008a). In more recent days, fMRI experiments have also shown that the DMN is highly susceptible to pharmacological challenges (Biskup et al., 2016; Helmbold et al., 2016; Klaassens et al., 2016; Klaassens et al., 2015; Kunisato et al., 2011; Lehmann et al., 2016; Scheidegger et al., 2012; van de Ven et al., 2013; Zanchi et al., 2016). This is, perhaps, due to the rich innervation of neurotransmitters among its regions (Nagano-Saito et al., 2009; Northoff et al., 2007) and its pivotal role in internal modes of cognition (Buckner et al., 2008a) and emotion processing (Spies et al., 2017). In our study, brain 5-HT synthesis was manipulated using tryptophan, the essential amino acid precursor of 5-HT. One clear advantage of tryptophan challenges is their almost exclusive impact on 5-HT levels (Moja et al., 1988), whereas other serotonergic interventions rarely act just on one neurotransmitter and often produce overlapping side effects (Khalili-Mahani et al., 2017). On the other hand, the major disadvantage of tryptophan manipulations (and other pharmacological interventions in humans) is the impossibility of measuring the real influx of 5-HT into the human brain (van Donkelaar et al., 2011). Since this study used a healthy sample, changes in mood or anxiety scores were neither evident nor related to DMN variations. However, changes in these scores after tryptophan interventions in relation to functional connectivity may be regarded as sensitive biomarkers in depressive patients (Gaffrey et al., 2012; Posner et al., 2013; Wang et al., 2015). Considering the advantages and disadvantages of our design, our findings provide compelling evidence for the role of the serotonergic system in the modulation of the DMN and suggest that similar changes may underlie the improvement of depressive symptomatology, after the administration of serotonergic agents.

## 4.4.    Integration of findings

In chapters 2-3, we have shown that resting-state functional connectivity is a valuable neuroimaging tool for the examination of spontaneous brain signals under resting conditions. Specifically, we were able to identify connectivity differences across decision-making profiles and in response to serotonergic manipulations.

Perhaps more interesting is the fact that the DMN was present in both studies. Recent research has expanded our knowledge about the function of this large-scale associative brain network, suggesting that its work is not limited to resting conditions, as it also plays a pivotal role during automated decision-making under predictable behavioral contexts (Vatansever et al., 2017). Moreover, Margulies et al. (2016) have proposed that the role of the DMN in cognition arises from its position at the top of a representational hierarchy, which acts as a hub

of integration across multiple sensory modalities. These observations, together with our findings, point towards an enhanced connectivity between the DMN and other brain systems supporting higher cognitive functions. The role of the DMN in emotion is perhaps more relevant to understand the findings of our second study. As displayed in Fig. 8, normal processes carried out by the DMN (i.e. self-directed cognition and self-referential mnemonic processes) may be abnormally laden with emotional content from the subgenual PFC (sgPFC). This interplay yields higher functional connectivity between these two systems at the neural level, and ruminative thoughts at the cognitive level (Hamilton et al., 2015). Although this model has received some support from experimental research (Berman et al., 2011; Drevets et al., 1997; Greicius et al., 2007), neuroanatomical studies have failed to find a direct link between these two systems (Johansen-Berg et al., 2008), proposing the role of the medial-dorsal thalamus as a functional mediator (Alexander et al., 1986). Overall, the results from both studies presented in this thesis corroborated the *raison d'être* of the DMN in the emergence of healthy and pathological conditions. In light of the current crisis of reproducibility in neuroimaging research, we believe that the large body of existing literature has already laid a solid groundwork for more hypothesis-driven and less exploratory DMN research.

A more recent application field of RSFC is the predictive value of this technique. For instance, several studies described how ICN's function can predict cognitive or clinical scores (Meskaldji et al., 2016), task-activity (Sala-Llonch et al., 2012), disease evolution (Emerson et al., 2017) and treatment outcomes (Drysdale et al., 2017). Although some similarities between this literature and our work exist, methodological differences prevent us from extrapolating our inferences to the predictive domain. Instead, results from our first study might expand the existing body of literature on normal ICN patterns among decision-making profiles. This would allow comparative analyses with pathological samples in which the activity of default-mode and frontoparietal networks is associated with aberrant decision-making (e.g. addictions (Costumero et al., 2017; Dalwani et al., 2014; Ding et al., 2013; Han et al., 2016; Wang et al., 2017)). In a similar manner, results from our second study may be relevant for the characterization of the intrinsic modulation of the DMN and its implication in the onset of psychopathological conditions (Whitfield-Gabrieli & Ford, 2012).
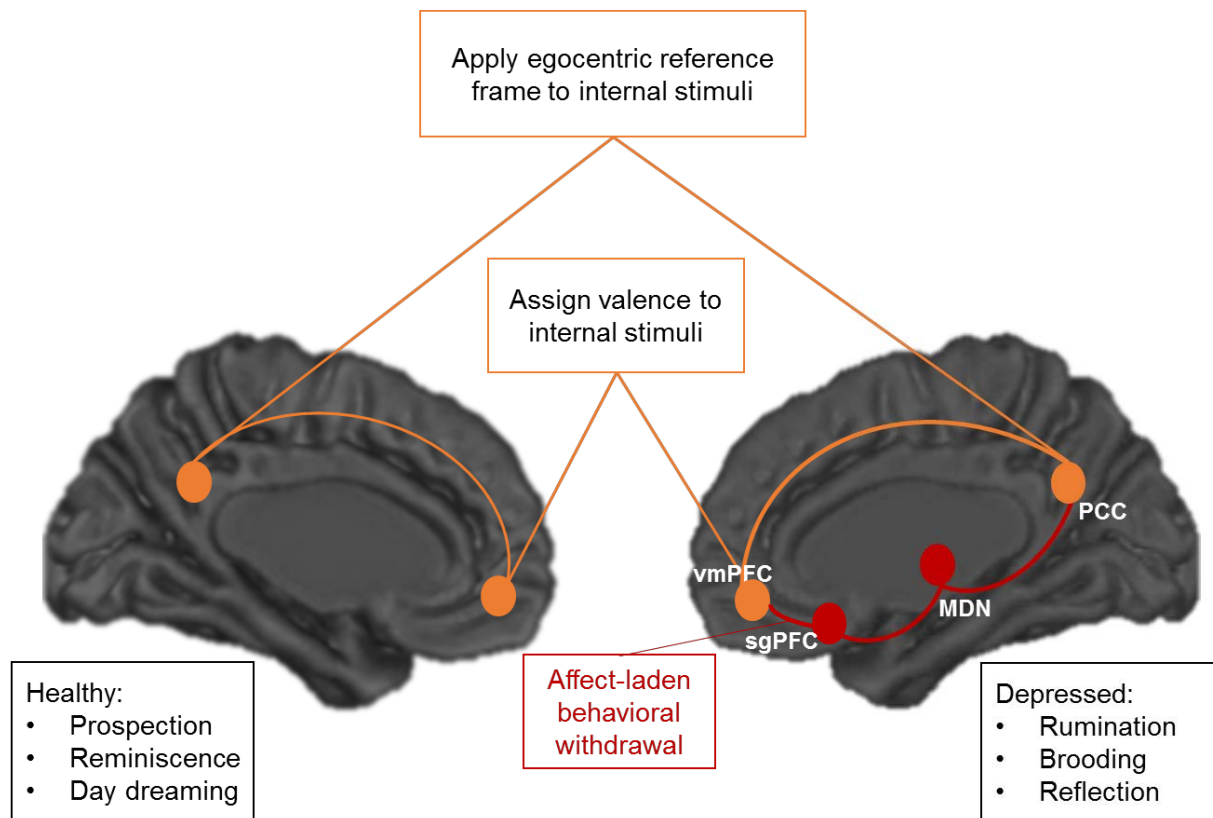
**Figure 8.** Schema of the model proposed by Hamilton et al. (2015) in which depressive rumination is the result of the excessive integration of DMN and sgPFC functions. These is also expressed in a hyperconnectivity between these two systems (adapted from Hamilton et al. (2015)).

### 4.5.    Limitations and future directions

Besides the inherent limitations of the studies presented in this thesis, more general controversies merit comment. As an emerging and not fully consolidated research field, RSFC faces several threats -mostly methodological- that should be carefully considered by current and future research. First, no consensus regarding preprocessing pipelines or statistical guidelines for RSFC analyses exist. However, comparative studies favored some methodological approaches over others (Dipasquale et al., 2017; Preibisch et al., 2015; Pruim et al., 2015b), providing a starting point for the implementation of more sophisticated analyses. Furthermore, due to the concerns about the replicability in neuroimaging research,

a dynamic community of neuroscientists has joined efforts and stablished guidelines for analyses, report of results and data sharing, with especial emphasis on resting-state data (e.g. COBIDAS, (Nichols et al., 2017), Consortium for Reliability and Reproducibility - CoRR[5]). These promising initiatives sought to systematically establish gold standards for data processing and for a successful open science tool for RSFC research. This is particularly important for the development of multimodal neuroimaging biomarkers (Drysdale et al., 2017; Emerson et al., 2017) in which resting-state datasets play a key role.

Second, the brain is a network itself subject to considerable individual differences shaped by anatomical, genetic and epigenetic factors. In RSFC research, such variability encourages the use of larger samples, taking into account the ongoing developmental trajectories of brain connections (Song et al., 2012; Supekar et al., 2010). An outstanding initiative to show the evolution of ICN's properties across the lifespan includes the Human Connectome Project and, more recently, the Baby Connectome project[6]. Despite the inherent challenges of participant recruitment and scanning, structural and functional imaging datasets of healthy adults and children between cero and five years old are being collected. More ambitious attempts to model network properties of the infant brain are *in utero* RSFC studies (Schopf et al., 2012), which have already provided evidence of altered RSFC in the preterm brain (see van den Heuvel and Thomason (2016) for a discussion). These studies will allow to separate intrauterine from extrauterine influences in the configuration of ICN, and thus establish a more comprehensive model of how emerging connectivity patterns shape pathological and normal behavior.

Finally, we need to mention that for a long time RSFC was assumed to be stationary, but recent work has revealed its dynamic nature (Preti et al., 2017). According to this postulate, RSFC has significant temporal variability that can be detected using "sliding window" procedures for example. These windows move across the timecourses, can be of fixed or varying length, and are analyzed at several time-frequency decompositions (Chang & Glover, 2010). Dynamic patterns of RSFC have been already investigated in depression (Kaiser et al., 2016), schizophrenia (Ma et al., 2014) and Alzheimer disease (Jones et al., 2012) among others. Differences between clinical populations and healthy samples are, presumably, due to neurometabolic changes (Thompson, 2017), but further work is necessary to confirm this postulate. To address this and other questions, the scan length is of particular

---

[5] COBIDAS: https://www.humanbrainmapping.org/i4a/pages/index.cfm?pageID=3728 and CoRR: http://fcon_1000.projects.nitrc.org/indi/CoRR/html/index.html respectively
[6] http://www.humanconnectomeproject.org/ and http://babyconnectomeproject.org/ respectively

relevance. Most dynamic RSFC studies focus on time ranges from around 30 seconds to two minutes (Hutchison et al., 2013) and stable estimations of static connectivity strengths are visible only around six minutes (Birn et al., 2013).

All these facts advocate for the design of longer and well-tailored resting-state studies, preferably entirely dedicated to the investigation of RSFC, without the influence of other tasks within the scanner. Ideally, the scan length should be longer than nine minutes to obtain reliable measures of connectivity (Birn, 2012).

### 4.6. General conclusion

This doctoral thesis has provided significant evidence of 1) individual differences in intrinsic network connectivity associated with decision-making profiles and 2) serotonergic modulation of the default mode network. Together, these results added to the existing literature highlighting the use of RSFC as a powerful tool for the noninvasive investigation of the human brain. Specifically, study 1 revealed the participation of default mode and frontoparietal systems in individuals who prefer to avoid sure losses. Interestingly, networks comprising appetite and reward-driven areas did not show any variation, pointing to a novel connectivity finding underlying a decision-making style never explored before. Study 2 revealed that higher serotonin brain synthesis is associated with decreased functional connectivity between the default mode network and emotion-related brain regions, which in turn, provides partial support to the connectivity model underlying depressive rumination. Critically, independent component analysis and dual regression methods were used to identify the networks of interest, lending credence to model-free techniques for the investigation of functional brain connectivity. Different analytical approaches and less-exploratory work is encouraged to yield myriad of functional measures, able to capture more subtle changes in the resting brain. Our work demonstrated that RSFC provides crucial information regarding spontaneous intrinsic brain activity, which may be diagnostically or therapeutically relevant for the understanding of the neurobiological foundations of normal and disruptive behaviors.

## 5. ZUSAMMENFASSUNG

### Hintergrund

Im Jahre 1985 bildeten Dr. Bharat Biswal und Kollegen zum ersten Mal, mithilfe der funktionellen Magnetresonanztomographie (fMRT), spontan entstehende Gehirnsignale im sensorisch-motororischen Kortex in Abwesenheit eines Stimulus oder einer Aufgabe ab. Diese Untersuchung zeigte zweifellos, dass das Gehirn im Wachzustand unter Ruhebedingungen weiterhin arbeitet, was das Konzept der Messung von funktionellen Konnektivitäten im Ruhezustand (RSFC) begründete; eine Technik, die spontane Gehirnfluktuationen im fMRT-Signal aufdeckt. Später begünstigte die dringende Nachfrage Ruhezustandssignale in einer kohärenten Weise darzustellen die Identifikation räumlich konsistenter Muster über mehrere Gehirnregionen hinweg, welche heute als „intrinsische Konnektivitätsnetzwerke" (ICN) bekannt sind. Unter diesen ICN ist das „default mode" Netzwerk (DMN) von besonderer Bedeutung, da es in höhere kognitive Funktionen, selbstbezogene Kognition und psychiatrische Symptomatologie involviert ist.

Insgesamt zeigt das Studium von RSFC, aufgegliedert in unterscheidbare und anti-korrelierte ICN, eine hohe Sensitivität und Spezifizität bei der Entdeckung individueller Unterschiede, die mit einer großen Spanne an Verhaltensmerkmalen und Zuständen assoziiert sind. Weiterhin zeigen die ICN wesentliche Änderungen als Reaktion auf kurzfristig vorangegangene Erfahrungen und pharmakologische Behandlungen; und kürzlich wurde gezeigt, dass diese Netzwerke als Biomarker für Erkrankungen benutzt werden können, sowie auch als Prädiktor für den Ausgang einer Behandlung. Um die oben genannte Informationsmenge zu erweitern, befasst sich diese Doktorarbeit mit der Untersuchung von Änderungen der ICN, die mit 1) phänotypischen Merkmalen und 2) pharmakologischen Manipulationen assoziiert sind. Zur Erreichung dieses Ziels verwendeten wir das Verfahren der Analyse unabhängiger Komponenten (ICA), ein multivariater und datengetriebener Ansatz, der keine a priori Hypothesen oder ein Modell der Gehirnaktivität benötigt.

### Fragestellung

Die zentrale Fragestellung dieser Doktorarbeit war es den Nutzen von RSFC als ein mächtiges Werkzeug zur Untersuchung spontaner Fluktuationen im neuronalen Signal, welches kohärent in ICN strukturiert ist, zu demonstrieren. Im Detail, basierend auf einer

postulierten phänotypischen Variabilität der ICN über mehrere Verhaltensdomänen, untersuchte Studie 1 den Zusammenhang zwischen einer Menge von Parametern zu wertebasiertem Entscheidungsverhalten (VBDM) und die ICN in einer großen Kohorte junger männlicher Erwachsener. Basierend auf einer serotonergen Manipulation des DMN und seiner potentiellen Implikation in der Pathogenese depressiven Grübelns, verwendete Studie 2 eine große Stichprobe gesunder Erwachsener, um zu untersuchen, wie unterschiedliche zentralnervöse Serotoninspiegel die DMN-Konnektivität beeinflussen, als auch ob es potentielle Zusammenhänge zwischen diesen neuronalen Effekten und Stimmungs-, Ängstlichkeits- und Schläfrigkeitsbewertungen gibt.

## Material und Methoden

Für Studie 1 wurden 145 18-jährige, rechtshändige Männer aus Dresden und Berlin rekrutiert, die Teil der andauernden fMRT-Studie „Learning dysfunctions in young adults as predictors for the development of alcohol use disorders" innerhalb des DFG geförderten Forschungsprojektes „Learning and habituation as predictors of the development and maintenance of alcoholism" sind. Am ersten Termin wurde an den Probanden eine ausführliche Erhebung klinischer Merkmale und des Verhaltens durchgeführt, welche auch die Batterie zum Entscheidungsverhalten (VBDM) beinhaltete. Die einzelnen Aufgaben der VBDM verwenden ein Lernschema basierend auf dem Theorem von Bayes, um Diskontierungsraten von Wartezeiten, Wahrscheinlichkeiten bei Gewinnen und Verlusten sowie das Ausmaß von Verlustaversion zu schätzen. Am zweiten Termin führten wir eine sechsminütige Messung der Gehirnaktivität im Ruhezustand, nachfolgend einer Aufgabe zum Entscheidungsverhalten, durch. Vierzehn ICN wurden in den Daten identifiziert; jedoch wurden die Gruppenanalysen unter Verwendung eines nicht-parametrischen Ansatzes ausschließlich mit den Netzwerken durchgeführt, von denen bereits bekannt war, dass sie eine Rolle bei Entscheidungsverhaltensprozessen spielen. Die signifikanten Regionen zeigen, dass die Stärke der Kopplung zwischen diesen Regionen und bestimmten Netzwerken mit einem gegebenen VBDM-Wert assoziiert war.

Für Studie 2 verwendeten wir ein randomisiertes Cross-Over-Design, mit einer Kontrollbedingung und zwei Interventionen, um die Serotoninsynthese im Gehirn mithilfe von Tryptophan, dem diätischen Vorgänger von Serotonin, zu erhöhen oder abzusenken. Fünfundachtzig gesunde Erwachsene nahmen an drei Erhebungen teil, in denen sie eines

der folgenden Getränke erhielten: eines zur akuten Absenkungen von Tryptophan (ATD), ein balanciertes (BAL) oder eines zur akuten Anreicherung von Tryptophan (ATL). Eine sechsminütige Messung der Gehirnaktivität im Ruhezustand wurde 3,5 Stunden nach der Einnahme des Getränkes durchgeführt. Für die fMRT-Analysen wurde das DMN für jeden Probanden zu jeder Sitzung bestimmt. Permutationstests wurden ausgeführt, um Voxel-zu-Netzwerk-Unterschiede zwischen allen Bedingungen zu vergleichen. Zusätzlich wurden Verhaltensmaße bezüglich Ängstlichkeit, Depression und Schläfrigkeit in jeder Sitzung erhoben, um den Einfluss von Tryptophan auf diese Maße zu beobachten, sowie deren mögliche Assoziation mit Veränderungen der Konnektivität des DMN.

Alle fMRT-Analysen dieser Studien wurden mit der Software Library FSL aus dem Softwarepaket Functional Magnetic Resonance Imaging of the Brain (FMRIB) durchgeführt.

## **Ergebnisse**

Die Befunde der ersten Studie zeigten, dass höhere Risikobereitschaft für Verluste mit einer stärkeren Konnektivität zwischen dem „default-mode" und linksseitigen frontoparietalen Systemen und benachbarten Gehirnregionen assoziiert waren, besonders zu denen, die an prospektivem Denken, affektivem Entscheidungsverhalten und visueller Verarbeitung beteiligt sind. Obwohl unsere Ergebnisse als explorativ präsentiert werden und einer recht konservativen statistischen Korrektur folgen, leisten sie einen wichtigen Beitrag zur kognitiven Neurowissenschaft und legen den Grundstein für ein tieferes Verständnis der neurobiologischen Grundlagen impulsiver und risikofreudiger Verhaltensweisen.

Die zweite Studie offenbarte, dass angereicherte Tryptophanspiegel die Konnektivität zwischen dem DMN und emotionsbezogenen Gehirnregionen verringerten. Dies legt nahe, dass diese funktionalen Änderungen ein Hauptmerkmal für das Verständnis der neuralen Basis depressiver Symptomatologie sind. Reduzierte Tryptophanspiegel beeinflussten nicht die Konnektivität. Verhaltensänderungen standen nicht im Zusammenhang mit DMN-Konnektivitätsveränderungen.

**<u>Schlussfolgerungen</u>**

Zusammengefasst leisten diese Ergebnisse einen Betrag zur existierenden Literatur, die den Nutzen von RSFC als mächtiges Werkzeug für die nicht-invasive Untersuchung des menschlichen Gehirns hervorhebt. Im Detail offenbarte Studie 1 die Teilnahme von „default-mode" und frontoparietaler Systeme in Individuen mit höherer Risikobereitschaft (für Verluste). Interessanterweise zeigten Netzwerke, die aus appetits- und belohnungsgetriebenen Arealen bestehen, keine Variation. Dies deutet auf eine neuartige Konnektivität hin, die einem noch nie zuvor erforschten Entscheidungsstil zugrunde liegt. Studie 2 offenbarte, dass eine höhere Serotoninsynthese im Gehirn mit einer reduzierten funktionalen Konnektivität zwischen dem DMN und emotionsbezogenen Gehirnregionen einhergeht, was wiederum anteilig das Konnektivitätsmodell bestärkt, dem depressives Grübeln zugrunde liegt. Entscheidend ist, dass Methoden der unabhängigen Komponentenanalyse und dualen Regression angewandt worden sind, um die interessierenden Netzwerke zu identifizieren, was die Verwendung modellfreier Techniken für die Untersuchung intrinsischer Gehirnkonnektivitäten unterstützt.

## 6. SUMMARY

### Background

In 1985 Dr. Bharat Biswal and colleagues mapped spontaneous brain signals in the human sensorimotor cortex in absence of a task or stimulus for the first time using functional magnetic resonance imaging (fMRI). This investigation undoubtedly demonstrated that the awake brain remains working under resting conditions and introduced the concept of Resting-State Functional-Connectivity (RSFC), a technique that uncovers spontaneous brain fluctuations in the fMRI signal. Later, the urgent demand for presenting resting-state signals in a coherent way promoted the identification of spatially consistent patterns across multiple brain regions, which are known as "intrinsic connectivity networks" (ICN). Among all the ICN, the default mode network (DMN) is of particular interest due to its involvement in higher cognitive functions, self-related cognition and psychiatric symptomatology.

Overall, the study of RSFC organized into consistent and anticorrelated ICN has demonstrated high sensitivity and specificity for detecting individual differences associated with a wide range of behavioral traits and states. Furthermore, ICN show relevant changes in response to recent experiences and pharmacological treatments. And it has been recently demonstrated that these networks can be used as a biomarker of diseases and predictor of treatment outcome. To expand on the above-mentioned body of information, this doctoral thesis investigated changes of ICN associated with 1) phenotypic traits and 2) pharmacological manipulations. For this objective we used Independent Component Analysis (ICA), a multivariate and data-driven approach that requires no a priori hypothesis or model of brain activity.

### Research question

The central question of this doctoral thesis was to demonstrate the utility of RSFC as a powerful tool to investigate spontaneous brain functions, which are coherently structured in ICN. Specifically, based on the postulated phenotypic variability of ICN across several behavioral domains, study 1 investigated the relationship between a set of value-based decision-making (VBDM) scores and ICN in a large cohort of young adult males. Based on the serotonergic modulation of the DMN and its potential implication in the pathogenesis of depressive rumination, study 2 used a large sample of healthy adults to investigate how

90

different brain serotonin levels affect the DMN connectivity as well as potential relationships between these neural effects with mood, anxiety, impulsive choice and sleepiness ratings.

**Material and Methods**

For study 1, 145 18-year-old, right-handed males were recruited from Dresden and Berlin as part of the ongoing longitudinal fMRI study "Learning dysfunctions in young adults as predictors for the development of alcohol use disorders". In the first session, participants completed an extensive behavioral and clinical assessment, which included the Value-Based Decision-Making battery (VBDM). This set of tasks employs a Bayesian learning scheme to estimate delay discounting rate as well as probability discounting rates for gains and losses, and loss aversion. During the second appointment, participants completed a six-minute resting-state scan after a decision-making task. Fourteen ICN were detected in the data, but the higher-level analyses were performed only in the networks previously implicated in decision-making processes using a non-parametric approach. The significant regions resulting from the analyses indicated that the strength of the coupling between these regions and a certain network was associated with a given VBDM score.

For study 2, we used a double-blind, randomized, cross-over design, with a control condition and two interventions to decrease and increase brain serotonin synthesis using tryptophan, the dietary precursor of serotonin. Eighty-five healthy adults took part in three assessments where they received one of the following drinks: acute tryptophan depletion (ATD), balanced (BAL) or acute tryptophan loading (ATL). A six-minute resting-state scan was performed 3.5 hours after the ingestion of the drink. For the fMRI analyses, the DMN was derived for each participant and session. Permutation testing was performed to compare voxel-to-network differences between all conditions. Additionally, behavioral measures of mood, anxiety, impulsive choice and sleepiness were acquired in each session to observe the influence of tryptophan on these measures and their possible association with DMN connectivity changes.

All the fMRI analyses of these studies were performed using the Functional Magnetic Resonance Imaging of the Brain (FMRIB) Software Library (FSL).

## Results

Findings of the first study showed that individuals who preferred to gamble in order to avoid a sure loss, exhibited stronger connectivity between the default mode and left frontoparietal systems to their adjacent brain regions, specially to those involved in prospective thinking, affective decision making and visual processing. Although our findings are presented as exploratory and follow a somewhat conservative statistical correction procedure, they represent an important contribution for cognitive neuroscience and lay the groundwork for a deeper understanding of the neurobiological bases of impulsive and risk-seeking behaviors.

The second study revealed that increased tryptophan levels decreased the connectivity between the DMN and emotion-related brain regions, suggesting that these functional changes represent a key feature for the understanding of the neural basis of depressive symptomatology. Decreased tryptophan levels did not affect brain connectivity. Behavioral scores were neither affected by any intervention nor associated with connectivity changes.

## Conclusion

Together, these results add to the existing literature highlighting the use of RSFC as a powerful tool for the noninvasive investigation of the human brain. Specifically, study 1 revealed the participation of default mode and frontoparietal systems in more risk-seeking (for losses) individuals. Interestingly, networks comprising appetite and reward-driven areas did not show any variation, pointing to a novel connectivity finding underlying a decision-making style never explored before. Study 2 revealed that higher serotonin brain synthesis is associated with decreased functional connectivity between the default mode network and emotion-related brain regions, which, in turn, provides partial support to the connectivity model underlying depressive rumination. Critically, independent component analysis and dual regression methods were used to identify the networks of interest, lending support to model-free techniques for the investigation of intrinsic brain connectivity.

## 7. REFERENCES

Adelstein, J. S., Shehzad, Z., Mennes, M., DeYoung, C. G., Zuo, X. N., Kelly, C., . . . Milham, M. P. (2011). Personality Is Reflected in the Brain's Intrinsic Functional Architecture. *PLoS One, 6*(11). doi:ARTN e2763310.1371/journal.pone.0027633

Ainslie, G. (1975). Specious reward: a behavioral theory of impulsiveness and impulse control. *Psychol Bull, 82*(4), 463-496.

Akerstedt, T., & Gillberg, M. (1990). Subjective and Objective Sleepiness in the Active Individual. *International Journal of Neuroscience, 52*(1-2), 29-37.

Alexander, G. E., Delong, M. R., & Strick, P. L. (1986). Parallel Organization of Functionally Segregated Circuits Linking Basal Ganglia and Cortex. *Annual Review of Neuroscience, 9*, 357-381. doi:DOI 10.1146/annurev.ne.09.030186.002041

Allen, E. A., Erhardt, E. B., Damaraju, E., Gruner, W., Segall, J. M., Silva, R. F., . . . Calhoun, V. D. (2011). A baseline for the multivariate comparison of resting-state networks. *Front Syst Neurosci, 5*, 2. doi:10.3389/fnsys.2011.00002

Altmann, A., Schroter, M. S., Spoormaker, V. I., Kiem, S. A., Jordan, D., Ilg, R., . . . Samann, P. G. (2016). Validation of non-REM sleep stage decoding from resting state fMRI using linear support vector machines. *Neuroimage, 125*, 544-555. doi:10.1016/j.neuroimage.2015.09.072

Aminoff, E. M., Kveraga, K., & Bar, M. (2013). The role of the parahippocampal cortex in cognition. *Trends Cogn Sci, 17*(8), 379-390. doi:10.1016/j.tics.2013.06.009

Amlung, M., Vedelago, L., Acker, J., Balodis, I., & MacKillop, J. (2017). Steep delay discounting and addictive behavior: a meta-analysis of continuous associations. *Addiction, 112*(1), 51-62. doi:10.1111/add.13535

Andrews-Hanna, J. R., Reidler, J. S., Sepulcre, J., Poulin, R., & Buckner, R. L. (2010). Functional-anatomic fractionation of the brain's default network. *Neuron, 65*(4), 550-562. doi:10.1016/j.neuron.2010.02.005

Anticevic, A., Cole, M. W., Murray, J. D., Corlett, P. R., Wang, X. J., & Krystal, J. H. (2012). The role of default network deactivation in cognition and disease. *Trends in Cognitive Sciences, 16*(12), 584-592. doi:10.1016/j.tics.2012.10.008

Baik, J. H. (2013). Dopamine signalling in reward-related behaviours. *Frontiers in Neural Circuits, 7*. doi:UNSP 15210.3389/fncir.2013.00152

Ball, I. L., Farnill, D., & Wangeman, J. F. (1984). Sex and Age-Differences in Sensation Seeking - Some National Comparisons. *British Journal of Psychology, 75*(May), 257-265.

Barkley-Levenson, E., & Galvan, A. (2014). Neural representation of expected value in the adolescent brain. *Proc Natl Acad Sci U S A, 111*(4), 1646-1651. doi:10.1073/pnas.1319762111

Bartra, O., McGuire, J. T., & Kable, J. W. (2013). The valuation system: a coordinate-based meta-analysis of BOLD fMRI experiments examining neural correlates of subjective value. *Neuroimage, 76*, 412-427. doi:10.1016/j.neuroimage.2013.02.063

Beaty, R. E., Benedek, M., Kaufman, S. B., & Silvia, P. J. (2015). Default and Executive Network Coupling Supports Creative Idea Production. *Sci Rep, 5*, 10964. doi:10.1038/srep10964

Beaty, R. E., Kenett, Y. N., Christensen, A. P., Rosenberg, M. D., Benedek, M., Chen, Q. L., . . . Silvia, P. J. (2018). Robust prediction of individual creative ability from brain functional

connectivity. *Proceedings of the National Academy of Sciences of the United States of America, 115*(5), 1087-1092. doi:10.1073/pnas.1713532115

Beck, A. T., Ward, C. H., Mendelson, M., Mock, J., & Erbaugh, J. (1961). An inventory for measuring depression. *Arch Gen Psychiatry, 4*, 561-571.

Beckmann, C. F., DeLuca, M., Devlin, J. T., & Smith, S. M. (2005). Investigations into resting-state connectivity using independent component analysis. *Philosophical Transactions of the Royal Society B-Biological Sciences, 360*(1457), 1001-1013. doi:10.1098/rstb.2005.1634

Beckmann, C. F., Mackay, C. E., Nicola, F., & Smith, S. M. (2009). Group comparison of resting-state FMRI data using multi-subject ICA and dual regression. *OHBM*.

Beckmann, C. F., & Smith, S. M. (2004). Probabilistic independent component analysis for functional magnetic resonance imaging. *IEEE Trans Med Imaging, 23*(2), 137-152. doi:10.1109/TMI.2003.822821

Bell, A. J., & Sejnowski, T. J. (1995). An Information Maximization Approach to Blind Separation and Blind Deconvolution. *Neural Computation, 7*(6), 1129-1159. doi:DOI 10.1162/neco.1995.7.6.1129

Berman, M. G., Peltier, S., Nee, D. E., Kross, E., Deldin, P. J., & Jonides, J. (2011). Depression, rumination and the default network. *Soc Cogn Affect Neurosci, 6*(5), 548-555. doi:10.1093/scan/nsq080

Bernhardt, N., Nebe, S., Pooseh, S., Sebold, M., Sommer, C., Birkenstock, J., . . . Smolka, M. N. (2017). Impulsive decision making in young adult social drinkers and detoxified alcohol-dependent patients: A cross-sectional and longitudinal study. *Alcoholism: Clinical and Experimental Research.* doi:10.1111/acer.13481

Birn, R. M. (2012). The role of physiological noise in resting-state functional connectivity. *Neuroimage, 62*(2), 864-870. doi:10.1016/j.neuroimage.2012.01.016

Birn, R. M., Molloy, E. K., Patriat, R., Parker, T., Meier, T. B., Kirk, G. R., . . . Prabhakaran, V. (2013). The effect of scan length on the reliability of resting-state fMRI connectivity estimates. *Neuroimage, 83*, 550-558. doi:10.1016/j.neuroimage.2013.05.099

Biskup, C. S., Helmbold, K., Baurmann, D., Klasen, M., Gaber, T. J., Bubenzer-Busch, S., . . . Zepf, F. D. (2016). Resting state default mode network connectivity in children and adolescents with ADHD after acute tryptophan depletion. *Acta Psychiatrica Scandinavica, 134*(2), 161-171. doi:10.1111/acps.12573

Biskup, C. S., Sanchez, C. L., Arrant, A., Van Swearingen, A. E., Kuhn, C., & Zepf, F. D. (2012). Effects of acute tryptophan depletion on brain serotonin function and concentrations of dopamine and norepinephrine in C57BL/6J and BALB/cJ mice. *PLoS One, 7*(5), e35916. doi:10.1371/journal.pone.0035916

Biswal, B., Yetkin, F. Z., Haughton, V. M., & Hyde, J. S. (1995). Functional connectivity in the motor cortex of resting human brain using echo-planar MRI. *Magn Reson Med, 34*(4), 537-541.

Biswal, B. B., Mennes, M., Zuo, X. N., Gohel, S., Kelly, C., Smith, S. M., . . . Milham, M. P. (2010). Toward discovery science of human brain function. *Proceedings of the National Academy of Sciences of the United States of America, 107*(10), 4734-4739. doi:10.1073/pnas.0911855107

Blum, R. W., & Nelson-Mmari, K. (2004). The health of young people in a global context. *Journal of Adolescent Health, 35*(5), 402-418. doi:10.1016/j.jadohealth.2003.10.007

Booth, M. (2000). Assessment of physical activity: an international perspective. *Res Q Exerc Sport, 71*(2 Suppl), S114-120.

Braams, B. R., van Duijvenvoorde, A. C., Peper, J. S., & Crone, E. A. (2015). Longitudinal changes in adolescent risk-taking: a comprehensive study of neural responses to rewards, pubertal development, and risk-taking behavior. *J Neurosci, 35*(18), 7226-7238. doi:10.1523/JNEUROSCI.4764-14.2015

Brainard, D. H. (1997). The Psychophysics Toolbox. *Spat Vis, 10*(4), 433-436.

Buckner, R. L., Andrews-Hanna, J. R., & Schacter, D. L. (2008a). The brain's default network - Anatomy, function, and relevance to disease. *Year in Cognitive Neuroscience 2008, 1124*, 1-38. doi:10.1196/annals.1440.011

Buckner, R. L., Andrews-Hanna, J. R., & Schacter, D. L. (2008b). The brain's default network: anatomy, function, and relevance to disease. *Ann N Y Acad Sci, 1124*, 1-38. doi:10.1196/annals.1440.011

Burnett, S., Bault, N., Coricelli, G., & Blakemore, S. J. (2010). Adolescents' heightened risk-seeking in a probabilistic gambling task. *Cognitive Development, 25*(2), 183-196. doi:10.1016/j.cogdev.2009.11.003

Buss, A. H., & Perry, M. (1992). The Aggression Questionnaire. *Journal of Personality and Social Psychology, 63*(3), 452-459. doi:Doi 10.1037//0022-3514.63.3.452

Calhoun, V. D., Adali, T., Pearlson, G. D., & Pekar, J. J. (2001). A method for making group inferences from functional MRI data using independent component analysis. *Human Brain Mapping, 14*(3), 140-151. doi:DOI 10.1002/hbm.1048

Carbonell, F., Nagano-Saito, A., Leyton, M., Cisek, P., Benkelfat, C., He, Y., & Dagher, A. (2014). Dopamine precursor depletion impairs structure and efficiency of resting state brain functional networks. *Neuropharmacology, 84*, 90-100. doi:10.1016/j.neuropharm.2013.12.021

Castellanos, F. X., Margulies, D. S., Kelly, C., Uddin, L. Q., Ghaffari, M., Kirsch, A., . . . Milham, M. P. (2008). Cingulate-precuneus interactions: A new locus of dysfunction in adult attention-deficit/hyperactivity disorder. *Biological Psychiatry, 63*(3), 332-337. doi:10.1016/j.biopsych.2007.06.025

Cha, J., Guffanti, G., Gingrich, J., Talati, A., Wickramaratne, P., Weissman, M., & Posner, J. (2018). Effects of Serotonin Transporter Gene Variation on Impulsivity Mediated by Default Mode Network: A Family Study of Depression. *Cerebral Cortex, 28*(6), 1911-1921. doi:10.1093/cercor/bhx097

Chang, C., & Glover, G. H. (2010). Time-frequency dynamics of resting-state brain connectivity measured with fMRI. *Neuroimage, 50*(1), 81-98. doi:10.1016/j.neuroimage.2009.12.011

Christopoulos, G. I., Tobler, P. N., Bossaerts, P., Dolan, R. J., & Schultz, W. (2009). Neural Correlates of Value, Risk, and Risk Aversion Contributing to Decision Making under Risk. *Journal of Neuroscience, 29*(40), 12574-12583. doi:10.1523/Jneurosci.2614-09.2009

Cohen, S., Kamarck, T., & Mermelstein, R. (1983). A global measure of perceived stress. *J Health Soc Behav, 24*(4), 385-396.

Cole, D. M., Beckmann, C. F., Oei, N. Y., Both, S., van Gerven, J. M., & Rombouts, S. A. (2013). Differential and distributed effects of dopamine neuromodulations on resting-state network connectivity. *Neuroimage, 78*, 59-67. doi:10.1016/j.neuroimage.2013.04.034

Cole, D. M., Smith, S. M., & Beckmann, C. F. (2010). Advances and pitfalls in the analysis and interpretation of resting-state FMRI data. *Front Syst Neurosci, 4*, 8. doi:10.3389/fnsys.2010.00008

Cools, R., Roberts, A. C., & Robbins, T. W. (2008). Serotoninergic regulation of emotional and behavioural control processes. *Trends Cogn Sci, 12*(1), 31-40. doi:10.1016/j.tics.2007.10.011

Costumero, V., Rosell-Negre, P., Bustamante, J. C., Fuentes-Claramonte, P., Llopis, J. J., Avila, C., & Barros-Loscertales, A. (2017). Left frontoparietal network activity is modulated by drug stimuli in cocaine addiction. *Brain Imaging Behav*. doi:10.1007/s11682-017-9799-3

Cowen, P. J., & Browning, M. (2015). What has serotonin to do with depression? *World Psychiatry, 14*(2), 158-160. doi:10.1002/wps.20229

Cox, C. L., Gotimer, K., Roy, A. K., Castellanos, F. X., Milham, M. P., & Kelly, C. (2010). Your Resting Brain CAREs about Your Risky Behavior. *PLoS One, 5*(8). doi:ARTN e1229610.1371/journal.pone.0012296

Craddock, R. C., Holtzheimer, P. E., 3rd, Hu, X. P., & Mayberg, H. S. (2009). Disease state prediction from resting state functional connectivity. *Magn Reson Med, 62*(6), 1619-1628. doi:10.1002/mrm.22159

Crittenden, B., Mitchell, D. J., & Duncan, J. (2015). Recruitment of the default mode network during a demanding act of executive control. *Elife, 4*. doi:ARTN e0648110.7554/eLife.06481

Crockett, M. J., Clark, L., Roiser, J. P., Robinson, O. J., Cools, R., Chase, H. W., . . . Robbins, T. W. (2012). Converging evidence for central 5-HT effects in acute tryptophan depletion. *Mol Psychiatry, 17*(2), 121-123. doi:10.1038/mp.2011.106

Crockford, D. N., Goodyear, B., Edwards, J., Quickfall, J., & el-Guebaly, N. (2005). Cue-induced brain activity in pathological gamblers. *Biological Psychiatry, 58*(10), 787-795. doi:10.1016/j.biopsych.2005.04.037

Cservenka, A., Casimo, K., Fair, D. A., & Nagel, B. J. (2014). Resting state functional connectivity of the nucleus accumbens in youth with a family history of alcoholism. *Psychiatry Res, 221*(3), 210-219. doi:10.1016/j.pscychresns.2013.12.004

Dainer-Best, J., Disner, S. G., McGeary, J. E., Hamilton, B. J., & Beevers, C. G. (2018). Negative self-referential processing is associated with genetic variation in the serotonin transporter-linked polymorphic region (5-HTTLPR): Evidence from two independent studies. *PLoS One, 13*(6). doi:ARTN e019895010.1371/journal.pone.0198950

Dalwani, M. S., Tregellas, J. R., Andrews-Hanna, J. R., Mikulich-Gilbertson, S. K., Raymond, K. M., Banich, M. T., . . . Sakai, J. T. (2014). Default mode network activity in male adolescents with conduct and substance use disorder. *Drug Alcohol Depend, 134*, 242-250. doi:10.1016/j.drugalcdep.2013.10.009

Damoiseaux, J. S., Rombouts, S. A. R. B., Barkhof, F., Scheltens, P., Stam, C. J., Smith, S. M., & Beckmann, C. F. (2006). Consistent resting-state networks across healthy subjects. *Proceedings of the National Academy of Sciences of the United States of America, 103*(37), 13848-13853. doi:10.1073/pnas.0601417103

Davis, F. C., Knodt, A. R., Sporns, O., Lahey, B. B., Zald, D. H., Brigidi, B. D., & Hariri, A. R. (2013). Impulsivity and the modular organization of resting-state neural networks. *Cereb Cortex, 23*(6), 1444-1452. doi:10.1093/cercor/bhs126

De Pisapia, N., Bacci, F., Parrott, D., & Melcher, D. (2016). Brain networks for visual creativity: a functional connectivity study of planning a visual artwork. *Scientific Reports, 6*. doi:ARTN 3918510.1038/srep39185

DeWitt, S. J., Aslan, S., & Filbey, F. M. (2014). Adolescent risk-taking and resting state functional connectivity. *Psychiatry Research-Neuroimaging, 222*(3), 157-164. doi:10.1016/j.pscychresns.2014.03.009

Deza Araujo, Y. I., Nebe, S., Neukam, P. T., Pooseh, S., Sebold, M., Garbusow, M., . . . Smolka, M. N. (2018). Risk seeking for losses modulates the functional connectivity of the default mode and left frontoparietal networks in young males. *Cognitive, Affective, & Behavioral Neuroscience*. doi:10.3758/s13415-018-0586-4

Di, X., Kim, E. H., Huang, C. C., Tsai, S. J., Lin, C. P., & Biswal, B. B. (2013). The influence of the amplitude of low-frequency fluctuations on resting-state functional connectivity. *Front Hum Neurosci, 7*, 118. doi:10.3389/fnhum.2013.00118

Dickman, S. J. (1990). Functional and dysfunctional impulsivity: personality and cognitive correlates. *J Pers Soc Psychol, 58*(1), 95-102.

Ding, W. N., Sun, J. H., Sun, Y. W., Zhou, Y., Li, L., Xu, J. R., & Du, Y. S. (2013). Altered default network resting-state functional connectivity in adolescents with Internet gaming addiction. *PLoS One, 8*(3), e59902. doi:10.1371/journal.pone.0059902

Dingerkus, V. L., Gaber, T. J., Helmbold, K., Bubenzer, S., Eisert, A., Sanchez, C. L., & Zepf, F. D. (2012). Acute tryptophan depletion in accordance with body weight: influx of amino acids across the blood-brain barrier. *J Neural Transm (Vienna), 119*(9), 1037-1045. doi:10.1007/s00702-012-0793-z

Dipasquale, O., Sethi, A., Lagana, M. M., Baglio, F., Baselli, G., Kundu, P., . . . Cercignani, M. (2017). Comparing resting state fMRI de-noising approaches using multi- and single-echo acquisitions. *PLoS One, 12*(3). doi:ARTN e017328910.1371/journal.pone.0173289

Dixon, W. J. (1960). Simplified Estimation from Censored Normal Samples. *Annals of Mathematical Statistics, 31*(2), 385-391. doi:DOI 10.1214/aoms/1177705900

Dosenbach, N. U., Fair, D. A., Miezin, F. M., Cohen, A. L., Wenger, K. K., Dosenbach, R. A., . . . Petersen, S. E. (2007). Distinct brain networks for adaptive and stable task control in humans. *Proc Natl Acad Sci U S A, 104*(26), 11073-11078. doi:10.1073/pnas.0704320104

Dougherty, D. M., Richard, D. M., James, L. M., & Mathias, C. W. (2010). Effects of acute tryptophan depletion on three different types of behavioral impulsivity. *Int J Tryptophan Res, 3*, 99-111.

Drevets, W. C., Price, J. L., & Furey, M. L. (2008a). Brain structural and functional abnormalities in mood disorders: implications for neurocircuitry models of depression. *Brain Struct Funct, 213*(1-2), 93-118. doi:10.1007/s00429-008-0189-x

Drevets, W. C., Price, J. L., Simpson, J. R., Todd, R. D., Reich, T., Vannier, M., & Raichle, M. E. (1997). Subgenual prefrontal cortex abnormalities in mood disorders. *Nature, 386*(6627), 824-827. doi:DOI 10.1038/386824a0

Drevets, W. C., Savitz, J., & Trimble, M. (2008b). The subgenual anterior cingulate cortex in mood disorders. *CNS Spectr, 13*(8), 663-681.

Drysdale, A. T., Grosenick, L., Downar, J., Dunlop, K., Mansouri, F., Meng, Y., . . . Liston, C. (2017). Resting-state connectivity biomarkers define neurophysiological subtypes of depression (vol 23, pg 28, 2016). *Nature Medicine, 23*(2), 264-264.

Eisner, P., Klasen, M., Wolf, D., Zerres, K., Eggermann, T., Eisert, A., . . . Mathiak, K. (2017). Cortico-limbic connectivity in MAOA-L carriers is vulnerable to acute tryptophan depletion. *Hum Brain Mapp, 38*(3), 1622-1635. doi:10.1002/hbm.23475

Eklund, A., Nichols, T. E., & Knutsson, H. (2016). Cluster failure: Why fMRI inferences for spatial extent have inflated false-positive rates. *Proc Natl Acad Sci U S A, 113*(28), 7900-7905. doi:10.1073/pnas.1602413113

Ekstrom, A. (2010). How and when the fMRI BOLD signal relates to underlying neural activity: the danger in dissociation. *Brain Res Rev, 62*(2), 233-244. doi:10.1016/j.brainresrev.2009.12.004

Emerson, R. W., Adams, C., Nishino, T., Hazlett, H. C., Wolff, J. J., Zwaigenbaum, L., . . . Network, I. (2017). Functional neuroimaging of high-risk 6-month-old infants predicts a diagnosis of autism at 24 months of age. *Science Translational Medicine, 9*(393). doi:ARTN eaag288210.1126/scitranslmed.aag2882

Esposito, F., Tessitore, A., Giordano, A., De Micco, R., Paccone, A., Conforti, R., . . . Tedeschi, G. (2013). Rhythm-specific modulation of the sensorimotor network in drug-naive patients with Parkinson's disease by levodopa. *Brain, 136*(Pt 3), 710-725. doi:10.1093/brain/awt007

Fair, D. A., Cohen, A. L., Dosenbach, N. U. F., Church, J. A., Miezin, F. M., Barch, D. M., . . . Schlaggar, B. L. (2008). The maturing architecture of the brain's default network. *Proceedings of the National Academy of Sciences of the United States of America, 105*(10), 4028-4032. doi:10.1073/pnas.0800376105

Fanelli, D., Costas, R., & Ioannidis, J. P. (2017). Meta-assessment of bias in science. *Proc Natl Acad Sci U S A, 114*(14), 3714-3719. doi:10.1073/pnas.1618569114

Faul, F., Erdfelder, E., Lang, A. G., & Buchner, A. (2007). G*Power 3: a flexible statistical power analysis program for the social, behavioral, and biomedical sciences. *Behav Res Methods, 39*(2), 175-191.

Filippini, N., MacIntosh, B. J., Hough, M. G., Goodwin, G. M., Frisoni, G. B., Smith, S. M., . . . Mackay, C. E. (2009). Distinct patterns of brain activity in young carriers of the APOE-epsilon4 allele. *Proc Natl Acad Sci U S A, 106*(17), 7209-7214. doi:10.1073/pnas.0811879106

Flodin, P., Gospic, K., Petrovic, P., & Fransson, P. (2012). Effects of L-dopa and oxazepam on resting-state functional magnetic resonance imaging connectivity: a randomized, cross-sectional placebo study. *Brain Connect, 2*(5), 246-253. doi:10.1089/brain.2012.0081

Fox, M. D., Snyder, A. Z., Vincent, J. L., Corbetta, M., Van Essen, D. C., & Raichle, M. E. (2005). The human brain is intrinsically organized into dynamic, anticorrelated functional networks. *Proceedings of the National Academy of Sciences of the United States of America, 102*(27), 9673-9678. doi:10.1073/pnas.0504136102

Franken, I. H., van Strien, J. W., Nijs, I., & Muris, P. (2008). Impulsivity is associated with behavioral decision-making deficits. *Psychiatry Res, 158*(2), 155-163. doi:10.1016/j.psychres.2007.06.002

Fusar-Poli, P., Allen, P., McGuire, P., Placentino, A., Cortesi, M., & Perez, J. (2006). Neuroimaging and electrophysiological studies of the effects of acute tryptophan

depletion: a systematic review of the literature. *Psychopharmacology, 188*(2), 131-143. doi:10.1007/s00213-006-0493-1

Gaffrey, M. S., Luby, J. L., Botteron, K., Repovs, G., & Barch, D. M. (2012). Default mode network connectivity in children with a history of preschool onset depression. *Journal of Child Psychology and Psychiatry, 53*(9), 964-972. doi:10.1111/j.1469-7610.2012.02552.x

Galvan, A., Hare, T., Voss, H., Glover, G., & Casey, B. J. (2007). Risk-taking and the adolescent brain: who is at risk? *Dev Sci, 10*(2), F8-F14. doi:10.1111/j.1467-7687.2006.00579.x

Gess, J. L., Fausett, J. S., Kearney-Ramos, T. E., Kilts, C. D., & James, G. A. (2014). Task-dependent recruitment of intrinsic brain networks reflects normative variance in cognition. *Brain and Behavior, 4*(5), 650-664. doi:10.1002/brb3.243

Glahn, D. C., Winkler, A. M., Kochunov, P., Almasy, L., Duggirala, R., Carless, M. A., . . . Blangero, J. (2010). Genetic control over the resting brain. *Proc Natl Acad Sci U S A, 107*(3), 1223-1228. doi:10.1073/pnas.0909969107

Goldstein, R. Z., & Volkow, N. D. (2011). Dysfunction of the prefrontal cortex in addiction: neuroimaging findings and clinical implications. *Nature Reviews Neuroscience, 12*(11), 652-669. doi:10.1038/nrn3119

Green, L., Myerson, J., & Ostaszewski, P. (1999). Amount of reward has opposite effects on the discounting of delayed and probabilistic outcomes. *J Exp Psychol Learn Mem Cogn, 25*(2), 418-427.

Greicius, M. D., Flores, B. H., Menon, V., Glover, G. H., Solvason, H. B., Kenna, H., . . . Schatzberg, A. F. (2007). Resting-state functional connectivity in major depression: abnormally increased contributions from subgenual cingulate cortex and thalamus. *Biol Psychiatry, 62*(5), 429-437. doi:10.1016/j.biopsych.2006.09.020

Greicius, M. D., Krasnow, B., Reiss, A. L., & Menon, V. (2003). Functional connectivity in the resting brain: A network analysis of the default mode hypothesis. *Proceedings of the National Academy of Sciences of the United States of America, 100*(1), 253-258. doi:10.1073/pnas.0135058100

Greve, D. N., & Fischl, B. (2009). Accurate and robust brain image alignment using boundary-based registration. *Neuroimage, 48*(1), 63-72. doi:10.1016/j.neuroimage.2009.06.060

Griffanti, L., Douaud, G., Bijsterbosch, J., Evangelisti, S., Alfaro-Almagro, F., Glasser, M. F., . . . Smith, S. M. (2017). Hand classification of fMRI ICA noise components. *Neuroimage, 154*, 188-205. doi:10.1016/j.neuroimage.2016.12.036

Grill-Spector, K., & Malach, R. (2004). The human visual cortex. *Annual Review of Neuroscience, 27*, 649-677. doi:10.1146/annurev.neuro.27.070203.144220

Grimes, M. A., Cameron, J. L., & Fernstrom, J. D. (2000). Cerebrospinal fluid concentrations of tryptophan and 5-hydroxyindoleacetic acid in Macaca mulatta: diurnal variations and response to chronic changes in dietary protein intake. *Neurochem Res, 25*(3), 413-422.

Hamilton, J. P., Farmer, M., Fogelman, P., & Gotlib, I. H. (2015). Depressive Rumination, the Default-Mode Network, and the Dark Matter of Clinical Neuroscience. *Biol Psychiatry, 78*(4), 224-230. doi:10.1016/j.biopsych.2015.02.020

Hamilton, J. P., Furman, D. J., Chang, C., Thomason, M. E., Dennis, E., & Gotlib, I. H. (2011). Default-mode and task-positive network activity in major depressive disorder:

implications for adaptive and maladaptive rumination. *Biol Psychiatry, 70*(4), 327-333. doi:10.1016/j.biopsych.2011.02.003

Han, D. H., Kim, S. M., Bae, S., Renshaw, P. F., & Anderson, J. S. (2016). A failure of suppression within the default mode network in depressed adolescents with compulsive internet game play. *J Affect Disord, 194*, 57-64. doi:10.1016/j.jad.2016.01.013

Hartmann, E. (1982). Effects of L-tryptophan on sleepiness and on sleep. *J Psychiatr Res, 17*(2), 107-113.

Hearne, L. J., Mattingley, J. B., & Cocchi, L. (2016). Functional brain networks related to individual differences in human intelligence at rest. *Scientific Reports, 6*. doi:ARTN 3232810.1038/srep32328

Helmbold, K., Zvyagintsev, M., Dahmen, B., Biskup, C. S., Bubenzer-Busch, S., Gaber, T. J., . . . Zepf, F. D. (2016). Serotonergic modulation of resting state default mode network connectivity in healthy women. *Amino Acids, 48*(4), 1109-1120. doi:10.1007/s00726-015-2137-4

Henle, T., Walter, H., Krause, I., & Klostermeyer, H. (1991). Efficient Determination of Individual Maillard Compounds in Heat-Treated Milk Products by Amino Acid Analysis. *International Dairy Journal, 1*(2), 125-135. doi:Doi 10.1016/0958-6946(91)90004-R

Hillman, E. M. C. (2014). Coupling Mechanism and Significance of the BOLD Signal: A Status Report. *Annual Review of Neuroscience, Vol 37, 37*, 161-181. doi:10.1146/annurev-neuro-071013-014111

Hornung, J. P. (2003). The human raphe nuclei and the serotonergic system. *Journal of Chemical Neuroanatomy, 26*(4), 331-343. doi:10.1016/j.jchemneu.2003.10.002

Hsu, W. T., Rosenberg, M. D., Scheinost, D., Constable, R. T., & Chun, M. M. (2018). Resting-state functional connectivity predicts neuroticism and extraversion in novel individuals. *Soc Cogn Affect Neurosci, 13*(2), 224-232. doi:10.1093/scan/nsy002

Hutchison, R. M., Womelsdorf, T., Gati, J. S., Everling, S., & Menon, R. S. (2013). Resting-state networks show dynamic functional connectivity in awake humans and anesthetized macaques. *Hum Brain Mapp, 34*(9), 2154-2177. doi:10.1002/hbm.22058

Ingvar, D. H. (1979). "Hyperfrontal" distribution of the cerebral grey matter flow in resting wakefulness; on the functional anatomy of the conscious state. *Acta Neurol Scand, 60*(1), 12-25.

Jenkins, T. A., Nguyen, J. C., Polglaze, K. E., & Bertrand, P. P. (2016). Influence of Tryptophan and Serotonin on Mood and Cognition with a Possible Role of the Gut-Brain Axis. *Nutrients, 8*(1). doi:10.3390/nu8010056

Jenkinson, M., Bannister, P., Brady, M., & Smith, S. (2002). Improved optimization for the robust and accurate linear registration and motion correction of brain images. *Neuroimage, 17*(2), 825-841. doi:10.1006/nimg.2002.1132

Jenkinson, M., Beckmann, C. F., Behrens, T. E., Woolrich, M. W., & Smith, S. M. (2012). Fsl. *Neuroimage, 62*(2), 782-790. doi:10.1016/j.neuroimage.2011.09.015

Johansen-Berg, H., Gutman, D. A., Behrens, T. E. J., Matthews, P. M., Rushworth, M. F. S., Katz, E., . . . Mayberg, H. S. (2008). Anatomical connectivity of the subgenual cingulate region targeted with deep brain stimulation for treatment-resistant depression. *Cerebral Cortex, 18*(6), 1374-1383. doi:10.1093/cercor/bhm167

Jones, D. T., Vemuri, P., Murphy, M. C., Gunter, J. L., Senjem, M. L., Machulda, M. M., . . . Jack, C. R., Jr. (2012). Non-stationarity in the "resting brain's" modular architecture. *PLoS One, 7*(6), e39731. doi:10.1371/journal.pone.0039731

Jutten, C., & Herault, J. (1991). Blind Separation of Sources .1. An Adaptive Algorithm Based on Neuromimetic Architecture. *Signal Processing, 24*(1), 1-10. doi:Doi 10.1016/0165-1684(91)90079-X

Kahneman, D., & Tversky, A. (1979). Prospect Theory - Analysis of Decision under Risk. *Econometrica, 47*(2), 263-291. doi:Doi 10.2307/1914185

Kahnt, T., Chang, L. J., Park, S. Q., Heinzle, J., & Haynes, J. D. (2012). Connectivity-based parcellation of the human orbitofrontal cortex. *J Neurosci, 32*(18), 6240-6250. doi:10.1523/JNEUROSCI.0257-12.2012

Kaiser, R. H., Andrews-Hanna, J. R., Wager, T. D., & Pizzagalli, D. A. (2015). Large-Scale Network Dysfunction in Major Depressive Disorder A Meta-analysis of Resting-State Functional Connectivity. *JAMA Psychiatry, 72*(6), 603-611. doi:10.1001/jamapsychiatry.2015.0071

Kaiser, R. H., Whitfield-Gabrieli, S., Dillon, D. G., Goer, F., Beltzer, M., Minkel, J., . . . Pizzagalli, D. A. (2016). Dynamic Resting-State Functional Connectivity in Major Depression. *Neuropsychopharmacology, 41*(7), 1822-1830. doi:10.1038/npp.2015.352

Kelly, C., de Zubicaray, G., Di Martino, A., Copland, D. A., Reiss, P. T., Klein, D. F., . . . McMahon, K. (2009). L-Dopa Modulates Functional Connectivity in Striatal Cognitive and Motor Networks: A Double-Blind Placebo-Controlled Study. *Journal of Neuroscience, 29*(22), 7364-7378. doi:10.1523/Jneurosci.0810-09.2009

Kelly, R. E., Alexopoulos, G. S., Wang, Z. S., Gunning, F. M., Murphy, C. F., Morimoto, S. S., . . . Hoptman, M. J. (2010). Visual inspection of independent components: Defining a procedure for artifact removal from fMRI data. *Journal of Neuroscience Methods, 189*(2), 233-245. doi:10.1016/j.jneumeth.2010.03.028

Khalili-Mahani, N., Rombouts, S. A., van Osch, M. J., Duff, E. P., Carbonell, F., Nickerson, L. D., . . . van Gerven, J. M. (2017). Biomarkers, designs, and interpretations of resting-state fMRI in translational pharmacological research: A review of state-of-the-Art, challenges, and opportunities for studying brain chemistry. *Hum Brain Mapp, 38*(4), 2276-2325. doi:10.1002/hbm.23516

Kirsch, M., Guldenmund, P., Bahri, M. A., Demertzi, A., Baquero, K., Heine, L., . . . Laureys, S. (2017). Sedation of Patients With Disorders of Consciousness During Neuroimaging: Effects on Resting State Functional Brain Connectivity. *Anesthesia and Analgesia, 124*(2), 588-598. doi:10.1213/Ane.0000000000001721

Kiviniemi, V., Jauhiainen, J., Tervonen, O., Paakko, E., Oikarinen, J., Vainionpaa, V., . . . Biswal, B. (2000). Slow vasomotor fluctuation in fMRI of anesthetized child brain. *Magnetic Resonance in Medicine, 44*(3), 373-378. doi:Doi 10.1002/1522-2594(200009)44:3<373::Aid-Mrm5>3.3.Co;2-G

Klaassens, B. L., Rombouts, S. A., Winkler, A. M., van Gorsel, H. C., van der Grond, J., & van Gerven, J. M. (2016). Time related effects on functional brain connectivity after serotonergic and cholinergic neuromodulation. *Hum Brain Mapp.* doi:10.1002/hbm.23362

Klaassens, B. L., van Gorsel, H. C., Khalili-Mahani, N., van der Grond, J., Wyman, B. T., Whitcher, B., . . . van Gervend, J. A. (2015). Single-dose serotonergic stimulation shows

widespread effects on functional brain connectivity. *Neuroimage, 122*, 440-450. doi:10.1016/j.neuroimage.2015.08.012

Klumpers, L. E., Cole, D. M., Khalili-Mahani, N., Soeter, R. P., Te Beek, E. T., Rombouts, S. A., & van Gerven, J. M. (2012). Manipulating brain connectivity with delta(9)-tetrahydrocannabinol: a pharmacological resting state FMRI study. *Neuroimage, 63*(3), 1701-1711. doi:10.1016/j.neuroimage.2012.07.051

Kong, X. Z., Zhen, Z., Li, X., Lu, H. H., Wang, R., Liu, L., . . . Liu, J. (2014). Individual differences in impulsivity predict head motion during magnetic resonance imaging. *PLoS One, 9*(8), e104989. doi:10.1371/journal.pone.0104989

Krishnan, G. P., Gonzalez, O. C., & Bazhenov, M. (2018). Origin of slow spontaneous resting-state neuronal fluctuations in brain networks. *Proc Natl Acad Sci U S A*. doi:10.1073/pnas.1715841115

Kroes, M. C. W., van Wingen, G. A., Wittwer, J., Mohajeri, M. H., Kloek, J., & Fernandez, G. (2014). Food can lift mood by affecting mood-regulating neurocircuits via a serotonergic mechanism. *Neuroimage, 84*, 825-832. doi:10.1016/j.neuroimage.2013.09.041

Kunisato, Y., Okamoto, Y., Okada, G., Aoyama, S., Demoto, Y., Munakata, A., . . . Yamawaki, S. (2011). Modulation of default-mode network activity by acute tryptophan depletion is associated with mood change: A resting state functional magnetic resonance imaging study. *Neuroscience Research, 69*(2), 129-134. doi:10.1016/j.neures.2010.11.005

Laird, A. R., Fox, P. M., Eickhoff, S. B., Turner, J. A., Ray, K. L., McKay, D. R., . . . Fox, P. T. (2011). Behavioral Interpretations of Intrinsic Connectivity Networks. *Journal of Cognitive Neuroscience, 23*(12), 4022-4037. doi:DOI 10.1162/jocn_a_00077

Lauritzen, M. (2005). Reading vascular changes in brain imaging: is dendritic calcium the key? *Nat Rev Neurosci, 6*(1), 77-85. doi:10.1038/nrn1589

Lee, M. H., Smyser, C. D., & Shimony, J. S. (2013). Resting-state fMRI: a review of methods and clinical applications. *AJNR Am J Neuroradiol, 34*(10), 1866-1872. doi:10.3174/ajnr.A3263

Lehmann, M., Seifritz, E., Henning, A., Walter, M., Boker, H., Scheidegger, M., & Grimm, S. (2016). Differential effects of rumination and distraction on ketamine induced modulation of resting state functional connectivity and reactivity of regions within the default-mode network. *Social Cognitive and Affective Neuroscience, 11*(8), 1227-1235. doi:10.1093/scan/nsw034

Lieben, C. K. J., Blokland, A., Westerink, B., & Deutz, N. E. P. (2004). Acute tryptophan and serotonin depletion using an optimized tryptophan-free protein-carbohydrate mixture in the adult rat. *Neurochemistry International, 44*(1), 9-16. doi:10.1016/S0197-0186(03)00102-5

Lieberman, M. D., & Cunningham, W. A. (2009). Type I and Type II error concerns in fMRI research: re-balancing the scale. *Social Cognitive and Affective Neuroscience, 4*(4), 423-428. doi:10.1093/scan/nsp052

Lindseth, G., Helland, B., & Caspers, J. (2015). The Effects of Dietary Tryptophan on Affective Disorders. *Archives of Psychiatric Nursing, 29*(2), 102-107. doi:10.1016/j.apnu.2014.11.008

Little, R. J. A., & Smith, P. J. (1987). Editing and Imputation for Quantitative Survey Data. *Journal of the American Statistical Association, 82*(397), 58-68. doi:Doi 10.2307/2289125

Lois, G., & Wessa, M. (2016). Differential association of default mode network connectivity and rumination in healthy individuals and remitted MDD patients. *Soc Cogn Affect Neurosci, 11*(11), 1792-1801. doi:10.1093/scan/nsw085

Ma, S., Calhoun, V. D., Phlypo, R., & Adali, T. (2014). Dynamic changes of spatial functional network connectivity in individuals and schizophrenia patients using independent vector analysis. *Neuroimage, 90*, 196-206. doi:10.1016/j.neuroimage.2013.12.063

Mann, L., Burnett, P., Radford, M., & Ford, S. (1997). The Melbourne Decision Making Questionnaire: An instrument for measuring patterns for coping with decisional conflict. *Journal of Behavioral Decision Making, 10*(1), 1-19. doi:Doi 10.1002/(Sici)1099-0771(199703)10:1<1::Aid-Bdm242>3.0.Co;2-X

Marco-Pallares, J., Mohammadi, B., Samii, A., & Munte, T. F. (2010). Brain activations reflect individual discount rates in intertemporal choice. *Brain Res, 1320*, 123-129. doi:10.1016/j.brainres.2010.01.025

Margulies, D. S., Ghosh, S. S., Goulas, A., Falkiewicz, M., Huntenburg, J. M., Langs, G., . . . Smallwood, J. (2016). Situating the default-mode network along a principal gradient of macroscale cortical organization. *Proceedings of the National Academy of Sciences of the United States of America, 113*(44), 12574-12579. doi:10.1073/pnas.1608282113

Mazur, J. E. (1988). Estimation of indifference points with an adjusting-delay procedure. *J Exp Anal Behav, 49*(1), 37-47. doi:10.1901/jeab.1988.49-37

McCabe, C., & Mishor, Z. (2011). Antidepressant medications reduce subcortical-cortical resting-state functional connectivity in healthy volunteers. *Neuroimage, 57*(4), 1317-1323. doi:10.1016/j.neuroimage.2011.05.051

McCabe, C., Mishor, Z., Filippini, N., Cowen, P. J., Taylor, M. J., & Harmer, C. J. (2011). SSRI administration reduces resting state functional connectivity in dorso-medial prefrontal cortex. *Molecular Psychiatry, 16*(6), 592-594. doi:10.1038/mp.2010.138

McClure, S. M., Laibson, D. I., Loewenstein, G., & Cohen, J. D. (2004). Separate neural systems value immediate and delayed monetary rewards. *Science, 306*(5695), 503-507. doi:10.1126/science.1100907

McDermott, J. H. (2009). The cocktail party problem. *Current Biology, 19*(22), R1024-1027. doi:10.1016/j.cub.2009.09.005

McKeown, M. J., Makeig, S., Brown, G. G., Jung, T. P., Kindermann, S. S., Bell, A. J., & Sejnowski, T. J. (1998). Analysis of fMRI data by blind separation into independent spatial components. *Human Brain Mapping, 6*(3), 160-188. doi:Doi 10.1002/(Sici)1097-0193(1998)6:3<160::Aid-Hbm5>3.3.Co;2-R

Meneses, A., & Liy-Salmeron, G. (2012). Serotonin and emotion, learning and memory. *Reviews in the Neurosciences, 23*(5-6), 543-553. doi:10.1515/revneuro-2012-0060

Mennes, M., Kelly, C., Zuo, X. N., Di Martino, A., Biswal, B. B., Castellanos, F. X., & Milham, M. P. (2010). Inter-individual differences in resting-state functional connectivity predict task-induced BOLD activity. *Neuroimage, 50*(4), 1690-1701. doi:10.1016/j.neuroimage.2010.01.002

Meskaldji, D. E., Preti, M. G., Bolton, T. A. W., Montandon, M. L., Rodriguez, C., Morgenthaler, S., . . . Van De Ville, D. (2016). Prediction of long-term memory scores in MCI based on resting-state fMRI. *Neuroimage-Clinical, 12*, 785-795. doi:10.1016/j.nicl.2016.10.004

Miyazaki, K., Miyazaki, K. W., & Doya, K. (2012). The role of serotonin in the regulation of patience and impulsivity. *Mol Neurobiol, 45*(2), 213-224. doi:10.1007/s12035-012-8232-6

Moeller, S. J., London, E. D., & Northoff, G. (2016). Neuroimaging markers of glutamatergic and GABAergic systems in drug addiction: Relationships to resting-state functional connectivity. *Neurosci Biobehav Rev, 61*, 35-52. doi:10.1016/j.neubiorev.2015.11.010

Moja, E. A., Stoff, D. M., Gessa, G. L., Castoldi, D., Assereto, R., & Tofanetti, O. (1988). Decrease in plasma tryptophan after tryptophan-free amino acid mixtures in man. *Life Sci, 42*(16), 1551-1556.

Monti, M. M., Lutkenhoff, E. S., Rubinov, M., Boveroux, P., Vanhaudenhuyse, A., Gosseries, O., . . . Laureys, S. (2013). Dynamic change of global and local information processing in propofol-induced loss and recovery of consciousness. *PLoS Comput Biol, 9*(10), e1003271. doi:10.1371/journal.pcbi.1003271

Mumford, J. A. (2017). A comprehensive review of group level model performance in the presence of heteroscedasticity: Can a single model control Type I errors in the presence of outliers? *Neuroimage, 147*, 658-668. doi:10.1016/j.neuroimage.2016.12.058

Mumford, J. A., Poline, J. B., & Poldrack, R. A. (2015). Orthogonalization of Regressors in fMRI Models. *PLoS One, 10*(4). doi:ARTN e012625510.1371/journal.pone.0126255

Murty, V. P., FeldmanHall, O., Hunter, L. E., Phelps, E. A., & Davachi, L. (2016). Episodic memories predict adaptive value-based decision-making. *J Exp Psychol Gen, 145*(5), 548-558. doi:10.1037/xge0000158

Muthuraman, M., Moliadze, V., Mideksa, K. G., Anwar, A. R., Stephani, U., Deuschl, G., . . . Siniatchkin, M. (2015). EEG-MEG Integration Enhances the Characterization of Functional and Effective Connectivity in the Resting State Network. *PLoS One, 10*(10), e0140832. doi:10.1371/journal.pone.0140832

Nagano-Saito, A., Liu, J. Q., Doyon, J., & Dagher, A. (2009). Dopamine modulates default mode network deactivation in elderly individuals during the Tower of London task. *Neuroscience Letters, 458*(1), 1-5. doi:10.1016/j.neulet.2009.04.025

Neukam, P. T., Kroemer, N. B., Deza Araujo, Y. I., Hellrung, L., Pooseh, S., Rietschel, M., . . . Smolka, M. N. (2018). Risk-seeking for losses is associated with 5-HTTLPR, but not with transient changes in 5-HT levels. *Psychopharmacology*. doi:10.1007/s00213-018-4913-9

Nichols, T. E., Das, S., Eickhoff, S. B., Evans, A. C., Glatard, T., Hanke, M., . . . Yeo, B. T. T. (2017). Best practices in data analysis and sharing in neuroimaging using MRI. *Nature Neuroscience, 20*(3), 299-303. doi:DOI 10.1038/nn.4500

Nichols, T. E., & Holmes, A. P. (2002). Nonparametric permutation tests for functional neuroimaging: A primer with examples. *Human Brain Mapping, 15*(1), 1-25. doi:DOI 10.1002/hbm.1058

Nishizawa, S., Benkelfat, C., Young, S. N., Leyton, M., Mzengeza, S., DeMontigny, C., . . . Diksic, M. (1997). Differences between males and females in rates of serotonin synthesis in human brain. *Proceedings of the National Academy of Sciences of the United States of America, 94*(10), 5308-5313. doi:DOI 10.1073/pnas.94.10.5308

Niu, H., & He, Y. (2014). Resting-state functional brain connectivity: lessons from functional near-infrared spectroscopy. *Neuroscientist, 20*(2), 173-188. doi:10.1177/1073858413502707

Northoff, G., Walter, M., Schulte, R. F., Beck, J., Dydak, U., Henning, A., . . . Boesiger, P. (2007). GABA concentrations in the human anterior cingulate cortex predict negative BOLD responses in fMRI. *Nature Neuroscience, 10*(12), 1515-1517. doi:10.1038/nn2001

Odum, A. L. (2011). Delay discounting: I'm a k, you're a k. *J Exp Anal Behav, 96*(3), 427-439. doi:10.1901/jeab.2011.96-423

Ogawa, S., Lee, T. M., Nayak, A. S., & Glynn, P. (1990). Oxygenation-Sensitive Contrast in Magnetic-Resonance Image of Rodent Brain at High Magnetic-Fields. *Magnetic Resonance in Medicine, 14*(1), 68-78. doi:DOI 10.1002/mrm.1910140108

Okazawa, H., Leyton, M., Benkelfat, C., Mzengeza, S., & Diksic, M. (2000). Statistical mapping analysis of serotonin synthesis images generated in healthy volunteers using positron-emission tomography and alpha-[11C]methyl-L-tryptophan. *J Psychiatry Neurosci, 25*(4), 359-370.

Ortiz, J. J., Portillo, W., Paredes, R. G., Young, L. J., & Alcauter, S. (2018). Resting state brain networks in the prairie vole. *Sci Rep, 8*(1), 1231. doi:10.1038/s41598-017-17610-9

Pandya, M., Altinay, M., Malone, D. A., & Anand, A. (2012). Where in the Brain Is Depression? *Current Psychiatry Reports, 14*(6), 634-642. doi:10.1007/s11920-012-0322-7

Pelli, D. G. (1997). The VideoToolbox software for visual psychophysics: Transforming numbers into movies. *Spatial Vision, 10*(4), 437-442. doi:Doi 10.1163/156856897x00366

Peters, J., & Buchel, C. (2011). The neural mechanisms of inter-temporal decision-making: understanding variability. *Trends Cogn Sci, 15*(5), 227-239. doi:10.1016/j.tics.2011.03.002

Pooseh, S., Bernhardt, N., Guevara, A., Huys, Q. J., & Smolka, M. N. (2017). Value-based decision-making battery: A Bayesian adaptive approach to assess impulsive and risky behavior. *Behav Res Methods*. doi:10.3758/s13428-017-0866-x

Posner, J., Cha, J., Wang, Z., Talati, A., Warner, V., Gerber, A., . . . Weissman, M. (2016). Increased Default Mode Network Connectivity in Individuals at High Familial Risk for Depression. *Neuropsychopharmacology, 41*(7), 1759-1767. doi:10.1038/npp.2015.342

Posner, J., Hellerstein, D. J., Gat, I., Mechling, A., Klahr, K., Wang, Z., . . . Peterson, B. S. (2013). Antidepressants normalize the default mode network in patients with dysthymia. *JAMA Psychiatry, 70*(4), 373-382. doi:10.1001/jamapsychiatry.2013.455

Power, J. D., Barnes, K. A., Snyder, A. Z., Schlaggar, B. L., & Petersen, S. E. (2012). Spurious but systematic correlations in functional connectivity MRI networks arise from subject motion. *Neuroimage, 59*(3), 2142-2154. doi:10.1016/j.neuroimage.2011.10.018

Preibisch, C., Castrillon, J. G., Buhrer, M., & Riedl, V. (2015). Evaluation of Multiband EPI Acquisitions for Resting State fMRI. *PLoS One, 10*(9). doi:ARTN e013696110.1371/journal.pone.0136961

Preti, M. G., Bolton, T. A. W., & Van De Ville, D. (2017). The dynamic functional connectome: State-of-the-art and perspectives. *Neuroimage, 160*, 41-54. doi:10.1016/j.neuroimage.2016.12.061

Preuschoff, K., Quartz, S. R., & Bossaerts, P. (2008). Human insula activation reflects risk prediction errors as well as risk. *J Neurosci, 28*(11), 2745-2752. doi:10.1523/JNEUROSCI.4286-07.2008

Pruim, R. H. R., Mennes, M., Buitelaar, J. K., & Beckmann, C. F. (2015b). Evaluation of ICA-AROMA and alternative strategies for motion artifact removal in resting state fMRI. *Neuroimage, 112*, 278-287. doi:10.1016/j.neuroimage.2015.02.063

Pruim, R. H. R., Mennes, M., van Rooij, D., Llera, A., Buitelaar, J. K., & Beckmann, C. F. (2015). ICA-AROMA: A robust ICA-based strategy for removing motion artifacts from fMRI data. *Neuroimage, 112*, 267-277. doi:10.1016/j.neuroimage.2015.02.064

Pruim, R. H. R., Mennes, M., van Rooij, D., Llera, A., Buitelaar, J. K., & Beckmann, C. F. (2015a). ICA-AROMA: A robust ICA-based strategy for removing motion artifacts from fMRI data. *Neuroimage, 112*, 267-277. doi:10.1016/j.neuroimage.2015.02.064

Rachlin, H., Raineri, A., & Cross, D. (1991). Subjective probability and delay. *J Exp Anal Behav, 55*(2), 233-244. doi:10.1901/jeab.1991.55-233

Raduntz, T., Scouten, J., Hochmuth, O., & Meffert, B. (2015). EEG artifact elimination by extraction of ICA-component features using image processing algorithms. *Journal of Neuroscience Methods, 243*, 84-93. doi:10.1016/j.jneumeth.2015.01.030

Raichle, M. E., MacLeod, A. M., Snyder, A. Z., Powers, W. J., Gusnard, D. A., & Shulman, G. L. (2001). A default mode of brain function. *Proc Natl Acad Sci U S A, 98*(2), 676-682. doi:10.1073/pnas.98.2.676

Ray, K. L., McKay, D. R., Fox, P. M., Riedel, M. C., Uecker, A. M., Beckmann, C. F., . . . Laird, A. R. (2013). ICA model order selection of task co-activation networks. *Front Neurosci, 7*, 237. doi:10.3389/fnins.2013.00237

Reineberg, A. E., Andrews-Hanna, J. R., Depue, B. E., Friedman, N. P., & Banich, M. T. (2015). Resting-state networks predict individual differences in common and specific aspects of executive function. *Neuroimage, 104*, 69-78. doi:10.1016/j.neuroimage.2014.09.045

Richard, D. M., Dawes, M. A., Mathias, C. W., Acheson, A., Hill-Kapturczak, N., & Dougherty, D. M. (2009). L-Tryptophan: Basic Metabolic Functions, Behavioral Research and Therapeutic Indications. *Int J Tryptophan Res, 2*, 45-60.

Ripke, S., Hubner, T., Mennigen, E., Muller, K. U., Li, S. C., & Smolka, M. N. (2015). Common Neural Correlates of Intertemporal Choices and Intelligence in Adolescents. *Journal of Cognitive Neuroscience, 27*(2), 387-399. doi:10.1162/jocn_a_00698

Ripke, S., Hubner, T., Mennigen, E., Muller, K. U., Rodehacke, S., Schmidt, D., . . . Smolka, M. N. (2012). Reward processing and intertemporal decision making in adults and adolescents: The role of impulsivity and decision consistency. *Brain Research, 1478*, 36-47. doi:10.1016/j.brainres.2012.08.034

Roberts, A. C. (2011). The Importance of Serotonin for Orbitofrontal Function. *Biological Psychiatry, 69*(12), 1185-1191. doi:10.1016/j.biopsych.2010.12.037

Romer, D. (2010). Adolescent risk taking, impulsivity, and brain development: implications for prevention. *Dev Psychobiol, 52*(3), 263-276. doi:10.1002/dev.20442

Rushworth, M. F., Noonan, M. P., Boorman, E. D., Walton, M. E., & Behrens, T. E. (2011). Frontal cortex and reward-guided learning and decision-making. *Neuron, 70*(6), 1054-1069. doi:10.1016/j.neuron.2011.05.014

Sala-Llonch, R., Pena-Gomez, C., Arenaza-Urquijo, E. M., Vidal-Pineiro, D., Bargallo, N., Junque, C., & Bartres-Faz, D. (2012). Brain connectivity during resting state and subsequent working memory task predicts behavioural performance. *Cortex, 48*(9), 1187-1196. doi:10.1016/j.cortex.2011.07.006

Salimi-Khorshidi, G., Douaud, G., Beckmann, C. F., Glasser, M. F., Griffanti, L., & Smith, S. M. (2014). Automatic denoising of functional MRI data: combining independent component analysis and hierarchical fusion of classifiers. *Neuroimage, 90*, 449-468. doi:10.1016/j.neuroimage.2013.11.046

Saulin, A., Savli, M., & Lanzenberger, R. (2012). Serotonin and molecular neuroimaging in humans using PET. *Amino Acids, 42*(6), 2039-2057. doi:10.1007/s00726-011-1078-9

Scheidegger, M., Walter, M., Lehmann, M., Metzger, C., Grimm, S., Boeker, H., . . . Seifritz, E. (2012). Ketamine Decreases Resting State Functional Network Connectivity in Healthy Subjects: Implications for Antidepressant Drug Action. *PLoS One, 7*(9). doi:ARTN e4479910.1371/journal.pone.0044799

Schoenbaum, G., Takahashi, Y., Liu, T. L., & McDannald, M. A. (2011). Does the orbitofrontal cortex signal value? *Ann N Y Acad Sci, 1239*, 87-99. doi:10.1111/j.1749-6632.2011.06210.x

Schopf, V., Kasprian, G., Schwindt, J., Kollndorfer, K., & Prayer, D. (2012). Visualization of resting-state networks in utero. *Ultrasound Obstet Gynecol, 39*(4), 487-488. doi:10.1002/uog.11119

Shannon, B. J., Raichle, M. E., Snyder, A. Z., Fair, D. A., Mills, K. L., Zhang, D., . . . Kiehl, K. A. (2011). Premotor functional connectivity predicts impulsivity in juvenile offenders. *Proc Natl Acad Sci U S A, 108*(27), 11241-11245. doi:10.1073/pnas.1108241108

Shead, N. W., & Hodgins, D. C. (2009). Probability discounting of gains and losses: implications for risk attitudes and impulsivity. *J Exp Anal Behav, 92*(1), 1-16. doi:10.1901/jeab.2009.92-1

Sheline, Y. I., Barch, D. M., Price, J. L., Rundle, M. M., Vaishnavi, S. N., Snyder, A. Z., . . . Raichle, M. E. (2009). The default mode network and self-referential processes in depression. *Proc Natl Acad Sci U S A, 106*(6), 1942-1947. doi:10.1073/pnas.0812686106

Shi, L., Sun, J., Ren, Z., Chen, Q., Wei, D., Yang, W., & Qiu, J. (2018). Large-scale brain network connectivity underlying creativity in resting-state and task fMRI: Cooperation between default network and frontal-parietal network. *Biol Psychol*. doi:10.1016/j.biopsycho.2018.03.005

Siegel, J. S., Ramsey, L. E., Snyder, A. Z., Metcalf, N. V., Chacko, R. V., Weinberger, K., . . . Corbetta, M. (2016). Disruptions of network connectivity predict impairment in multiple behavioral domains after stroke. *Proceedings of the National Academy of Sciences of the United States of America, 113*(30), E4367-E4376. doi:10.1073/pnas.1521083113

Silber, B. Y., & Schmitt, J. A. (2010). Effects of tryptophan loading on human cognition, mood, and sleep. *Neurosci Biobehav Rev, 34*(3), 387-407. doi:10.1016/j.neubiorev.2009.08.005

Smith, S. M., Fox, P. T., Miller, K. L., Glahn, D. C., Fox, P. M., Mackay, C. E., . . . Beckmann, C. F. (2009a). Correspondence of the brain's functional architecture during activation and rest. *Proceedings of the National Academy of Sciences of the United States of America, 106*(31), 13040-13045. doi:10.1073/pnas.0905267106

Smith, S. M., Fox, P. T., Miller, K. L., Glahn, D. C., Fox, P. M., Mackay, C. E., . . . Beckmann, C. F. (2009b). Correspondence of the brain's functional architecture during activation and rest. *Proc Natl Acad Sci U S A, 106*(31), 13040-13045. doi:10.1073/pnas.0905267106

Smith, S. M., Hyvarinen, A., Varoquaux, G., Miller, K. L., & Beckmann, C. F. (2014). Group-PCA for very large fMRI datasets. *Neuroimage, 101*, 738-749. doi:10.1016/j.neuroimage.2014.07.051

Smith, S. M., & Nichols, T. E. (2009). Threshold-free cluster enhancement: addressing problems of smoothing, threshold dependence and localisation in cluster inference. *Neuroimage, 44*(1), 83-98. doi:10.1016/j.neuroimage.2008.03.061

Smith, S. M., Nichols, T. E., Vidaurre, D., Winkler, A. M., Behrens, T. E. J., Glasser, M. F., . . . Miller, K. L. (2015). A positive-negative mode of population covariation links brain connectivity, demographics and behavior. *Nature Neuroscience, 18*(11), 1565-1567. doi:10.1038/nn.4125

Smoski, M. J., Lynch, T. R., Rosenthal, M. Z., Cheavens, J. S., Chapman, A. L., & Krishnan, R. R. (2008). Decision-making and risk aversion among depressive adults. *Journal of Behavior Therapy and Experimental Psychiatry, 39*(4), 567-576. doi:10.1016/j.jbtep.2008.01.004

Smucny, J., Wylie, K. P., & Tregellas, J. R. (2014). Functional magnetic resonance imaging of intrinsic brain networks for translational drug discovery. *Trends in Pharmacological Sciences, 35*(8), 397-403. doi:10.1016/j.tips.2014.05.001

Snaith, R. P., Hamilton, M., Morley, S., Humayan, A., Hargreaves, D., & Trigwell, P. (1995). A scale for the assessment of hedonic tone the Snaith-Hamilton Pleasure Scale. *Br J Psychiatry, 167*(1), 99-103.

Sohn, W. S., Yoo, K., Lee, Y. B., Seo, S. W., Na, D. L., & Jeong, Y. (2015). Influence of ROI selection on resting state functional connectivity: an individualized approach for resting state fMRI analysis. *Frontiers in Neuroscience, 9*. doi:ARTN 28010.3389/fnins.2015.00280

Song, J., Desphande, A. S., Meier, T. B., Tudorascu, D. L., Vergun, S., Nair, V. A., . . . Prabhakaran, V. (2012). Age-Related Differences in Test-Retest Reliability in Resting-State Brain Functional Connectivity. *PLoS One, 7*(12). doi:ARTN e4984710.1371/journal.pone.0049847

Spielberger, C. (1983). Special Issue - Behavioral Medicine - Foreword. *International Review of Applied Psychology-Revue Internationale De Psychologie Appliquee, 32*(1), 1-4.

Spies, M., Kraus, C., Geissberger, N., Auer, B., Klobl, M., Tik, M., . . . Lanzenberger, R. (2017). Default mode network deactivation during emotion processing predicts early antidepressant response. *Translational Psychiatry, 7*. doi:ARTN e100810.1038/tp.2016.265

Spreng, R. N. (2012). The fallacy of a "task-negative" network. *Front Psychol, 3*, 145. doi:10.3389/fpsyg.2012.00145

Steinberg, L. (2008). A social neuroscience perspective on adolescent risk-taking. *Developmental Review, 28*(1), 78-106. doi:10.1016/j.dr.2007.08.002

Story, G. W., Vlaev, I., Seymour, B., Darzi, A., & Dolan, R. J. (2014). Does temporal discounting explain unhealthy behavior? A systematic review and reinforcement learning perspective. *Front Behav Neurosci, 8*, 76. doi:10.3389/fnbeh.2014.00076

Supekar, K., Uddin, L. Q., Prater, K., Amin, H., Greicius, M. D., & Menon, V. (2010). Development of functional and structural connectivity within the default mode network in young children. *Neuroimage, 52*(1), 290-301. doi:10.1016/j.neuroimage.2010.04.009

Szewczyk-Krolikowski, K., Menke, R. A., Rolinski, M., Duff, E., Salimi-Khorshidi, G., Filippini, N., . . . Mackay, C. E. (2014). Functional connectivity in the basal ganglia network differentiates PD patients from controls. *Neurology, 83*(3), 208-214. doi:10.1212/WNL.0000000000000592

Talbot, P. S., & Cooper, S. J. (2006). Anterior cingulate and subgenual prefrontal blood flow changes following tryptophan depletion in healthy males. *Neuropsychopharmacology, 31*(8), 1757-1767. doi:10.1038/sj.npp.1301022

Tamura, M., Moriguchi, Y., Higuchi, S., Hida, A., Enomoto, M., Umezawa, J., & Mishima, K. (2012). Neural Network Development in Late Adolescents during Observation of Risk-Taking Action. *PLoS One, 7*(6). doi:ARTN e39527

10.1371/journal.pone.0039527

Thompson, G. J. (2017). Neural and metabolic basis of dynamic resting state fMRI. *Neuroimage*. doi:10.1016/j.neuroimage.2017.09.010

Tom, S. M., Fox, C. R., Trepel, C., & Poldrack, R. A. (2007). The neural basis of loss aversion in decision-making under risk. *Science, 315*(5811), 515-518. doi:10.1126/science.1134239

Turner, C., & McClure, R. (2003). Age and gender differences in risk-taking behaviour as an explanation for high incidence of motor vehicle crashes as a driver in young males. *Inj Control Saf Promot, 10*(3), 123-130. doi:10.1076/icsp.10.3.123.14560

Uddin, L. Q., Supekar, K. S., Ryali, S., & Menon, V. (2011). Dynamic reconfiguration of structural and functional connectivity across core neurocognitive brain networks with development. *J Neurosci, 31*(50), 18578-18589. doi:10.1523/JNEUROSCI.4465-11.2011

Vaidya, C. J., & Gordon, E. M. (2013). Phenotypic variability in resting-state functional connectivity: current status. *Brain Connect, 3*(2), 99-120. doi:10.1089/brain.2012.0110

van de Ven, V., Wingen, M., Kuypers, K. P. C., Ramaekers, J. G., & Formisano, E. (2013). Escitalopram Decreases Cross-Regional Functional Connectivity within the Default-Mode Network. *PLoS One, 8*(6). doi:ARTN e6835510.1371/journal.pone.0068355

van den Heuvel, M. I., & Thomason, M. E. (2016). Functional Connectivity of the Human Brain in Utero. *Trends in Cognitive Sciences, 20*(12), 931-939. doi:10.1016/j.tics.2016.10.001

van Donkelaar, E. L., Blokland, A., Ferrington, L., Kelly, P. A., Steinbusch, H. W., & Prickaerts, J. (2011). Mechanism of acute tryptophan depletion: is it only serotonin? *Mol Psychiatry, 16*(7), 695-713. doi:10.1038/mp.2011.9

Varnas, K., Halldin, C., & Hall, H. (2004). Autoradiographic distribution of serotonin transporters and receptor subtypes in human brain. *Hum Brain Mapp, 22*(3), 246-260. doi:10.1002/hbm.20035

Vatansever, D., Menon, D. K., & Stamatakis, E. A. (2017). Default mode contributions to automated information processing. *Proceedings of the National Academy of Sciences of the United States of America, 114*(48), 12821-12826. doi:10.1073/pnas.1710521114

Vogt, B. A., Nimchinsky, E. A., Vogt, L. J., & Hof, P. R. (1995). Human cingulate cortex: surface features, flat maps, and cytoarchitecture. *J Comp Neurol, 359*(3), 490-506. doi:10.1002/cne.903590310

Vytlacil, J., Kayser, A., Miyakawa, A., & D'Esposito, M. (2014). An Approach for Identifying Brainstem Dopaminergic Pathways Using Resting State Functional MRI. *PLoS One, 9*(1). doi:ARTN e8710910.1371/journal.pone.0087109

Wang, L., Shen, H., Lei, Y., Zeng, L. L., Cao, F., Su, L., . . . Hu, D. (2017). Altered default mode, fronto-parietal and salience networks in adolescents with Internet addiction. *Addict Behav, 70*, 1-6. doi:10.1016/j.addbeh.2017.01.021

Wang, L., Xia, M., Li, K., Zeng, Y., Su, Y., Dai, W., . . . Si, T. (2015). The effects of antidepressant treatment on resting-state functional brain networks in patients with major depressive disorder. *Hum Brain Mapp, 36*(2), 768-778. doi:10.1002/hbm.22663

Wang, L. B., Su, L. F., Shen, H., & Hu, D. W. (2012). Decoding Lifespan Changes of the Human Brain Using Resting-State Functional Connectivity MRI. *PLoS One, 7*(8). doi:ARTN e4453010.1371/journal.pone.0044530

Weber, B. J., & Huettel, S. A. (2008). The neural substrates of probabilistic and intertemporal decision making. *Brain Res, 1234*, 104-115. doi:10.1016/j.brainres.2008.07.105

Wei, Z., Alcauter, S., Jin, K., Peng, Z. W., & Gao, W. (2013). Graph theoretical analysis of sedation's effect on whole brain functional system in school-aged children. *Brain Connect, 3*(2), 177-189. doi:10.1089/brain.2012.0125

Wei, Z. D., Yang, N. N., Liu, Y., Yang, L. Z., Wang, Y., Han, L., . . . Zhang, X. C. (2016). Resting-state functional connectivity between the dorsal anterior cingulate cortex and thalamus is associated with risky decision-making in nicotine addicts. *Scientific Reports, 6*. doi:ARTN 2177810.1038/srep21778

Weiland, B. J., Heitzeg, M. M., Zald, D., Cummiford, C., Love, T., Zucker, R. A., & Zubieta, J. K. (2014). Relationship between impulsivity, prefrontal anticipatory activation, and striatal dopamine release during rewarded task performance. *Psychiatry Res, 223*(3), 244-252. doi:10.1016/j.pscychresns.2014.05.015

Weissman, D. G., Schriber, R. A., Fassbender, C., Atherton, O., Krafft, C., Robins, R. W., . . . Guyer, A. E. (2015). Earlier adolescent substance use onset predicts stronger connectivity between reward and cognitive control brain networks. *Dev Cogn Neurosci, 16*, 121-129. doi:10.1016/j.dcn.2015.07.002

Whelan, R., Conrod, P. J., Poline, J. B., Lourdusamy, A., Banaschewski, T., Barker, G. J., . . . Consortium, I. (2012). Adolescent impulsivity phenotypes characterized by distinct brain networks. *Nature Neuroscience, 15*(6), 920-925. doi:10.1038/nn.3092

Whitfield-Gabrieli, S., & Ford, J. M. (2012). Default Mode Network Activity and Connectivity in Psychopathology. *Annual Review of Clinical Psychology, Vol 8, 8*, 49-+. doi:10.1146/annurev-clinpsy-032511-143049

Williams, W. A., Shoaf, S. E., Hommer, D., Rawlings, R., & Linnoila, M. (1999). Effects of acute tryptophan depletion on plasma and cerebrospinal fluid tryptophan and 5-hydroxyindoleacetic acid in normal volunteers. *J Neurochem, 72*(4), 1641-1647.

Winkler, A. M., Ridgway, G. R., Douaud, G., Nichols, T. E., & Smith, S. M. (2016a). Faster permutation inference in brain imaging. *Neuroimage, 141*, 502-516. doi:10.1016/j.neuroimage.2016.05.068

Winkler, A. M., Webster, M. A., Brooks, J. C., Tracey, I., Smith, S. M., & Nichols, T. E. (2016b). Non-parametric combination and related permutation tests for neuroimaging. *Human Brain Mapping, 37*(4), 1486-1511. doi:10.1002/hbm.23115

Winkler, A. M., Webster, M. A., Vidaurre, D., Nichols, T. E., & Smith, S. M. (2015). Multi-level block permutation. *Neuroimage, 123*, 253-268. doi:10.1016/j.neuroimage.2015.05.092

Woodward, N. D., & Cascio, C. J. (2015). Resting-State Functional Connectivity in Psychiatric Disorders. *JAMA Psychiatry, 72*(8), 743-744. doi:10.1001/jamapsychiatry.2015.0484

Wu, L., Calhoun, V. D., Jung, R. E., & Caprihan, A. (2015). Connectivity-based whole brain dual parcellation by group ICA reveals tract structures and decreased connectivity in schizophrenia. *Human Brain Mapping, 36*(11), 4681-4701. doi:10.1002/hbm.22945

Ye, M., Yang, T., Qing, P., Lei, X., Qiu, J., & Liu, G. (2015). Changes of Functional Brain Networks in Major Depressive Disorder: A Graph Theoretical Analysis of Resting-State fMRI. *PLoS One, 10*(9), e0133775. doi:10.1371/journal.pone.0133775

Yeo, B. T. T., Krienen, F. M., Sepulcre, J., Sabuncu, M. R., Lashkari, D., Hollinshead, M., . . . Buckner, R. L. (2011). The organization of the human cerebral cortex estimated by intrinsic functional connectivity. *Journal of Neurophysiology, 106*(3), 1125-1165. doi:10.1152/jn.00338.2011

Young, S. N. (2007). How to increase serotonin in the human brain without drugs. *Journal of Psychiatry & Neuroscience, 32*(6), 394-399.

Young, S. N., & Gauthier, S. (1981). Effect of tryptophan administration on tryptophan, 5-hydroxyindoleacetic acid and indoleacetic acid in human lumbar and cisternal cerebrospinal fluid. *J Neurol Neurosurg Psychiatry, 44*(4), 323-328.

Zanchi, D., Meyer-Gerspach, A. C., Suenderhauf, C., Janach, K., le Roux, C. W., Haller, S., . . . Borgwardt, S. (2016). Differential effects of L-tryptophan and L-leucine administration on brain resting state functional networks and plasma hormone levels. *Scientific Reports, 6*. doi:ARTN 3572710.1038/srep35727

Zanto, T. P., & Gazzaley, A. (2013). Fronto-parietal network: flexible hub of cognitive control. *Trends in Cognitive Sciences, 17*(12), 602-603. doi:10.1016/j.tics.2013.10.001

Zepf, F. D., & Poustka, F. (2008). 5-HT functioning and aggression in children with ADHD and disruptive behaviour disorders. *Human Psychopharmacology-Clinical and Experimental, 23*(5), 438-438. doi:10.1002/hup.948

Zermatten, A., Van der Linden, M., d'Acremont, M., Jermann, F., & Bechara, A. (2005). Impulsivity and decision making. *J Nerv Ment Dis, 193*(10), 647-650.

Zhang, S., & Li, C. S. R. (2012). Functional networks for cognitive control in a stop signal task: Independent component analysis. *Human Brain Mapping, 33*(1), 89-104. doi:10.1002/hbm.21197

Zhang, Y. Y., Brady, M., & Smith, S. (2001). Segmentation of brain MR images through a hidden Markov random field model and the expectation-maximization algorithm. *Ieee Transactions on Medical Imaging, 20*(1), 45-57. doi:Doi 10.1109/42.906424

Zhou, Y., Li, S., Dunn, J., Li, H., Qin, W., Zhu, M., . . . Jiang, T. (2014). The neural correlates of risk propensity in males and females using resting-state fMRI. *Front Behav Neurosci, 8*, 2. doi:10.3389/fnbeh.2014.00002

Zhu, X., Cortes, C. R., Mathur, K., Tomasi, D., & Momenan, R. (2015). Model-free functional connectivity and impulsivity correlates of alcohol dependence: a resting-state study. *Addict Biol*. doi:10.1111/adb.12272

Zhu, X. L., Wang, X., Xiao, J., Liao, J., Zhong, M. T., Wang, W., & Yao, S. Q. (2012). Evidence of a Dissociation Pattern in Resting-State Default Mode Network Connectivity in First-

Episode, Treatment-Naive Major Depression Patients. *Biological Psychiatry, 71*(7), 611-617. doi:10.1016/j.biopsych.2011.10.035

Zuo, X. N., Kelly, C., Adelstein, J. S., Klein, D. F., Castellanos, F. X., & Milham, M. P. (2010). Reliable intrinsic connectivity networks: Test-retest evaluation using ICA and dual regression approach. *Neuroimage, 49*(3), 2163-2177. doi:10.1016/j.neuroimage.2009.10.080

## 8. ANNEX

### 8.1. Publikationsverzeichnis

**Zeitschriftenbeiträge:**

**Deza Araujo, Y.I**., Neukam, P.T., Marxen, M., Müller, D. K., Henle, T., Smolka, M.N. (2018). Acute Tryptophan Loading Decreases Functional Connectivity between the Default Mode Network and Emotion-Related Brain Regions. *Human Brain Mapping*. doi:10.1002/hbm.24494

**Deza Araujo, Y. I.,** Nebe, S., Neukam, P. T., Pooseh, S., Sebold, M., Garbusow, M., . . . Smolka, M. N. (2018). Risk seeking for losses modulates the functional connectivity of the default mode and left frontoparietal networks in young males. *Cognitive, Affective, & Behavioral Neuroscience*. doi:10.3758/s13415-018-0586-4

Neukam, P. T., Kroemer, N. B., **Deza Araujo, Y. I**., Hellrung, L., Pooseh, S., Rietschel, M.,. .. Smolka, M. N. (2018). Risk-seeking for losses is associated with 5-HTTLPR, but not with transient changes in 5-HT levels. *Psychopharmacology*. doi:10.1007/s00213-018-4913-9

**Deza Araujo, Y.I*.,** Fang, X*., Marxen, M., Spreer., M., Petzold, J., Riedel, P., Zimmerman, U., Smolka, M. N., Acute effects of alcohol on DMN connectivity (*under prep.)*

Boehm, I., Geisler, D., King, J. A., Ritschel, F., Seidel, M., **Deza Araujo, Y**., . . . Ehrlich, S. (2014). Increased resting state functional connectivity in the frontoparietal and default mode network in anorexia nervosa. *Front Behav Neurosci*, 8, 346. doi:10.3389/fnbeh.2014.00346

**Konferenzbeiträge:**

- **Yacila I. Deza Araujo**, Nils B. Kroemer, Lydia Hellrung, Stephan Nebe, Michael N. Smolka. Increased discounting behavior in young men is associated with greater fronto-precuneus resting-state functional connectivity. *DGPPN Kongress*, Berlin, Deutschland 25.-28 November 2015.

- **Yacila I. Deza Araujo,** Lydia Hellrung, Nils B. Kroemer, Stephan Nebe, Michael N. Smolka. Negative correlation between rs-FC of the rostrolateral PFC and risk-seeking behavior in young males. *OHBM* in Genf, Schweiz, 26.-30 Juni, 2016.

- **Yacila I. Deza Araujo,** Lydia Hellrung, Nils B. Kroemer., Stephan Nebe, Michael N. Smolka. Risk-seeking behavior is negatively correlated with functional connectivity in the frontal pole in young males. *Resting state and Brain Connectivity*, Wien, Österreich, 21.-23 September, 2016.

- **Yacila I. Deza Araujo,** Philipp T. Neukam, Lydia Hellrung, Nils B. Kroemer, Michael N. Smolka. Serotonergic modulation of large-scale brain networks. Presented at the *Late-summer school of Non-invasive brain stimulation*, Freiburg, Deutschland, 12.-16 Oktober, 2016.

- **Yacila I. Deza Araujo,** Philipp T. Neukam, Michael Marxen, Dirk Müller, Michael N. Smolka. Serotonergic modulation of large-scale brain networks, *TeaP*, Dresden, Deutschland, 26.-29 März, 2017.

Ort, Datum                                              Unterschrift des Doktoranden

114

## 8.2. Danksagung

## 8.3. Erklärungen zur Eröffnung des Promotionsverfahrens

1. Hiermit versichere ich, dass ich die vorliegende Arbeit ohne unzulässige Hilfe Dritter und ohne Benutzung anderer als der angegebenen Hilfsmittel angefertigt habe; die aus fremden Quellen direkt oder indirekt übernommenen Gedanken sind als solche kenntlich gemacht.

2. Bei der Auswahl und Auswertung des Materials sowie bei der Herstellung des Manuskripts habe ich Unterstützungsleistungen von folgenden Personen erhalten:

   a. Prof. Dr. med. Michael Smolka

   b. M.Sc. Philipp T. Neukam

   c. Dr. rer. nat. Stephan Nebe

   d. M.Sc. Julianne Fröhner

   e. Shakoor Pooseh Ph.D

   f. Michael Marxen Ph.D

   g. M.Sc. Dipl.-Inf. Dirk K. Müller

   h. Dr. rer. nat. Maria Garbusow

   i. Dr. rer nat. Mirian Sebold

   j. Prof. MD. Ph.D Andreas Heinz

   k. Prof. Dr. Thomas Henle

3. Weitere Personen waren an der geistigen Herstellung der vorliegenden Arbeit nicht beteiligt. Insbesondere habe ich nicht die Hilfe eines kommerziellen Promotionsberaters in Anspruch genommen. Dritte haben von mir weder unmittelbar noch mittelbar Geldwerte Leistungen für Arbeiten erhalten, die im Zusammenhang mit dem Inhalt der vorgelegten Dissertation stehen.

4. Die Arbeit wurde bisher weder im Inland noch im Ausland in gleicher oder ähnlicher Form einer anderen Prüfungsbehörde vorgelegt.

5. Die Inhalte dieser Dissertation wurden in folgender Form veröffentlicht:

   a. Research article     Risk seeking for losses modulates the functional connectivity of the default mode and left frontoparietal networks in young males

   b. Research article     Acute Tryptophan Loading Decreases Functional Connectivity between the Default Mode Network and Emotion-Related Brain Regions

6. Ich bestätige, dass es keine zurückliegenden erfolglosen Promotionsverfahren gab.

7. Ich bestätige, dass ich die Promotionsordnung der Medizinischen Fakultät der Technischen Universität Dresden anerkenne.

8. Ich habe die Zitierrichtlinien für Dissertationen an der Medizinischen Fakultät der Technischen Universität Dresden zur Kenntnis genommen und befolgt.

Ort, Datum                                                     Unterschrift des Doktoranden

**8.4. Erklärung zur Einhaltung gesetzlicher Vorgaben**

Hiermit bestätige ich die Einhaltung der folgenden aktuellen gesetzlichen Vorgaben im Rahmen meiner Dissertation

- das zustimmende Votum der Ethikkommission bei Klinischen Studien, epidemiologischen Untersuchungen mit Personenbezug oder Sachverhalten, die das Medizinproduktegesetz betreffen:

- Aktenzeichen der zuständigen Ethikkommission: EK 227062011 (Studie 1)
- Aktenzeichen der zuständigen Ethikkommission: EK 42022012 (Studie 2)

- die Einhaltung der Bestimmungen des Tierschutzgesetzes

- Aktenzeichen der Genehmigungsbehörde zum Vorhaben/ zur Mitwirkung: Entfällt

- die Einhaltung des Gentechnikgesetzes

- Projektnummer: Entfällt

- die Einhaltung von Datenschutzbestimmungen der Medizinischen Fakultät und des Universitätsklinikums Carl Gustav Carus.

Ort, Datum                                          Unterschrift des Doktoranden

**8.5. Erklärungen zur Publikation**

*Risk seeking for losses modulates the functional connectivity of the default mode and left frontoparietal networks in young males* **und** *Acute Tryptophan Loading Decreases Functional Connectivity between the Default Mode Network and Emotion-Related Brain Regions*

Als Erstautorin der beiden Manuskripte habe ich diese mit Unterstützung meiner Kollegen eigenständig verfasst. Unter der Leitung meines Betreuers Herr Prof. Dr. med. Michael N. Smolka habe ich die Qualitätskontrolle der fMRI- und Verhaltensdaten sowie die weiteren statistischen Analysen durchgeführt. Außerdem habe ich die von den Coautoren und nach dem Peer-Review-Verfahren die von den Gutachtern vorgeschlagenen Änderungen umgesetzt.

Für die erste Studie entwarf mein Kollege Herr Dr. rer. nat. Stephan Nebe das Design und sammelte die Daten in Dresden, während Frau Dr. rer. nat. Maria Garbusow und Frau Dr. rer. nat. Miriam Sebold die zweite Hälfte der Daten in Berlin unter der Leitung von Herrn Prof. Dr. med. Andreas Heinz erhoben. Herr Shakoor Pooseh, Ph.D. implementierte die für die Erhebung der Verhaltensdaten verwendeten mathematischen Algorithmen und Herr M.Sc. Philipp Neukam unterstützte die Arbeit durch anregende Diskussionen und Interpretation der Ergebnisse. Alle genannten Autoren haben die endgültige Fassung des Manuskripts zur Veröffentlichung freigegeben. Die Studie wurde in der Zeitschrift Cognitive Affective and Behavioral Neurosciences mit einem Impact Factor von 3.26 (5 Jahre Impact Factor: 3.51) veröffentlicht. Diese Zeitschrift wird im aktuellen Journal Citation Report in der Kategorie Behavioral Sciences auf Platz 12 von 51 und in der Kategorie Neurowissenschaften auf Platz 103 von 259 geführt. Die Zeitschrift veröffentlicht im Peer-Review-Verfahren psychologisch motivierte Studien über Beziehungen zwischen Gehirn und Verhalten, die unter anderem Aufmerksamkeit, Gedächtnis, Problemlösung, Argumentation und Entscheidungsfindung beinhalten. Diese Themen werden sowohl in der normalen Funktion als auch bei neurologischen Störungen und psychiatrischen Erkrankungen behandelt. Die Zeitschrift bekennt sich zu den Grundsätzen der Integrität und der guten wissenschaftlichen Praxis.

Für die zweite Studie war mein Kollege Herr M.Sc. Philipp Neukam für die Organisation und das Studiendesign zuständig. Wir waren beide an der Datenerhebung und Qualitätskontrolle der Verhaltens- und MRT-Datensätze beteiligt. All diese Aktivitäten wurden durch Herrn Prof. Dr. med. Michael N. Smolka beaufsichtigt. Herr Michael Marxen, Ph.D. und Herr Dipl.-Inf. Dirk K. Müller beteiligten sich an der Implementierung der Algorithmen für die Gruppenanalysen und Diskussionen über die statistischen Analysen und Ergebnisse. Herr Prof. Dr. Thomas

Henle überwachte die Analyse der Aminosäuren im Blutplasma. Alle genannten Autoren haben die endgültige Fassung des Manuskripts zur Veröffentlichung freigegeben. Das Manuskript wurde in der Zeitschrift Human Brain Mapping mit einem Impact Factor von 4.92 (5 Jahre Impact Factor: 5.09) veröffentlicht. Diese Zeitschrift wird im aktuellen Journal Citation Report in der Kategorie Neurowissenschaften auf Platz 57 von 259, in der Kategorie Neuroimaging auf Platz 2 von 14 und in der Kategorie Medizin und Medical Imaging auf Platz 13 von 127 geführt. Die Zeitschrift veröffentlicht Forschung im Peer-Review-Verfahren in den Bereichen Grundlagenforschung, klinische, theoretische und technische Forschung. Die Zeitschrift enthält Studien mit Ergebnissen der Neuroimaging-Forschung in den Bereichen kognitive Neurowissenschaften, Neurologie, Psychiatrie, Entwicklung, Alterung und Auswirkungen von systemischen Störungen auf das Gehirn. Studien, die neuartige oder komplexe Bildaufnahmemethoden (z.B. Kombination mehrerer bildgebender Verfahren) und analytische Methoden verwenden, werden für die Veröffentlichung in dieser Zeitschrift besonders empfohlen.

Ort, Datum                                                          Unterschrift des Doktoranden